UNIVERSITY OF SOUTHAMPTON

An Assessment of Approximate and Efficient Methods for The Dynamic Analysis of Non-linear Beams

by

Ieng Kit Daniel Gus Tang

Master of Philosophy

SCHOOL OF ENGINEERING SCIENCES

July 2002

UNIVERSITY OF SOUTHAMPTON

ABSTRACT

FACULTY OF ENGINEERING AND APPLIED SCIENCE
SCHOOL OF ENGINEERING SCIENCES

Master of Philosophy

AN ASSESSMENT OF APPROXIMATE AND EFFICIENT METHODS FOR THE DYNAMIC ANALYSIS OF NON-LINEAR BEAMS

by Ieng Kit Daniel Gus Tang

A literature survey on the field of non-linear vibrations of beams and thin panels has been performed with the aim of identifying efficient and accurate techniques which might be used in the aerospace industry. Attention is then focused on beam systems to allow candidate methods to be assessed.

Emphasis is placed on the study of geometrically non-linear vibration of isotropic slender beams with simply-supported end conditions when exposed to external excitation. The Duffing's equation has been derived and its applicability in describing non-linear beam vibrations is justified. The characteristics of non-linear harmonic vibration of the beam are studied. The non-linear response is first approximated by the Harmonic Balance Method based on the Duffing's equation and then compared with three sets of published results. The single-degree-of-freedom (SDOF) Duffing's equation is solved by a time-domain numerical method. An ANSYS® Finite Element Analysis is carried out to simulate the vibration problem. These solutions are compared with the Harmonic Balance results.

The non-linear response of a simply-supported beam to uniformly distributed random white-noise pressure is further studied. The non-linear root-mean-square displacement responses are approximated by applying the Direct Equivalent Linearisation Method to the SDOF Duffing's equation. The accuracy of the approximation is assessed by comparing the results with those obtained by the numerical integration of the SDOF Duffing's equation with simulated Gaussian white noise.

The total non-linear displacement response due to the first two modes of vibrations for the simply-supported beam subjected to various excitations are computed by solving both the uncoupled and coupled Duffing's equations by a step-by-step numerical integration scheme. The differences between the uncoupled and coupled responses are analysed.

Conclusions are drawn about the precision of the various methods of analysis and the importance of mode-coupling in non-linear beam vibrations.

List of Contents

List of Figures

List of Tables

ACKNOWLEDGEMENTS

The author would like to express his gratitude in particular to his supervisor Dr. Guglielmo Aglietti for his friendly advice and guidance.

The author wishes to acknowledge Professor Robin Langley at Cambridge University, for his technical suggestions and counsel have been a great support.

Financially, the author thanks the School of Engineering Sciences at the University of Southampton in the United Kingdom for their sponsorship of the research program.

In Aeronautics and Astronautics at the University of Southampton, the author wishes to show his gratitude to all his colleagues, especially Dr. Guo-Hua Xu for his opinion, Ajay Modha for his succour, Dr. Paul Cunningham for his help and Mrs. Allison Gunn for her assistance.

The author is indebted to his parents for their love and patience over the years. Their continual support is very much appreciated. The gratefulness cannot be expressed in a word.

Last, but not least, to all his family and friends, the author would love to say thank-you for keeping him amused.

This work is dedicated to the memory of my late grandfather.

Chapter 1

INTRODUCTION

1.1 The Need for the Prediction of Non-linear Random Response

With the current interest in high-speed vehicles and the ever increasing need for stronger, lighter structures, the problem of predicting the response of aircraft structures to random acoustic excitation is being reconsidered, with the emphasis being placed on the thermo-acoustic environment, and the non-linear response of lightweight panels. Since the implementation of gas turbine engines in the aerospace industry, a considerable amount of work has been carried out in an attempt to predict the stresses that could be encountered in service due to the random acoustic loading produced by the gas turbine engines. Most of the earlier methods employed to evaluate the response of aircraft structures only consider the linear case and the response dominated by low frequency dynamics. However some part of the aircraft structures, such as thin fuselage panels, close to the engine outlet exhibit a highly non-linear behaviour. Negligence of large deflection effects has been recognised as a major factor for the huge disagreement between measured test data and computed results.

In order to improve the prediction of acoustic fatigue damage, a better understanding of the non-linear response of random vibration of structures is needed. This is because

acoustic fatigue life prediction methods generally include the prediction of the random acoustic loads, the estimation of the stress response of the vibrating structure and the forecast of the life from stress versus cycles to failure curves for the material and fastener configuration [1]. The stress response becomes more non-linear and more difficult to predict as the acoustic load becomes larger.

The development of the structural response prediction model, combined with the understanding of acoustic sources will then enable the engineer to design against acoustic fatigue.

Efficient analysis methods and techniques, with a certain high level of accuracy in the prediction of the response due to the high level of acoustic loads, are necessary to be developed.

1.2 Brief Review of Acoustic Fatigue

A method for predicting the response of acoustically excited metallic structures was first developed by Miles [2]. He developed a cumulative damage hypothesis and used it to estimate the fatigue life of the structures subjected to random excitation. Powell [3] then carried out a general analysis of vibration of a structure caused by pressure fluctuations random in time and space, using ideas of vibration theory and spectrum analysis. He assumed that forced response of vibration could be approximated by the composition of the motions of the uncoupled natural modes. He had also considered multiple-modal effects. The results could be used to estimate fatigue life on the hypothesis of cumulative damage, on assuming normal randomness. From Powell's work, Clarkson [4] concentrated on the problem of the estimation of the stresses induced in typical structures by jet noise. The aim was to produce a single comprehensive design chart for each type of construction. He presented a simplified theory of Powell's work for panel-type structures by assuming that the major part of the response results from the contribution of one predominant mode. He carried out tests on flat plates, control surfaces and integrally stiffened skins to verify the applicability of the theory, and

concluded that it was satisfactory. Some other investigators have also worked on the problem since then.

As an extension to Miles' work, Blevins [5] has developed approximate analytical methods for the determination of linear response of plate and shell structures to surface pressures associated with sound and turbulence. It is capable of predicting higher mode response as well as response to both random and deterministic stationary surface pressures. This is done by simultaneously considering the spatial characteristics of both the structural modes and the sound field, and relating the two.

With improved computational power during the past forty years, some advanced analytical tools such as the finite element method have been developed and employed to tackle the problem of acoustic fatigue and estimate the response of aircraft panels subjected to strong random acoustic loads. Zienkiewicz [6] , for example, has given formulations for the properties of an element of a panel-type structure which undergoes large-displacements of vibration.

For more topics on acoustic fatigue and random vibrations, the reader is referred to excellent monographs such as references [7, 8, 9, 10].

1.3 Non-linearities in Structural Dynamics

The problem of non-linear dynamics has attracted a lot of investigators. In fact, almost all natural problems are of a non-linear character. The most distinct difference between linear and non-linear systems is that whilst the principle of superposition can be applied to linear systems, it may no longer be applicable to non-linear systems. Moreover, there are various phenomena such as the "drop-jump" phenomenon and internal resonance, which do not exist in the linear systems. Some descriptions in non-linear dynamic analysis of structures are documented in monographs such as Nayfeh [11] and Sathyamoorthy [12].

In dynamic systems, non-linearities are classified into three major categories [13]:

1. Geometric non-linearity due to large deflections in elastic elements

2. Material non-linearity due to the case when Hooke's Law is no longer valid, which results in a hysteresis loop

3. Topological non-linearity where a discrete finite change in the basic form of the differential equation occurs

The reason for the importance and sometimes puzzling effects of non-linearity is the very sudden transition from conditions in which linear theory is valid, to a state in which non-linear effects completely change the behaviour of a structure. The major effect of non-linearity is to introduce instabilities which can completely alter the mode shape of the vibrating structure [14]. Moreover, Ibrahim [13] indicated that despite many methods of solution exist there can be no universally applicable theory of predicting vibration behaviour in the non-linear regime. Each particular problem has to be approached from basic assumptions and a specific theory developed.

1.4 A Review of Non-linear Random Vibrations

In the study of forced vibration problems, two types of excitation are usually considered. They are deterministic and random excitation. The non-linear deterministic or sinusoidal cases result in a "jump phenomenon", the topic on which references [11, 15] have discussions. The random excitation case usually results in stochastic chaos. However, it is also known that the steady-state response of a non-linear system subjected to the harmonic forces may not only be harmonic, but also may be subharmonic, superharmonic, almost periodic or even chaotic, although the periodic responses often exist in a full or nearly full range of excitation frequency. Caughey [16] thoroughly reviewed the literature on non-linear random analysis prior to 1971. Thompson [17] has presented the basic concepts of non-linear dynamics and chaos. Random processes are described by many others in the literature [8, 18].

For engineering purposes, the random process is generally assumed to be stationary or weakly stationary. The random process is said to be stationary if the probability distributions obtained for the ensemble do not depend on absolute time. A stationary

process can be described as an ergodic process if, in addition to all the ensemble averaging being stationary with respect to time, the averages along any sample are the same as the ensemble averages [18]. Strictly speaking, a random process cannot be predicted exactly in advanced.

According to Spanos [19], the problem of predicting non-linear random vibrations has not been fully solved. The study of non-linear random vibrations raised great mathematical difficulties and to overcome these, four different principal methods have been proposed. They are the use of the perturbation method, Fokker-Planck-Kolmogorov (FPK) equations, the method of equivalent linearisation and the time-domain Monte-Carlo approach. A perturbation technique to study random non-linear vibration problems was proposed and applied by Crandall [20]. It is an extension to random vibrations of the perturbation method used for weakly non-linear deterministic systems. However, this method generally only yields results of reasonable accuracy for the case of small non-linearity. A new perturbation method where large parameters can be permitted has recently been proposed by He [21].

The most general extension of the FPK equation to non-linear multi-degree-of-freedom (MDOF) dynamic systems has been developed by Caughey [16, 22]. One advantage of this method over all other approaches is that it gives an exact solution. However, only for certain restricted classes of problems can the exact solutions of the steady-state probability function be found [23]. For example, the Fokker-Planck method can only be applied for the case of white noise random forces [24]. Lin [25] has introduced the procedures to obtain the stationary state solutions governed by the reduced Fokker-Planck equations.

Caughey [26] applied the Krylov and Bogoliubov method of equivalent linearisation [27] to a variety of non-linear random problems and compared the results with the exact solutions of the Fokker-Planck equation. Booton [28] and Caughey have developed independently the method of stochastic linearisation, which is the extension of the equivalent linearisation. Various texts have described the technique [19, 29, 30]. The objective of the equivalent linearisation method is to replace the non-linear elements in a model by linear forms, where the coefficients of linearisation can be found using the specific criterion of linearisation. Spanos [19] has given an in-depth discussion on the applicability

of this method in structural dynamics. This traditional method of equivalent linearisation is also known as the force error minimisation method when a new stochastic linearisation method based on potential (strain) energy error minimisation has recently been proposed by Elishakoff *et al.* [31]. Statistical linearisation methods generally have been wildly used [29, 32, 33, 34, 35] because of their ability to accurately capture the response statistics over a wide range of response levels while keeping a comparatively light computational load. However, the application is limited by the assumption that the response has to be Gaussian, and that the system is not strongly non-linear [36].

Numerical simulation techniques give the response in the time domain, from which the statistics of the random response may be retrieved. Vaicaitis [37] presented a review and illustrated the application of various time domain approaches to solve a variety of non-linear dynamic problems. The time-domain Monte Carlo method is the most general time-domain approach. It consists of three basic steps:

1. Realisations of random inputs and/or random system parameters are generated utilising simulation procedures of random processes [38, 39].

2. The equations of motion are solved numerically for each realisation.

3. Quantities of the random response process are computed from the ensemble solutions.

However, when the complexity of the physical system to be investigated increases, the computational expense gets dramatically higher.

Recently, Elishakoff and Colombi [36] have proposed a hybrid type of analysis by combining a stochastic linearisation and numerical Monte Carlo techniques in the study of non-linear systems under stochastic excitation.

The other widely used approximate methods [37] include the cumulant-neglect closure, stochastic averaging and energy dissipation balancing. It has to be noted, however, that there can be no general rule about the suitability of any method for a particular non-linear problem. Moreover, the application of different techniques to the same problem may lead to different results. Texts such as those by Blaquiére [40] as well as Dincă

and Teodosiu [30] have presented several approaches to find non-linear responses with random inputs.

1.5 Review of Non-linear Response of Beams and Panels

The non-linear response of thin panels has attracted the interests of numerous structural engineers. For a background study on classical linear and non-linear plate theories, the reader is referred to an excellent monograph by Leissa [41]. Leissa [42] and Reddy [43] have also written review papers in which they have discussed non-linear problems of plates of various geometries, composite laminated plates and sandwich plates. In cases where the deflections are small compared to the plate thickness, the linear bending of Timoshenko [44] is usually adequate. An overview of the subject of non-linear vibrations of plates and shells, and a summary of the literature from the 1960s up to the early 1980s were presented by Leissa [42]. Sathyamoorthy [12] published a comprehensive review of the development on the non-linear vibrations of plates in 1987.

The reader is recommended to refer to the tables of references in Appendix D for a brief description of the literature to be discussed in the following sections.

1.5.1 Free Vibration Problems

The geometric non-linear or large-amplitude vibrations of beams and plates have been studied by a number of investigators using various approximate analytical and numerical methods.

Woinowsky-Krieger [45] considered the free-oscillation problem of simply supported beams with immovable ends. The effects of axial loading and pre-stressing were taken into account the analysis. Expressing the solution as a product of a function of time and a linear free-oscillation mode, he solved the non-linear equation for the temporal function exactly using Jacobian elliptic functions.

McDonald JR. and Rayleigh [46] worked with a similar problem but did not consider axial pre-stressing. He treated the analysis by representing the deflection curve at any instant by a Fourier expansion in terms of the linear free-oscillation modes. He was able to solve the non-linear equations for the coefficients in terms of elliptic functions. He suggested that the problem be inherently non-linear even for small-amplitude vibrations and that there be always dynamic coupling of the modes.

Singh *et al.* [47] discussed the various formulations and assumptions, including the finite element method for large-amplitude free vibrations of beams. The vibration problem was formulated wherein the axial displacement is neglected and, further, the quadratic term in the strain displacement relation was linearised. This formulation would lead to the equation of motion which, when solved based on the simple harmonic oscillation assumption, would give exactly the same non-linear frequency as would the perturbation method, the Ritz-Galerkin method and the elliptical integral solution with axial displacement included, without linearisation of non-linear terms and without the harmonic oscillation assumption.

Benamar *et al.* [48] presented a method for calculating the first three non-linear mode shapes and natural frequencies of simply-supported (S-S) and clamped-clamped (C-C) beams at large amplitudes. A general model based on Hamilton's principle and spectral analysis for non-linear free vibrations occurring at large displacement amplitudes of fully clamped beams was set up. Rectangular homogeneous and composite plates subjected to the same problem were also developed [49, 50, 51].

Benamar *et al.* [52] studied the effects of large amplitudes on the fundamental mode shapes of fully clamped plates. Aluminium alloy plates were studied both experimentally and theoretically which exhibited a high degree of geometrical non-linearity. This was attributed to high in-plane stiffness inducing a higher contribution of the axial strain energy to the total strain energy at large displacement amplitudes. Even higher non-linearities were obtained with composite plates.

Continuing Benamar's work [49], El Kadiri *et al.* [53] calculated the second non-linear mode shape of the non-linear free vibration of fully clamped rectangular plates by the use of a hybrid method combining the steepest descent and Newton's methods.

They analysed the effect of non-linearity on the induced bending stresses associated with the second non-linear mode shape.

Rao *et al.* [54] presented a finite element method for the large amplitude free flexural vibration of plates and stiffened plates. The formulation assumes that the material of the plate and the stiffener obeys Hooke's law, that the lateral deflection is moderate and that Mindlin's hypothesis is followed.

Lee *et al.* [55] employed the Finite Element approach to derive a time-domain formulation for large-amplitude free vibrations of generally laminated thin composite rectangular plates.

Reddy [43] has presented a review on the finite element method (FEM) of natural vibrations of laminated composite plates from 1980 to 1985. A historical background of the development of shear deformation theories was also presented in the article.

Moussaoui *et al.* [56] recently studied the non-linear free response of a circular cylindrical shell of infinite length and determined the effects of large vibration amplitudes on the first and second coupled transverse-circumferential mode shapes and their corresponding natural frequencies.

1.5.2 Harmonically Forced Vibration Problems

There have been numerous theoretical and experimental analyses of non-linear vibrations of beams and plates excited harmonically. In particular, the topic of non-linear vibration of beams is of continuing interest, due to their frequent use as experimental test pieces [1, 57]. They comprise the simplest case of a continuous system, since their motion is expressed by one-dimensional partial differential equations in space. A well studied non-linear equation of motion is the Duffing's equation which has the form given in equation (1.1).

$$\frac{d^2x}{dt^2} + \xi\frac{dx}{dt} + \omega_0^2 x \pm \Pi x^3 = q\sin(\Omega t) \tag{1.1}$$

The parameter Π is a function of ω_0 and can be a positive *(hardening spring)* or a negative *(softening spring)* constant. In the case of a positive value of Π, the Duffing's equation can be used to describe the geometrically non-linear transverse vibrations of a beam subjected to a sinusoidal force. In this case, the transverse displacement is represented by x which is a function of time t. The parameter ξ is a damping coefficient, ω_0 is the natural angular frequency, and q and Ω are the amplitude and frequency of the external forcing function respectively. The equation includes damping and stiffness with cubic non-linearity. The basic solution of the Duffing's equation is the so-called "backbone curve". Many texts [11, 17, 40, 15, 58] have descriptions on the topic.

A number of approximate methods can be used to solve equation (1.1) analytically, as the equation cannot be solved exactly in closed form. One of the most widely used approach is by obtaining the perturbation method [30, 15].

Hsu [59] has presented analyses to find approximate solutions of a Duffing system to forced vibration. As the free vibration response of a system whose equation of motion is represented by equation (1.1) can be obtained exactly in the form of elliptic functions [45], he suggested that, if the external excitation of equation (1.1) is a simple elliptic forcing function, an elliptic function response can be obtained as the exact solution. By using a multiple-term elliptic response, Hsu also concluded that the simple harmonic forcing function and the corresponding perturbation solution was merely the first order approximation of the simple elliptic forcing function and the associated elliptic function response.

Srinivasan [60] applied a general modal approach to determine the response of beams and plates having moderately large amplitude steady state oscillations.

Bennett and Eisley [61] studied the steady-state response and stability for large deflection of a beam with clamped ends subjected to a concentrated harmonic force. Elastic restraint of the ends was included to relate theory with experiment. He used a multiple-mode (3 modes) analytical and numerical technique to obtain theoretical solutions for both response and stability. He concluded that there were situations where a multiple-mode analysis was essential to predict the observed results.

Azrar *et al.* [62] recently developed a semi-analytical approach to the non-linear dynamic response problem for the vibration of beams to determine the amplitude-frequency

dependence of S-S and C-C beams. He has developed a multi-dimensional form of the Duffing's equation having cubic non-linear stiffness for free and forced responses by using Lagrange's equations. The free vibration equations resulted were identical to that derived by Benamar [48] who used Hamilton's principle. Extending Azrar's work, Kadiri *et al.* [63] recently came up with a more practical simple multi-mode theory based on the linearisation of the non-linear algebraic equations, written on the modal basis, in the neighbourhood of each resonance. The method has been applied to explicitly determine the non-linear steady-state periodic forced response of C-C and clamped-simply supported (C-SS) beams for both small and large vibration amplitudes, excited harmonically with concentrated and distributed forces.

Leung and Chui [64] studied the non-linear vibration of a square plate subjected to a lateral symmetric sinusoidal force. Sherif [65] and Yamaki *et al.* [66] independently studied the non-linear vibration of a clamped circular plate to uniform distributed harmonic force.

Finite Element Analysis has also been employed by a number of researchers. Busby JR. and Weingarten [67] studied the multiple-modal forced responses of simply-supported beams subjected to periodic loading. Lee *et al.* [68] employed the FEM approach to derive a time-domain formulation and applied it for large-amplitude harmonically excited forced vibrations of generally laminated thin composite rectangular plates, considering also the effect of temperature. Chiang, Mei and Gray JR. [69] used a finite element formulation for determining the large-amplitude free and steady-state forced vibration of arbitrarily laminated anisotropic composite rectangular thin plates.

Ribeiro and Petyt [70] recently employed the hierarchical finite element method (HFEM) to study the geometrically non-linear free and steady state forced vibrations of uniform, slender beams with internal resonance. They concluded that the use of HFEM could significantly reduce the computational time when compared with FEM.

For the steady state, geometrically non-linear, periodic vibration of thin rectangular plates under harmonic external excitation, Ribeiro and Petyt [71, 72] presented and analysed the model by applying the principle of virtual work and the hierarchical finite element method. The stability of the obtained solutions was investigated. The convergence studies indicate that the HFEM and the harmonic balance method (HBM) allow

one to model the geometrical non-linear, forced periodic vibrations of plates accurately and with a small number of degrees of freedom.

1.5.3 Acoustic Random Forced Vibration Problems

Non-linear acoustic vibrations have been studied by many investigators. New theories have been proposed, established analytical methods have been employed and experimental work has been carried out to enhance the understanding of this topic.

Theoretical analysis

Vaicaitis [37] illustrated the application of the time domain approach to solve a variety of problems such as the non-linear response of panels and fatigue of surface panels subjected to high intensity turbulent flow and/or engine exhaust noise.

Herbert [33, 73] used the method of the Markoff process and the associated Fokker-Planck equation to study the multi-mode response of non-linear beams and plates subjected to purely random loading. However, he discovered that it was impossible to investigate the problem of whether the reduction of stresses due to the effect of membrane force would be the same as that of the displacement. Using the method of equivalent linearisation, he then carried on investigating the response of a non-linear beam subjected to a realistic random loading-a random loading with finite power [74]. He could then conclude that the percentage reduction of the mean square stresses could indeed be substantially less than that of the mean square displacements, and that the difference between the two percentage reductions would become greater as the spectral density of the load got wider.

Seide [75] also employed the equivalent linearisation technique to investigate the non-linear mean-square multi-mode stress add deflection responses of beams subjected to uniform pressure which is not correlated in time. It was concluded that determination of non-linear stresses would require many more modal functions than that of non-linear deflections would.

Prasad and Mei [76] studied the multiple-mode non-linear analysis for beams subjected to acoustic excitation including the effects of both non-linear damping and large-deflection. The effects have great influences on the deflections, strains and the modal frequencies, especially the restraining influence of non-linear damping on the modal frequencies. Schudt [77] investigated the non-linear response of beams to random excitation using an externally excited "hardening Duffing oscillator" (see equation (1.1)). Peak broadening phenomenon was studied by producing a family of typical response characteristics. The effect of the damping and the cubic non-linearity coefficients is to change the characteristics of the response peak in the Duffing oscillator.

Busby JR. and Weingarten [32] used the Finite Element Method to obtain the non-linear differential equations of motion which are expressed in terms of normal-mode co-ordinates. They studied the forced responses of the first two symmetric modes of simply-supported and clamped-clamped beams by the equivalent linearisation method. They concluded that if damping was included in the system, the effect of dynamic coupling could be reduced. Mei and Chiang [78] also used the FEM approach to develop the equations for the multi-modal representation of the large deflection random response of beams and plates subjected to acoustic loading. The excitation is assumed to be stationary, ergodic and Gaussian with zero mean; its magnitude and phase are uniform over the panel surfaces.

Elishakoff *et al.* [31] recently employed a new stochastic linearisation technique based on potential (strain) energy error minimisation for large amplitude random vibrations of a simply-supported or a clamped beam on elastic foundation. The stochastic loading acting on the beam is space-wise either (a) white noise or (b) uniformly distributed load and time-wise white noise. By using a three-term approximation, they found the mean square deflection at the mid-span of the beam for the various loading conditions. When comparing the results with the Fokker-Planck equation method and the conventional stochastic linearisation technique, they concluded that the proposed method was superior to the classical stochastic linearisation technique, especially in the high non-linearity range of the parameters.

Hwang and Pi [79] used a conforming plate element together with a non-linear plate stiffness element which is dependent on the modal response of the structure for the

non-linear response analysis of plate structures. Numerical results are obtained for a simply supported rectangular plate subjected to rain-drop type and uniform intensity random acoustic loading. Ahmadi *et al.* [24] studied the response of non-linear simply supported rectangular plates with stress free in-plane boundary conditions to stationary random excitation. Using one term in Galerkin's method, the resulting equation has been solved by different methods. Mei and Paul [23] determined the large-amplitude random response of clamped rectangular panels analytically, with the inclusion of multiple modes in the analysis. They obtained accurate mean-square deflections with the use of six terms in the Fourier-type series deflection function. Srinivasan and Krishnan [80] applied the integral equation technique to a non-linear stationary random response of an isotropic rectangular plate exposed to Gaussian white noise excitation.

Mei and Wentz [81], using series solution with one term, considered the geometric non-linearity of large-amplitude response of anti-symmetric angle-ply laminated rectangular plates subjected to broadband random acoustic excitation. Gray JR. *et al.* [82] presented an analytical solution for determining large deflection static bending, large-amplitude free and forced vibrations, and large-amplitude random response of a clamped, symmetrically laminated, rectangular, thin plate subjected to a uniformly distributed transverse loading.

Vaicaitis and Kavallieratos [83] employed the time-domain Monte-Carlo approach to study the non-linear response of simply-supported rectangular fibre reinforced laminated composite panel to random surface pressure with thermal heating. Vaicaitis and Arnold [84] developed a time-domain analytical model for non-linear response and fatigue life prediction of simple metallic and composite panels. Non-linear stresses have been investigated, and an acoustic fatigue damage model of surface panels has been constructed. Dhanaut *et al.* [85] recently developed a new analytical method using the Finite Element method and numerical integration time-domain approach to predict the non-linear random acoustic response of composite panels subjected to acoustic pressure at elevated temperature. It was shown to be able to predict the three types of panel motions, namely the linear random vibration about one of the buckled position, the snap-through between the two buckled positions, and the non-linear random response over the two thermally buckled positions.

Dogan and Vaicaitis [86] have carried out an analytical study of non-linear flexural vibrations of simply-supported cylindrical shells to random excitation, with the inclusion of thermal effects for a uniform temperature rise through the shell thickness in the formulation. A Monte-Carlo simulation technique of stationary random processes, multi-mode Galerkin-like approach and numerical integration procedures have been employed to find the non-linear response solutions

The time-domain Finite Element modelling has been widely used in recent decades. Green and Killey [87] explain how this technique can be used to assist in the design of aircraft against acoustic fatigue. They reasoned that although Finite Element Method is computationally intensive, it enhances the understanding of complex vibrations, such as the response of structures to spatially correlated jet noise excitations, or interactions between sound pressure loads and thermal loads.

McEwan *et al.* [88] has recently proposed a combined modal/finite element analysis technique for modelling large deflection forced response of a beam subjected to harmonic excitation. The proposed method, which involves non-linear coupled multiple vibration modes and imposes no linearisation scheme, has been applied to the case of a homogeneous isotropic beam, with fully simply-supported and fully clamped boundary conditions. The results have been shown to compare well with the standard direct integration finite element approach, with a significant saving in computational expense.

Experimental analysis

Bennouna and White [57] studied the effects of large vibration amplitudes on dynamic strain response, near to the fundamental resonance, of a clamped-clamped thin aluminium alloy beam excited sinusoidally and randomly. A set of fatigue experiments was carried out. A statistical approach was used and this gave a good correlation between predicted and measured fatigue life. High values of increase of beam curvatures were noticed near the clamps of the structures with constrained ends, causing a highly non-linear increase in bending strain with increasing deflections. It has also been shown that such a non-linear effect may have a significant impact on the structural fatigue life.

Wolfe *et al.* [1] carried out experiments to investigate the non-linear behaviour of beams and plates excited in high levels of dynamic response and developed a method for incorporating effects of multiple-modal response of simple structures.

Galea and White [89] determined the response of composite plates by exposing them to broadband acoustic excitation at elevated temperatures. They compared the experimental results with those predicted by the single, fundamental mode formula. An investigation was further carried out to find the variations in modal response of a clamped plate with temperature effect. It was found that the natural frequencies of the composite plates decreased slightly with increasing temperature. However, the elevated temperature did not noticeably changed the bending strain response of the plates tested under broad-band acoustic excitation. It was also found that the single mode response method accurately predicted the root-mean-square bending strains at room temperature and at various elevated temperatures under broadband acoustic random excitation.

Chen *et al.* [90],using a finite element formulation combined with the equivalent linearisation and normal mode methods, analysed the non-linear random response of beams subjected to acoustic and thermal loads applied simultaneously and carried out experiments to verify the analytical results. It was shown that the computed deflection results were very close to the measured ones. However, the difference between the computed and measured strains was much larger than the difference in deflection results.

Using theoretical and experimental approaches, Steinwolf, Ferguson and White [91] have investigated the dynamic behaviour of a beam, subjected to stationary random excitation for the situation in which the response is different from the model of a Gaussian random process. The study was restricted to the case of symmetric non-Gaussian probability density functions of beam vibrations.

1.5.4 Damping Considerations

It is known that damping is a major factor in determining the resonant peak response of a structure [1]. However, there are no theoretical methods to derive the exact damping factor of typical structures, and measurements have been relied upon to estimate the

frequency average value. In non-linear systems, if the coefficients to the cubic coupling terms are large, the phenomenon of "coupling resonance" [61] will appear which may change the shape of the response curve. It is noted that if damping is included, the effect of coupling resonance will be reduced remarkably [67].

A common approach to damping in the solution of dynamic problems is to include only viscous damping in the modal equations so that the equations of motion are linear in the damping term and thus economical to solve. The viscous damping coefficient is often expressed as a certain percentage of the critical damping. The damping ratio in most flight-vehicle structural members ranges from 0.005 to 0.04 [92]. In linear models, this viscous damping coefficient used is sometimes chosen on the basis of the type of material and system concerned in vibration. Richards and Mead [7] have discussions on the damping of jet-excited structures.

Schudt's studies [77] in the non-linear response of beams excited by random excitation with damping included in the governing equation indicates that peak broadening can be modelled by including cubic stiffness terms and also higher damping factors in the equations of motion.

Some investigators have also carried out research in non-linear forced vibrations of structures with non-linear damping. For example, Prasad and Mei [76] showed that non-linear damping had the greatest influence on the first mode and that its effects were significant on deflection as well as strains for small values. Strain response peaks at high acoustic excitations was shown to become broad and rounded under the effect of non-linear damping.

Ghanbari and Dunne [93] used an empirical three-term non-linear damping model for use with a single-degree-of-freedom Duffing's equation to describe the motion of clamped-clamped beam vibrations. The beam has been driven with band-limited white-noise excitation. The model has been calibrated by using experimental measurements. Calibration has utilised a Markov moment method and finite element solutions of the stationary Fokker-Planck equation. It has been shown that the individual parts within the damping model have a profound effect on the accuracy of prediction, even at low level response amplitudes. Comparison between measurement and prediction by using the full

calibrated model shows excellent agreement for probability density functions associated with the central beam displacement only up to moderately large amplitudes. At higher amplitudes, the differences between the two sets of results are significant. Nonlinear beam coupling was identified as the most likely cause for this difference. Furthermore, it has been suggested that forced random vibrations of a clamped-clamped beam can be accurately predicted with a single-degree-of-freedom model up to moderately large amplitudes, but only a little beyond this a multiple-degree-of-freedom model is required.

1.6 Comments on the State-of-the-art

The non-linear vibration of beams and simple plates has been studied extensively. It was suggested that neglecting the non-linear coupling terms and considering each mode separately for the prediction of the response do not affect very much on the accuracy, provided that the non-linear coupling is weak [62] and the excitation is harmonic [67]. It was found that the effect of non-linearity could be reduced by several ways, e.g., by adding damping, but non-linear coupling cannot be neglected in all cases, especially when non-linearity effect is large.

In random vibrations, particularly for a white-noise excitation, it was found that considering the one-mode response could obtain a very good estimate of the maximum displacement [75]. Thus, it can be seen that much research work on the non-linear response of white-noise-excitation of beams and panels has considered only the fundamental mode, as non-linear coupling is weak for a white noise with uniformly spatial distribution. However, in order to determine accurately the stresses, many more modal functions are necessary. As a result, it is certainly worthwhile to investigate the non-linear behaviour of higher response modes of forced vibration, especially with the inclusion of mode-coupling effects, on the vibration response of beams and panels.

There is a concern about the use of linearisation techniques in solving response of structures to high-level random loading. Time domain analyses have shown that due to the presence of non-linearities, the response is non-Gaussian, whilst linearised analyses would have predicted a Gaussian response [83, 84, 85]. Hence, some linearised methods

which assume a Gaussian output response to a Gaussian input excitation should be used with care.

1.7 Scope of The Present Work

Since a variety of problems regarding the structural strength of thin panels which arise in modern aircraft constructions cannot be adequately analysed on the basis of the classical linear theory of vibration, the development of a structural response prediction model which would take into account the non-linear response behaviour in the treatment of panel vibration is necessary. Moreover, although the phenomenon of "coupling-resonance" due to the coupling of modes has been known for some time, its effect has very often been neglected in the study of beam vibration problems.

The objective of the current study is to improve the understanding of the vibration behaviour of non-linear response of thin aircraft beam structures when exposed to different loads by using several different methods, with effects of mode-coupling taken into consideration. The investigation may serve as a background study for the development of predicting non-linear vibrations of aircraft panel-type structures.

In Chapter 2, the equation of motion of the geometrically non-linear beam vibrations is derived. The equation is then used in subsequent chapters to help understand vibration problems of beams in different excitation. In Chapter 3, the non-linear responses of a simply-supported beam under harmonic loading are obtained by various methods and the solutions are studied. The accuracy of the use of the methods is justified.

The non-linear vibrations of a simply-supported beam in Gaussian white-noise random pressure are investigated by analytical and numerical approaches. This study is presented in Chapter 4. The single-mode solutions are studied. The use of approximate analytical schemes is assessed on its accuracy to capture non-linear random response of beams.

The coupling effects on non-linear response of simply-supported beams subjected to harmonic and random pressures are investigated in Chapter 5 . Different excitations are

investigated. The numerical solutions of the equations of motion including the first two symmetric modes are studied. Conclusions are drawn.

Finally, conclusions of the current work are presented and future work proposed by the author is given.

Chapter 2

EQUATION OF MOTION OF NON-LINEAR BEAM VIBRATIONS

The case of a simply-supported isotropic beam can be regarded as a simplified case of the more complex structural models used in the design of high-speed aircraft components [88]. Moreover, the intense loading acting on the aircraft structures can affect fatigue life by introducing large-deflection geometrical non-linearity, modal coupling and multiple-mode participation [90]. In this chapter, the governing equations of motion is derived for the geometrically non-linear forced vibration of a simply-supported isotropic beam. This is a set of multiple-degree-of-freedom (MDOF) equation which is considered to be a multiple-mode form of the very well-known Duffing's equation.

2.1 General Multiple-Degree-of-Freedom Theory

Consider an inextensible slender beam. The end hinges of the beams are restrained against both vertical and horizontal displacements. If one end moves away from the

other horizontally, a tensile force is produced in the beam, which is proportional to the amount of that motion. Similarly, if one end approaches the other one, the force produced is compressive. The deflection of the beam does not need to be small when compared with its transverse dimensions. However, the curvatures need to be restricted to be small so that the approximate expression $\partial^2 w/\partial x^2$ can be applicable to represent the curvature of the beam. Here, w represents the transverse deflection of the beam at any point x, and x is measured along the beam neutral axis. In the following analysis, both shear deformations and longitudinal inertia are neglected.

2.1.1 Transverse Vibrations of Beams

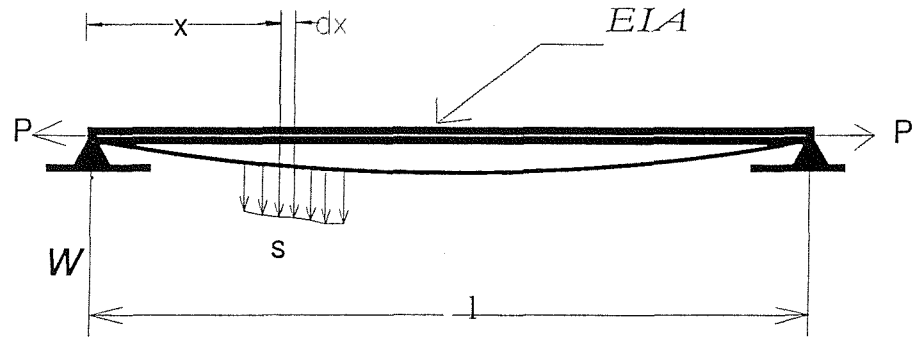

Figure 2.1: Beam with Hinged End Supports Axially Restrained under An Axial Force

If the beam is subjected to an axial tensile force P as shown in Figure 2.1, the differential equation of the deflection under static transverse loading is [94]:

$$EI\frac{d^2w}{dx^2} = M + Pw \tag{2.1}$$

where E and I are the Young's Modulus and the second moment of inertia, and the flexural rigidity of the beam is denoted by EI. M represents the bending moment produced by a transverse loading of intensity s. By double differentiation of equation (2.1) with respect to x, the following can be obtained:

$$\frac{d^2}{dx^2}\left(EI\frac{d^2w}{dx^2}\right) = s + P\frac{d^2w}{dx^2} \tag{2.2}$$

Furthermore, by substituting the inertial force per unit length for s, the general differential equation for transverse vibrations can be expressed as:

$$\frac{\partial^2}{\partial x^2}\left(EI\frac{\partial^2w}{\partial x^2}\right) - P\frac{\partial^2w}{\partial x^2} = -\mu\frac{\partial^2w}{\partial t^2} \tag{2.3}$$

If the flexural rigidity of the beam is constant, equation (2.3) may be given by:

$$EI\frac{\partial^4w}{\partial x^4} + \mu\frac{\partial^2w}{\partial t^2} - P\frac{\partial^2w}{\partial x^2} = 0 \tag{2.4}$$

2.1.2 Large Deflection Formulation

Assume a uniform and isotropic beam, i.e., EI and A are constant in Figure 2.1. From equation (2.4), the partial differential equation describing the transverse vibration of a beam which is axially restrained and in which large deflections are permitted is given by:

$$EI\frac{\partial^4w}{\partial x^4} + \mu\frac{\partial^2w}{\partial t^2} - (P_0 + P_1)\frac{\partial^2w}{\partial x^2} = f(x,t) \tag{2.5}$$

where

μ = vibration mass per unit length of beam

P_0 = initial axial tensile force of beam

P_1 = axial tensile force due to deflection

f = external load per unit length

This is a forced vibration problem. If the right-hand side of (2.5) is set to zero, the problem becomes a free vibration one [45].

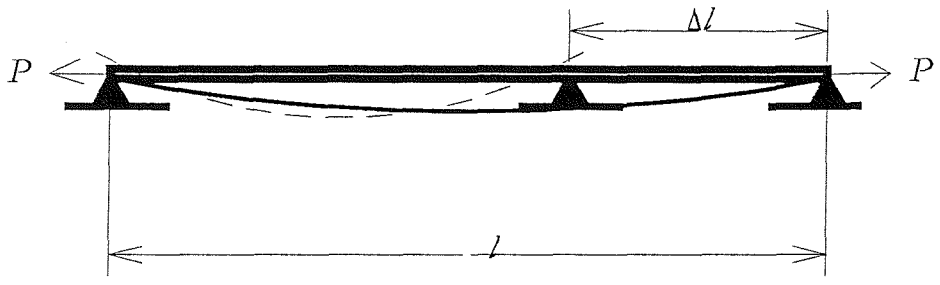

Figure 2.2: Beam Stretched by Axial Force P

The axial tensile force due to the deflection P_1 can be expressed in terms of the deflection w. If one support were free to move horizontally, the beam would be represented by the dashed line in Figure 2.2. The amount of axial movement of both simply-supported ends of the beam due to deflection is [45, 95]:

$$\Delta l = \frac{1}{2}\int_0^l \left(\frac{\partial w}{\partial x}\right)^2 dx \tag{2.6}$$

Equation (2.6) has been derived by numerous authors. For example, Langley [96] has used an alternative procedure in which $\frac{1}{2l}\int_0^l \left(\frac{\partial w}{\partial x}\right)^2 dx$ is identified as the non-linear axial Green's strain which is assumed to be constant along the neutral axis. The constant axial Green's strain is given by:

$$\epsilon_a = \frac{\partial u}{\partial x} + \frac{1}{2}\left(\frac{\partial w}{\partial x}\right)^2 \tag{2.7}$$

where u is the axial displacement of the beam neutral axis.

Integrating equation (2.7) with respect to x gives

$$u = \epsilon_a x + C - \frac{1}{2}\int_0^x \left(\frac{\partial w}{\partial x}\right)^2 dx \tag{2.8}$$

where C is a constant of integration. Applying the boundary conditions $u(0) = u(l) = 0$ gives an expression for ϵ_a in the form

$$\epsilon_a = \frac{1}{2l}\int_0^l \left(\frac{\partial w}{\partial x}\right)^2 dx. \tag{2.9}$$

Now, assuming that Hooke's law applies, the axial force P_1 produces an elongation of the beam, Δl which is:

$$\Delta l = \frac{P_1 l}{EA} \tag{2.10}$$

where l = length of the beam

A = cross-sectional area of the beam

E = Young's Modulus

Equating the equations (2.6) and (2.10), one gets the axial tensile force P_1:

$$P_1 = \frac{EA\Delta l}{l} = \frac{EA}{2l}\int_0^l \left(\frac{\partial w}{\partial x}\right)^2 dx \tag{2.11}$$

Then, substituting (2.11) into (2.5) gives a fourth-order partial differential equation that describes the transverse vibrations of a beam which is axially restrained and in which large deflections are permitted.

$$EI\frac{\partial^4 w}{\partial x^4} - \left[P_0 + \frac{EA}{2l}\int_0^l \left(\frac{\partial w}{\partial x}\right)^2 dx\right]\frac{\partial^2 w}{\partial x^2} + \mu\frac{\partial^2 w}{\partial t^2} + \beta\frac{\partial w}{\partial t} = f(x,t) \qquad (2.12)$$

The boundary conditions associated with equation (2.12) are $w(0) = 0$ and $w(l) = 0$. Equation (2.12) also includes damping and axial-prestressing. The damping coefficient is denoted by β. This equation is the basis for most of the studies of non-linear beam vibrations [11].

In the case of no axial-prestressing, P_0 in equation (2.12) is zero. The resulting equation of motion is given by the expression (2.13) and has been used by a number of investigators to study geometrically non-linear vibrations of isotropic beams [60, 74, 75, 76, 93].

$$EI\frac{\partial^4 w}{\partial x^4} - \left[\frac{EA}{2l}\int_0^l \left(\frac{\partial w}{\partial x}\right)^2 dx\right]\frac{\partial^2 w}{\partial x^2} + \mu\frac{\partial^2 w}{\partial t^2} + \beta\frac{\partial w}{\partial t} = f(x,t) \qquad (2.13)$$

The transverse deflection w can be represented by an expansion in terms of the linear free oscillation modes $\Phi_n(x)$ so that

$$w(x,t) = \sum_{n=1}^{\infty} Ru_n(t)\Phi_n(x) \qquad (2.14)$$

where n=1, 2,3,..., R is the radius of gyration, and u_n are functions of time only and are to be determined.

Specify also that $\Phi_n(x)$ satisfies the associated linear problem:

$$EI\frac{\partial^4 w}{\partial x^4} + \mu\frac{\partial^2 w}{\partial t^2} = 0 \qquad (2.15)$$

and the appropriate boundary conditions: $\Phi_n = \frac{d^2\Phi_n}{dx^2} = 0$ at a simply-supported end.

The following derivation procedures can also be found from various texts [11, 61, 75, 76]. Substituting (2.14) into equation (2.13) gives:

$$EIR\sum_{n=1}^{\infty} u_n \frac{d^4\Phi_n}{dx^4} + R\mu\sum_{n=1}^{\infty}\frac{d^2u_n}{dt^2}\Phi_n + R\beta\frac{du_n}{dt}\Phi_n$$
$$-\frac{EAR^2}{2l}\sum_{m,n=1}^{\infty} u_m u_n \int_0^l \frac{d\Phi_n}{dx}\frac{d\Phi_m}{dx}\,dx R\sum_{m=1}^{\infty} u_n\frac{d^2\Phi_n}{dx^2} = f(x,t) \qquad (2.16)$$

Equation (2.16) can be approximated by applying Galerkin's method [76], which basically involves the multiplying of the entire equation by Φ_m and then integrating it over the length of the beam.

$$EIR\sum_{n=1}^{\infty} u_n \int_0^l \Phi_m \frac{d^4\Phi_n}{dx^4}\,dx + R\mu\sum_{n=1}^{\infty}\int_0^l \Phi_m\Phi_n\frac{d^2u_n}{dt^2}\,dx$$
$$+ R\beta\frac{du_n}{dt}\int_0^l \Phi_m\Phi_n\,dx - \frac{EAR^2}{2l}\sum_{n,p,q=1}^{\infty} u_n u_p u_q \int_0^l \frac{d\Phi_p}{dx}\frac{d\Phi_q}{dx}\,dx\int_0^l \Phi_m\frac{d^2\Phi_n}{dx^2}\,dx$$
$$= \int_0^l f(x,t)\Phi_m\,dx \qquad (2.17)$$

The orthogonality relationships [97] are:

$$\int_0^l \mu\Phi_m\Phi_n\,dx = 0 \qquad \text{and} \qquad \int_0^l EI\Phi_m\frac{d^4\Phi_n}{dx^4} = 0 \qquad \text{for } m \neq n$$

$$\int_0^l EI\Phi_m\frac{d^4\Phi_n}{dx^4}\,dx = \omega_m^2\mu\int_0^l \Phi_m^2\,dx \quad \text{for} \qquad m = n \qquad (2.18)$$

where ω_m is the natural angular frequency which may be obtained from:

$$EI\frac{d^4\Phi_m}{dx^4} - \mu\omega_m^2\Phi_m = 0$$

As a result,

$$M_m \frac{d^2u_m}{dt^2} - \sum_{n,p,q=1}^{\infty} \left(\frac{EAR^2}{2l} \int_0^l \frac{d\Phi_p}{dx}\frac{d\Phi_q}{dx}\,dx \int_0^l \Phi_m \frac{d^2\Phi_n}{dx^2} \right) u_n u_p u_q + \beta \frac{du_m}{dt} \int_0^l \Phi_m^2 dx + \omega_m^2 M_m u_m = \frac{\int_0^l f(x,t)\Phi_m\,dx}{R} \tag{2.19}$$

where M_m is the generalised mass. Also, from the relation

$$\int_0^l \Phi_m \frac{d^2\Phi_n}{dx^2} = \left[\Phi_m \frac{d\Phi_n}{dx}\right]_0^l - \int_0^l \frac{d\Phi_m}{dx}\frac{d\Phi_n}{dx}\,dx = -K_{mn} \tag{2.20}$$

where,

$$K_{mn} = \int_0^l \frac{d\Phi_m}{dx}\frac{d\Phi_n}{dx}\,dx \tag{2.21}$$

the following set of non-linear ordinary differential equations results:

$$M_m \frac{d^2u_m}{dt^2} + \beta \int_0^l \Phi_m^2 dx \frac{du_m}{dt} + \omega_m^2 M_m u_m + \frac{EAR^2}{2l} \sum_{n,p,q=1}^{\infty} K_{mn}K_{pq}u_m u_p u_q = \frac{\int_0^l f(x,t)\Phi_m\,dx}{R} \tag{2.22}$$

Dividing (2.22) by M_m yields the following system of ordinary differential equations

$$\frac{d^2u_m}{dt^2} + \xi_m \frac{du_m}{dt} + \omega_m^2 u_m + \sum_{n,p,q=1}^{\infty} \Pi_{mnpq} u_n u_p u_q = \frac{f_0 f(t)\int_0^l f_m(x)\Phi_m\,dx}{RM_m} = F_{0m}(t) \tag{2.23}$$

where ξ_m is the generalised damping and Π_{mnpq} is the generalised non-linear stiffness coefficient. Moreover, the external force has been decomposed into its magnitude f_0, the time function $f(t)$ and the space function $f_m(x)$. The generalised force is denoted by $F_{0m}(t)$. Alternatively, (2.23) can be written as:

$$\frac{d^2u_m}{dt^2} + \xi_m \frac{du_m}{dt} + \omega_m^2 u_m + \Gamma_m = \frac{f(t)}{G_m} = F_{0m}(t) \tag{2.24}$$

The notations in equations (2.23) and (2.24) are as follows.

$$\Pi_{mnpq} = \frac{EAR^2}{2lM_m} K_{mn} K_{pq} \tag{2.25}$$

$$\xi_m = \frac{\beta}{M_m} \int_0^l \Phi_m^2 \, dx \; ; \qquad \Gamma_m = \frac{EAR^2}{2l} \sum_{n,p,q=1}^{\infty} K_{mn} K_{pq} u_m u_p u_q \tag{2.26}$$

$$M_m = \mu \int_0^l \Phi_m^2 \, dx \; ; \qquad G_m = \frac{RM_m}{\int_0^l f_m(x) \Phi_m \, dx} \tag{2.27}$$

Particularly, for the simply-supported (S-S) boundary conditions [76], where the modal functions in equation (2.14) is $\Phi_m(x) = \sin(m\pi x/l)$ and,

$$K_{mn} = \begin{cases} \frac{m^2\pi^2}{2l} & \text{if} \quad m = n; \\ 0 & \text{if} \quad m \neq n. \end{cases}$$

$$\xi_m = \frac{\beta}{M_m} \int_0^l \Phi_m^2 \, dx = \frac{\beta}{\mu}, \quad M_m = \mu \int_0^l \Phi_m^2 \, dx, \quad \omega_m^2 = \frac{EI}{\mu} \left(\frac{m\pi}{l}\right)^4 \tag{2.28}$$

Hence the geometrically non-linear transverse vibrations of a slender beam can be described by a set of second-order non-linear ordinary differential equations shown in equation (2.23).

2.2 The One-Mode Duffing's Equation

If only one mode is considered, then from equation (2.24), the single-degree-of-freedom (SDOF) Duffing's equation with cubic non-linearity and modal damping for simply-supported end conditions, is given by:

$$\frac{d^2u_1}{dt^2} + \xi_1 \frac{du_1}{dt} + \omega_1^2 u_1 + \Pi_{1111} u_1^3 = F_{01}(t) \tag{2.29}$$

where

$$\begin{aligned} \xi_1 &= \beta/\mu \\ \omega_1^2 &= \frac{\pi^4 EI}{\mu l^4} \\ \Pi_{1111} &= \frac{\pi^4 EI}{4\mu l^4} \end{aligned} \tag{2.30}$$

The corresponding Duffing's equation without damping is expressed as:

$$\frac{d^2u_1}{dt^2} + \omega_1^2 u_1 + \Pi_{1111} u_1^3 = F_{01}(t) \tag{2.31}$$

The single-mode Duffing's equation has been adopted by a number of investigators to study the non-linear vibrations of beams. Equation (2.31) can also be derived by using the energies of the beam and the Lagrange's equation [96]. The procedure is presented briefly here. Assuming that the non-linear Green's strain is constant along the neutral axis of a simply-supported beam whose ends are restrained from axial movement, the strain energy, V, can be written as:

$$V = \frac{1}{2} EAl\epsilon_a^2 + \frac{1}{2} EI \int_0^l \left(\frac{\partial^2 w}{\partial x^2} \right)^2 dx \tag{2.32}$$

where ϵ_a has been defined in equation (2.7). Suppose the transverse deflection of the beam $w(x,t)$ can be expressed in the form:

$$w(x,t) = Ru(t) sin(\pi x/l). \tag{2.33}$$

With the use of equations (2.33) and (2.9), equation (2.32) becomes:

$$V = \frac{EIR^2 l}{4} \left(\frac{\pi}{l} \right)^4 u^2 + \frac{EIR^2 l}{32} \left(\frac{\pi}{l} \right)^4 u^4 \tag{2.34}$$

The kinetic energy of the beam T with longitudinal inertia neglected can be written as:

$$T = \frac{1}{2}\mu \int_0^l \left(\frac{dw}{dt}\right)^2 dx = \frac{1}{4}\mu l R^2 \left(\frac{du}{dt}\right)^2 \tag{2.35}$$

By substituting equations (2.34) and (2.35) into the Lagrange's equation given by:

$$\left(\frac{d}{dt}\right)\left(\frac{\partial T}{\partial \dot{u}}\right) - \frac{\partial T}{\partial u} + \frac{\partial V}{\partial u} = f, \tag{2.36}$$

where $f = R\int_0^l f(x,t)sin(\pi x/l)dx$ is the generalised force caused by the external load, the equations of motion of the beam which is the same as equation (2.31) can then be obtained:

$$\frac{d^2u_1}{dt^2} + \omega_1^2 u_1 + \Pi_{1111}u_1^3 = F_{01}(t) \tag{2.37}$$

where the parameters have been defined in expressions in equation (2.30)

2.3 Chapter Summary

A multiple-degree-of-freedom model describing the geometrically non-linear transverse vibrations of slender isotropic beams has been set up. The beam under consideration has end hinges which are restrained against both vertical and horizontal displacements. Both shear deformations and longitudinal inertia are neglected.

A fourth-order differential equation has been derived in which large-deflection and axial-prestressing are included. The equation in which no axial-prestressing has been further analysed. By utilising the Galerkin's method and the orthogonality relationships, a set of MDOF ordinary differential equations has been derived. The corresponding SDOF Duffing's equation has also been obtained.

It has been shown that the same single-mode Duffing's equation can also be derived using a different approach utilising the beam energies and the Lagrange's equation.

Chapter 3

HARMONIC VIBRATIONS OF NON-LINEAR BEAM

The non-linear response of structures to harmonic excitation has been studied by numerous researchers. One reason is that the understanding of the response of structures to harmonic excitation provides insight into how the system will respond to other types of forces.

In this chapter, the non-linear response of beams subjected to harmonic excitation is investigated. The equations of motion derived in Chapter 2 are employed to study the vibration behaviour of simply-supported beam with immovable end conditions. Both analytical and numerical approaches are used to obtain the solutions of the non-linear response.

3.1 The MDOF Undamped Equations of Motion

The non-linear undamped forced response of simply-supported beams with immovable end conditions due to a time-domain harmonically varying load will be studied. The

equations of motion for an undamped systems can be obtained by simply neglecting the damping term in (2.23) and (2.24). The equations thus obtained are:

$$\frac{d^2u_m}{dt^2} + \omega_m^2 u_m + \sum_{n,p,q=1}^{\infty} \Pi_{mnpq} u_n u_p u_q = F_{0m}(t) \tag{3.1}$$

$$\frac{d^2u_m}{dt^2} + \omega_m^2 u_m + \Gamma_m = F_{0m}(t) \tag{3.2}$$

The MDOF undamped large-deflection transverse vibrations of a slender beam can be described by an expression either in the form of equation (3.1) or of equation (3.2).

3.2 Harmonic Response

3.2.1 Solution based upon the Harmonic Balance Method

Since there is no known exact analytical solution to (3.1), an approximate solution by the harmonic balance method will be sought. This method can be found from various texts such as Blaquière [40]. Bennett and Eisley [61] have outlined the method briefly. A solution of the mode $u_m(t)$ is assumed to have the form for harmonic forcing

$$u_m(t) = A_m \sin \Omega t \tag{3.3}$$

where Ω= angular frequency and A_m= constant to be determined.

Substituting (3.3) into (3.1), expressing $\sin^3 \Omega t = (3 \sin \Omega t - \sin 3\Omega t)/4$, and neglecting the terms that contain $\sin 3\Omega t$, the following is obtained:

$$-A_m\Omega^2 + \omega_m^2 A_m + \frac{3}{4} \sum_{n,p,q=1}^{j} \Pi_{mnpq} A_n A_p A_q = \frac{F_{0m}(t)}{\sin \Omega t} = Q_{0m} \tag{3.4}$$

The negligence of the terms that contain $\sin 3\Omega t$ is merely one assumption of the Harmonic Balance which states that any harmonics which arise in the substitution

which are not included in the assumed solution (equation 3.3) are neglected. Equation (3.4) only considers the first j modes. It is a set of j non-linear algebraic equations relating the terms of A_m's and Ω. An iterative method (see Appendix A.2) can then be employed to find the relations between the amplitudes A_m and the angular frequency Ω. The expression of equations (3.1) and (3.4) have been expanded up to the first three modes and is shown in Appendix A.1.

If the external force, $f(x,t)$ is assumed to be harmonic in the time domain, then it can either be a concentrated force, $f^c(x,t) = f_0^c \sin(\Omega t)\delta(x - x_0)$ at a particular point x_0 along it, or a distributed uniform load, $f^d(x,t) = f_0 \sin(\Omega t) f^d(x)$, across the span. The generalised forces $F_{0m}^c(t)$ and $F_{0m}^d(t)$ to be implemented in (3.1) for each case are respectively:

$$F_{0m}^c(t) = \frac{f_0}{RM_m} \sin(\Omega t)\Phi_m(x_0) \tag{3.5}$$

$$F_{0m}^d(t) = \frac{f_0}{RM_m} \sin(\Omega t) \int_0^l f(x)\Phi_m(x)\, dx \tag{3.6}$$

3.2.2 One-mode Non-linear Frequency Response Functions

The beam is approximated by an equivalent single-degree-of-freedom (SDOF) Duffing oscillator derived from equation (3.1). Equation (3.7) presents the Duffing's equation with only the first mode considered.

$$\frac{d^2u_1}{dt^2} = -\omega_1^2 u_1 - \Pi_{1111} u_1^3 + F_{01}(t) \tag{3.7}$$

The excitation, $F_{01}(t)$, varies harmonically with time and can be obtained from equations (3.5) and (3.6). From (3.4),

$$-A_1\Omega^2 + \omega_1^2 A_1 + \frac{3}{4}\Pi_{1111} A_1^3 = \frac{F_{01}(t)}{\sin \Omega t} = Q_{01} \tag{3.8}$$

Rearranging equation (3.8) gives the following frequency-amplitude relation approximation:

$$\frac{\Omega}{\omega_1} = \sqrt{1 + \frac{3}{4}\frac{\Pi_{1111}A_1^2}{\omega_1^2} - \frac{F_{01}(t)}{\omega_1^2 A_1 \sin \Omega t}} = \sqrt{1 + \frac{3}{4}\frac{\Pi_{1111}A_1^2}{\omega_1^2} - \frac{Q_{01}}{\omega_1^2 A_1}} \tag{3.9}$$

The force parameter Q_{01} is independent of time and related to the actual force by the expression $Q_{01} = \left[\frac{f_0}{RM_1}\int_0^l \Phi_1 f_0(x)\,dx\right]$, where f_0 and $f(x)$ specify the force magnitude and force spatial mode respectively. After obtaining the values of Ω for the corresponding values of pre-defined A_1 and the force parameter Q_{01}, the frequency-amplitude-force relation curves can be plotted, and the time dependent function $u_1(t)$ can also be approximated if desired (see Appendix B.2).

3.2.3 A Particular Example

In the numerical example, the beam shown in Figure 3.1 studied is studied and has a circular cross section. Its properties is given in Table 3.1. The use of such a beam is merely for the purpose of comparing the solutions by the various computational methods and the published results.

Young's Modulus E	207×10^9 Pa	Length of beam l	2.5 m
Radius of gyration R	0.025 m	2^{nd} moment of inertia I	4.909×10^{-6} m^4
Density of beam ρ	7850 kg/m^3	diameter d	0.1 m

Table 3.1: Parameters Used for Analysis of Beam in the Particular Numerical Example

From (2.14), let $\Phi_m(x) = \sin(m\pi x/l)$, so that

$$w(x,t) = Ru_m(t)\sin\frac{m\pi x}{l} \tag{3.10}$$

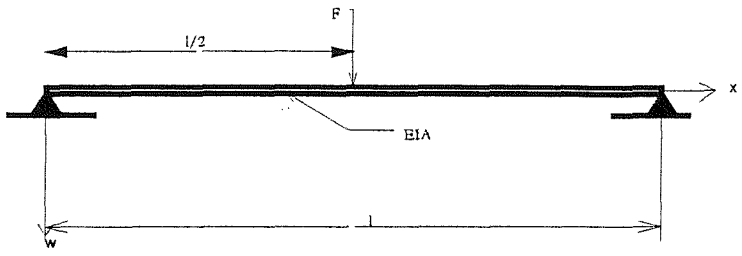

Figure 3.1: Beam with Immovable Ends Simply-supported and Load at Mid-span

where m is an integer. This example involves only a single mode so that m is equal to 1 in equation (3.10). Moreover, from equation (2.25) and expressions in (2.28), the following can be obtained:

$$\Pi_{1111} = \frac{\pi^4 EI}{4\mu l^4}\ ; \qquad M_1 = \frac{\mu l}{2}\ ; \qquad \omega_1^2 = \frac{\pi^4 EI}{\mu l^4}. \tag{3.11}$$

Now, consider two loading cases. In one case, an external concentrated force $F_{01}^c(t) = Q_{01}^c \sin(\Omega t)$ with normalised magnitude $Q_{01}^c = \frac{2f_0}{R\mu l}$ is applied at the mid-span of the beam. In the second case, a uniformly distributed force which acts on the beam can take the form of the expression

$$F_{01}^d(t) = Q_{01}^d \sin(\Omega t) \int_0^l \sin(\frac{\pi x}{l})\, dx = \frac{4f_0}{R\mu\pi} \sin(\Omega t)$$

Hence, substituting (3.11) into (3.9) and the forcing functions for each case as $F_{01}(t)$ in (3.9) will result in the following expressions for the frequency-amplitude relation:

$$\left(\frac{\Omega}{\omega_1}\right)_{concentrated} = \sqrt{1 + \frac{3}{16}A_1^2 - \frac{2f_0 l^3}{\pi^4 EIRA_1}} = \sqrt{1 + \frac{3}{16}A_1^2 - \frac{\overline{F_{01}^c}}{A_1}} \tag{3.12}$$

$$\left(\frac{\Omega}{\omega_1}\right)_{distributed} = \sqrt{1+\frac{3}{16}A_1^2 - \frac{4f_0 l^4}{\pi^5 EIRA_1}} = \sqrt{1+\frac{3}{16}A_1^2 - \frac{\overline{F_{01}^d}}{A_1}} \qquad (3.13)$$

Here, $A_1 = |w_{max}/R|$, and w_{max} is the maximum amplitude response for the single mode. Figures 3.2 and 3.3 are typical response curves for the hard spring Duffing's oscillator. They can be found by plotting the frequency ratio in (3.12) and (3.13) as a function of A_1.

3.2.4 Results and Discussions

Table 3.2 compares the free vibration frequency ratios for pre-defined response amplitudes with the exact theoretical solutions given by the elliptic function solutions [45, 98]. The Harmonic Balance solutions overestimates the solutions in free vibrations. The differences between the two solutions increase with increase in amplitude. However, their differences are acceptable, as the Harmonic Balance is simply an approximation to the Duffing's equation.

A_1	Elliptic function solution [45, 98] Ω/ω_1	HBM [equation (3.9) with $Q_{01}=0$] Ω/ω_1	% difference
1	1.0892	1.089725	0.048
2	1.3178	1.322876	0.385
3	1.6257	1.639360	0.840
4	1.9760	2.000000	1.215
5	2.3501	2.384848	1.479

Table 3.2: Free Vibration Frequency ratios Ω/ω_1 for a S-S Beam with Immovable End Conditions for Selected Amplitudes A_1

In the case of forced vibrations, the numerical results and other published results are shown in Tables 3.3 and Tables 3.4 for selected values of A_1. Figures 3.2 and 3.3 are

the "backbone curves" for the concentrated loading case and the uniformly distributed loading case respectively. As only the fundamental mode is concerned, the forcing frequencies have been chosen to be lower than and away from the next responding resonance frequency.

A_1	Elliptic solution [59, 98] Ω/ω_1	Perturbation solution [98] Ω/ω_1	F.E.M. [98] Ω/ω_1	HBM [equation (3.12)] Ω/ω_1
-1	1.6607	1.6608	1.6425	1.660812
$\pm$ 2	0.9695	0.9821	0.8497	0.982141
	1.5894	1.5923	1.5143	1.592293
$\pm$ 3	1.4519	1.4710	1.217	1.471021
	1.7815	1.7920	1.6326	1.791954
$\pm$ 4	1.8711	1.8993	1.6229	1.899290
	2.0751	2.0959	1.8495	2.095877
$\pm$ 5	2.2801	2.3181	1.9621	2.318047
	2.4179	2.4498	2.1165	2.449828

Table 3.3: Forced Vibration Frequency Ratios Ω/ω_1 for a S-S Beam with Immovable End Conditions under a Harmonic Concentrated Force ($\overline{F_{01}^c} = \pi/2$, $Q_{01}^c = \omega_1^2\pi/2$, $f_0 = 124379.73N$)

Tables 3.3 and 3.4 are represented graphically by Figures 3.4 and 3.5 respectively. When compared to the first two published results by the classical methods in Table 3.5, the present SDOF model matches very well with the elliptic and perturbation solutions, but not the F.E.M. solutions by reference [67], in both the concentrated and the distributed forced vibration case.

Since the methods to generate the published results are not exact, the accuracy cannot be verified. Hence, the time domain response amplitudes from the Finite Element

A_1	Elliptic solution [59, 98] Ω/ω_1	Perturbation solution [98] Ω/ω_1	F.E.M. [98] Ω/ω_1	HBM [equation (3.13)] Ω/ω_1
-1	1.7852	1.7854	1.7856	1.785357107
$\pm$ 2	0.8472	0.8660	0.8460	0.866025404
	1.6557	1.6583	1.6512	1.658312395
$\pm$ 3	1.4003	1.4126	1.3760	1.421560176
	1.8217	1.8314	1.8002	1.831438415
$\pm$ 4	1.8413	1.8708	1.7846	1.870828693
	2.1013	2.1213	2.0495	2.121320344
$\pm$ 5	2.2606	2.2995	2.1619	2.299456458
	2.4361	2.4673	2.3432	2.467285958

Table 3.4: Forced Vibration Frequency Ratios Ω/ω_1 for a S-S Beam with Immovable End Conditions under a Harmonic Uniformly Distributed Pressure ($\overline{F_{01}^d} = 2$, $Q_{01}^d = 2\omega_1^2$, $f_0 = 99503.78N/m$)

A_1	Perturbation method, c (%)	Elliptic solution, c (%)	F.E.M. [98], c (%)	Perturbation method, d (%)	Elliptic solution, d (%)	F.E.M. [98], d (%)
-1	-0.0674	-0.00674	-1.10259	+0.0024	-0.0088	+0.014
-2	-0.18169	-0.18169	-4.89816	-0.00075	-0.16	-0.43
-3	-1.29985	-0.58339	-8.89275	-0.0021	-0.53	-1.71
-4	-0.99133	-0.99133	-11.7553	-0.00096	-0.94	-3.39
-5	-0.00114	-1.30328	-13.6062	+0.00057	-1.26	-5.03
+2	-0.00417	-1.28709	-13.4849	-0.0029	-2.17	-2.31
+3	-0.00143	-1.29985	-13.5498	-0.63	-1.50	-3.20
+4	0.000527	-1.48425	-14.5523	+3.46	+1.83	-1.31
+5	0.002286	-1.63702	-15.3555	+0.0019	-1.69	-5.98

Table 3.5: Percentage Differences of (Ω/ω) between HBM results and Various Published Results, c=concentrated loading, d=distributed loading (from Tables 3.2, 3.3 and 3.4)

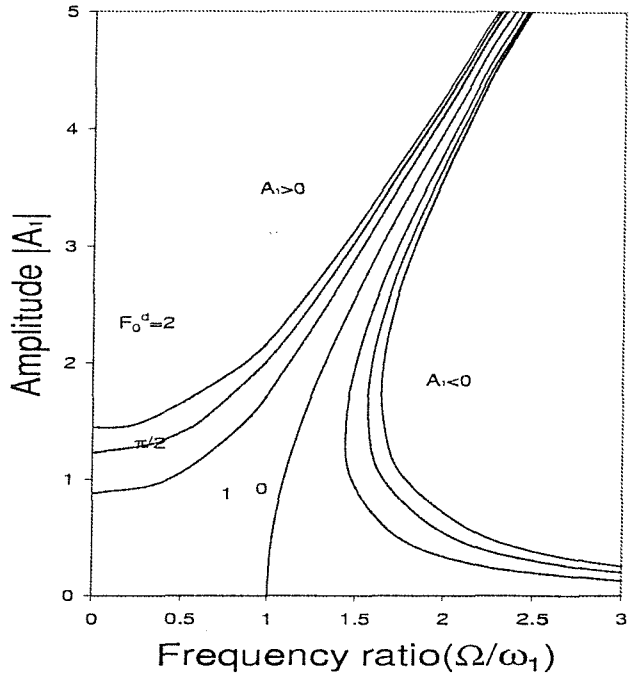

Figure 3.2: Harmonic Balance: Amplitude Versus Frequency for a S-S Beam with Immovable End Conditions under Concentrated Force with Magnitudes $\overline{F_{01}^c}$=1 (f_0=79182.59 N), $\overline{F_{01}^c}$=$\pi/2$ (f_0 = 124379.73N and $\overline{F_{01}^c}$=2 (f_0=158365.20 N)

software ANSYS® have been obtained to further check the validity of the present vibration model (2.13) (See Appendix C.1). This approach generally consists of three phases, the "Preprocessor" phase which generates the model, the "Solution" phase which analyses the model and calculates the solutions and the "Postprocessor" phase where the numerical results are retrieved. In the current study, linear solutions have been obtained through the use of "Harmonic" and "Transient" analysis within the "Solution" phase in ANSYS®. In ANSYS® 5.7, "Harmonic" can only perform frequency domain analysis without geometrically non-linearity effects. With the inclusion of non-linear effects but solutions in the time domain have been obtained via "Transient" analysis.

The time domain first-mode amplitude response has also been calculated by numerical integration of the governing ordinary differential equation (3.7) with the use of a

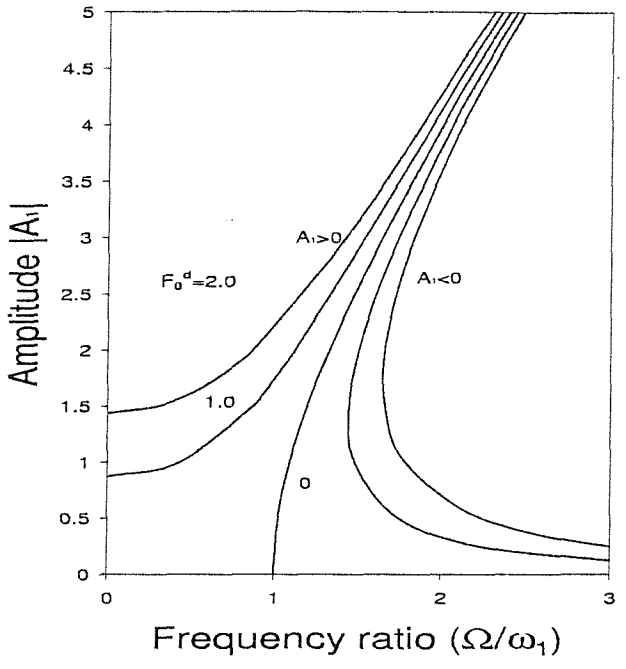

Figure 3.3: Harmonic Balance: Amplitude Versus Frequency for a S-S Beam with Immovable End Conditions under Uniformly Distributed Force with Magnitudes $\overline{F_{01}^d}$=1 (f_0=49751.89 N/m), and $\overline{F_{01}^d}$=2 (f_0=99503.78 N/m)

Newmark-Beta time integration method [99, 100]. This would give the exact solution of the first-mode response, if equation (3.7) were an exact interpretation of the motion of the beam under investigation. This approach checks the accuracy of the use of the Harmonic Balance Method which applies to equation (3.7).

The frequency response curve can be constructed from solutions obtained by the numerical methods. For each pre-defined forcing frequency Ω, the numerical analysis (both by ANSYS® "Transient" analysis and by Newmark-Beta time integration method) is performed and the steady-state maximum amplitude of the displacement response, $|A|$ is obtained. The time-domain numerical approaches give only the stable solutions of the differential equation although the present method using HBM is able to calculate all three (two stable and one unstable) solutions. Nevertheless, only the appropriate stable

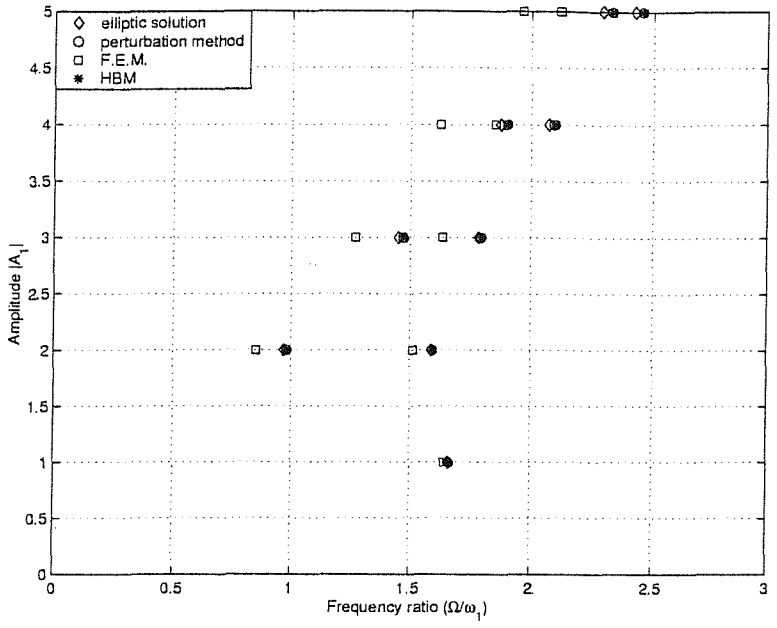

Figure 3.4: A Comparison of Amplitude $|A_1|$ at Selected Frequency Ratios among the Four Methods (Concentrated Load $\overline{F_{01}^c}=\pi/2$)

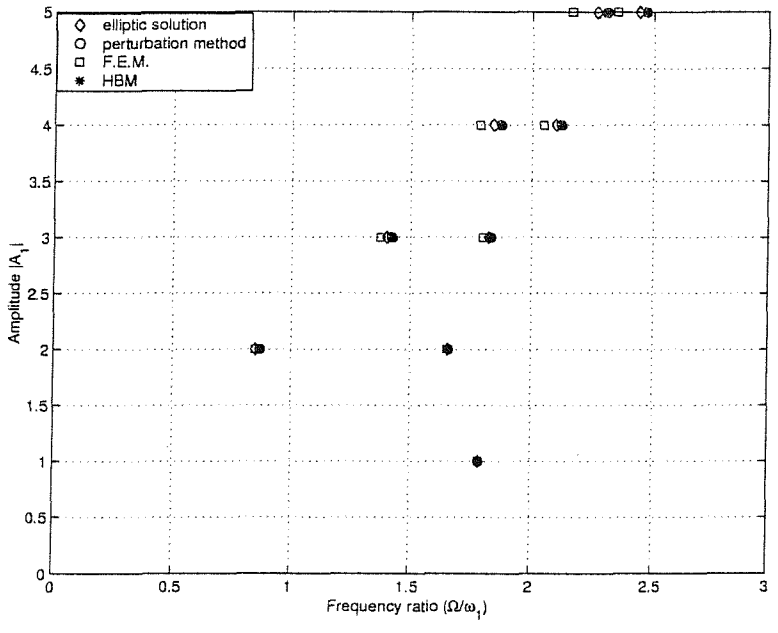

Figure 3.5: A Comparison Amplitude $|A_1|$ at Selected Frequency Ratios among the Four Methods (Distributed Load $\overline{F_{01}^d}=2$)

solution will be used for the purpose of comparison.

(Ω/ω_1)	$\|A\|$ (HBM)	$\|A\|$ (ANSYS® time-domain)	$\|A\|$ (Newmark-Beta time-domain)
0.0152	0.8747	0.856	0.848
0.0967	0.8803	0.8400	0.8513
0.4243	0.9946	1.014	1.1820
0.856	1.4777	1.518	1.508
1.0957	1.9504	2.000	1.984
1.3035	2.4332	2.429	2.4751
1.4162	2.7079	2.742	2.7543
1.5716	0.7299	0.580	0.7289
1.7005	0.5446	0.480	0.5438
1.7033	0.5416	0.460	0.5408
2.0203	0.3266	0.325	0.3261
2.096	0.2961	0.268	0.2957
2.3778	0.2153	0.168	0.2150
2.6987	0.1593	0.124	0.1591

Table 3.6: Forced Vibration Amplitudes $|A| = |w_{max}/R|$ for a S-S Beam with Immovable End Conditions under a Concentrated Force $\overline{F_{01}^c} = 1(f_0 = 79182.59N)$

Table 3.6 and Figure 3.6 show some results in the concentrated forcing case while Table 3.7 and Figure 3.7 show those in the uniformly distributed loading case. Figures 3.6 and 3.7 show the simulated backbone curves by the two time-domain analyses, together with that by the present model. Table 3.8 summarises the areas on the plots of Figures 3.6 and 3.7, where the "jump" phenomenon happens to occur (see Appendix B). To use the Harmonic Balance Method to estimate the frequency at which the "jump" occurs, the first derivative of equations (3.12) or (3.13) is set to zero. The value of $|A_1|$ is then obtained and by substituting $|A_1|$ back to equations (3.12) or (3.13), the

(Ω/ω_1)	$\|A\|$ (HBM)	$\|A\|$ (ANSYS® time-domain)	$\|A\|$ (Newmark-Beta time-domain)
0.0155	1.4402	1.3540	1.365
0.4330	1.5694	1.5000	1.7000
0.8660	2	1.9858	2.0800
1.1713	2.5	2.3285	2.5600
1.4216	3	2.4287	3.066
1.5	3.1677	1.9300	3.2373
1.6583	3.516	3.548	3.5920
1.7854	3.8404	3.825	3.8843
1.8314	0.9095	0.7554	0.9076
1.8718	0.8438	0.7080	0.8433
2.1213	0.5820	0.5054	0.5815
2.2465	0.5	0.4385	0.4994
2.2894	0.4763	0.4194	0.4760
3.0020	0.25	0.2600	0.2497

Table 3.7: Forced Vibration Amplitudes $|A| = |w_{max}/R|$ for a S-S Beam with Immovable End Conditions under a Uniformly Distributed Load $\overline{F_{01}^d} = 2(f_0 = 99503.78N/m)$

resulting value of (Ω/ω_1) corresponds to the frequency ratio where the backbone curve is vertical. This is where the jump of the amplitude should occur. The precise value of the "jump" frequency ratio has not been obtained from the numerical solutions given by the Newmark-Beta integration and ANSYS® results. This is because an excessively large number of numerical computation would be needed in order to generate enough data points to retrieve an exact value of (Ω/ω_1).

It can be seen that when predicting the frequency when this jump phenomenon takes place, the Harmonic Balance method will give a higher value than that by the ANSYS® FEA, and a lower one than that predicted by solving the SDOF Duffing numerically by Newmark-Beta time-domain approach.

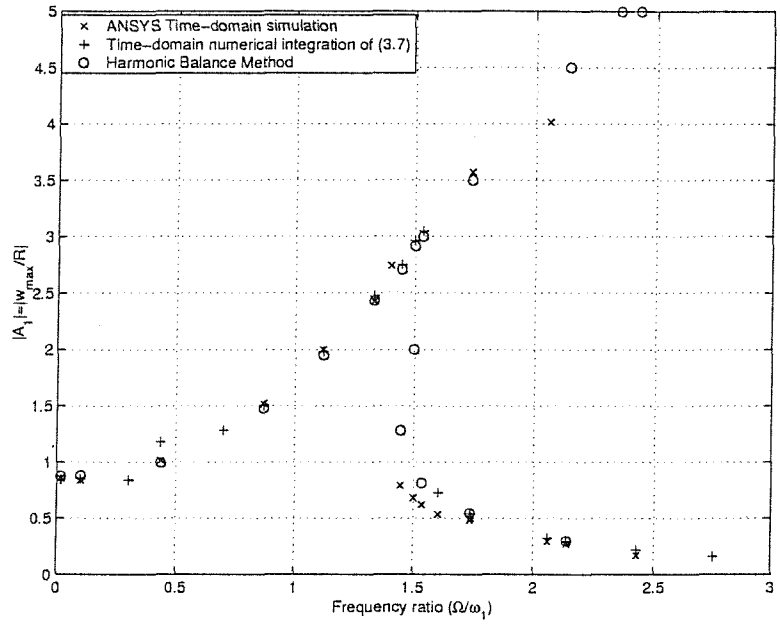

Figure 3.6: Comparison of Amplitudes $|A_1| = |w_{max}/R|$ at Selected Frequency Ratios by Different Solutions in the Concentrated Load Case, $\overline{F_{01}^c}$=1

Table 3.9 gives the difference in percentage between amplitudes given by the Newmark-Beta numerical integration method and by HBM, as well as that between amplitudes by ANSYS® and by HBM. It can be seen that, in general, the solutions by HBM agree better with those obtained by the numerical integration approach than with those by

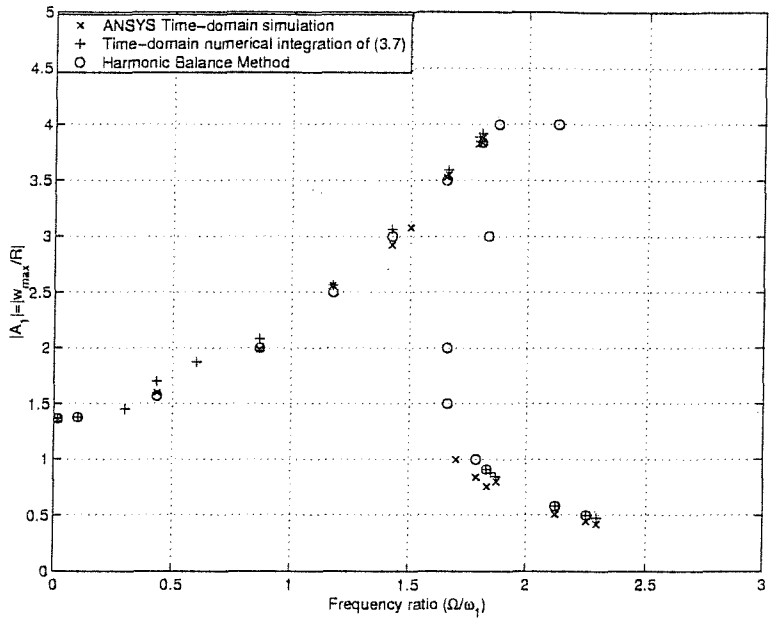

Figure 3.7: Comparison of Amplitudes $|A_1| = |w_{max}/R|$ at Selected Frequency Ratios by Different Solutions in the Distributed Load Case, $\overline{F_{01}^d}$=2

	Newmark-Beta time-domain	ANSYS® time domain simulation	Harmonic Balance Method
Point Force $\overline{F_{01}^c}$=1	$(\Omega/\omega_1) = 1.52$	$1.12 < (\Omega/\omega_1) < 1.32$	$(\Omega/\omega_1) = 1.44$
Distributed Load $\overline{F_{01}^d}$=2	$1.80 < (\Omega/\omega_1) < 1.83$	$1.43 < (\Omega/\omega_1) < 1.50$	$(\Omega/\omega_1) = 1.65$

Table 3.8: Frequency Ratio at which the "Jump Phenomenon" Occurs for the Three Analyses

ANSYS® simulation. This could be due to the fact that both the HBM and Newmark-Beta time-domain method solve the SDOF Duffing's equation whilst ANSYS® utilises the Finite Element Approach to model and solve the beam vibration problem. The damping which has to be employed in the ANSYS® analysis and the Newmark-Beta integration scheme to remove transient effects also affects the results when compared with the undamped solutions by HBM, especially near resonance.

3.2.5 Remarks on Mode-coupling in Non-linear Harmonic Vibrations

Finite Element Analysis by ANSYS® has been used to obtain the linear and non-linear responses subjected to harmonic excitation. The solutions are compared with those obtained by solving the Duffing's equation. Some of the solutions are compared and shown in the graphs in Figures 3.8 and 3.9 for different forcing conditions. The effects of non-linearity can indeed be identified from the diagrams. It can be seen that the effects of mode-coupling are not significant in the cases under investigation. This is deduced by the closeness between the numerical time-domain solutions of the SDOF Duffing's equation and the ANSYS® non-linear solutions which takes into account of all the responding modes. This implies that the effect of the resonances of the third and of subsequent modes are very small compared to that of the first mode. This finding, without any surprise, has widely been accepted for weakly non-linear systems.

However, it has to be borne in mind that for forcing frequencies close to the natural resonance, the response is very dependent on the amount of damping applied. Although no damping is considered in the analytical model, some damping has to be introduced when running the time-domain integration analysis in order to remove the "transients".

Figure 3.10 shows the frequency response curves for the first two symmetric modes (first and third) in the concentrated loading case, obtained using the Harmonic Balance Method and an iterative scheme (Appendices A.1.1 and A.2). Solutions obtained by ANSYS® non-linear time-domain analysis are also presented at selected frequency ratios (Ω/ω_1). It can be seen that the total response is indeed affected by resonances of both the

(Ω/ω_1)	Time domain Newmark-Beta, c (%)	Time domain simulation, c (ANSYS®) (%)	(Ω/ω_1)	Time domain Newmark-Beta, d (%)	Time domain simulation, d (ANSYS®) (%)
0.0152	3.15	2.14	0.0155	5.22	5.99
0.0967	3.41	4.58	0.4330	8.39	1.95
0.4243	15.9	1.95	0.8660	4.00	0.7093
0.856	2.00	0.156	1.1713	2.40	2.40
1.0957	1.69	6.48	1.4216	2.20	2.60
1.3035	1.69	0.173	1.5	2.15	2.88
1.4162	1.68	1.26	1.6583	2.12	0.893
1.5716	0.137	26.8	1.7854	1.13	0.553
1.7005	0.147	23.6	1.8314	0.209	7.64
1.7033	0.148	23.9	1.8718	0.0593	5.19
2.0203	0.153	21.6	2.1213	0.0859	13.2
2.096	0.135	21.6	2.2465	0.120	10.8
2.3778	0.140	22.0	2.2894	0.0630	13.6
2.6987	0.126	22.2	3.0020	0.120	4.00

Table 3.9: Percentage Differences of Response Amplitudes A_1 for Selected Frequency Ratios between HBM Model and Time-domain Simulations, c =concentrated load, d= distributed load (from Tables 3.6 and 3.7)

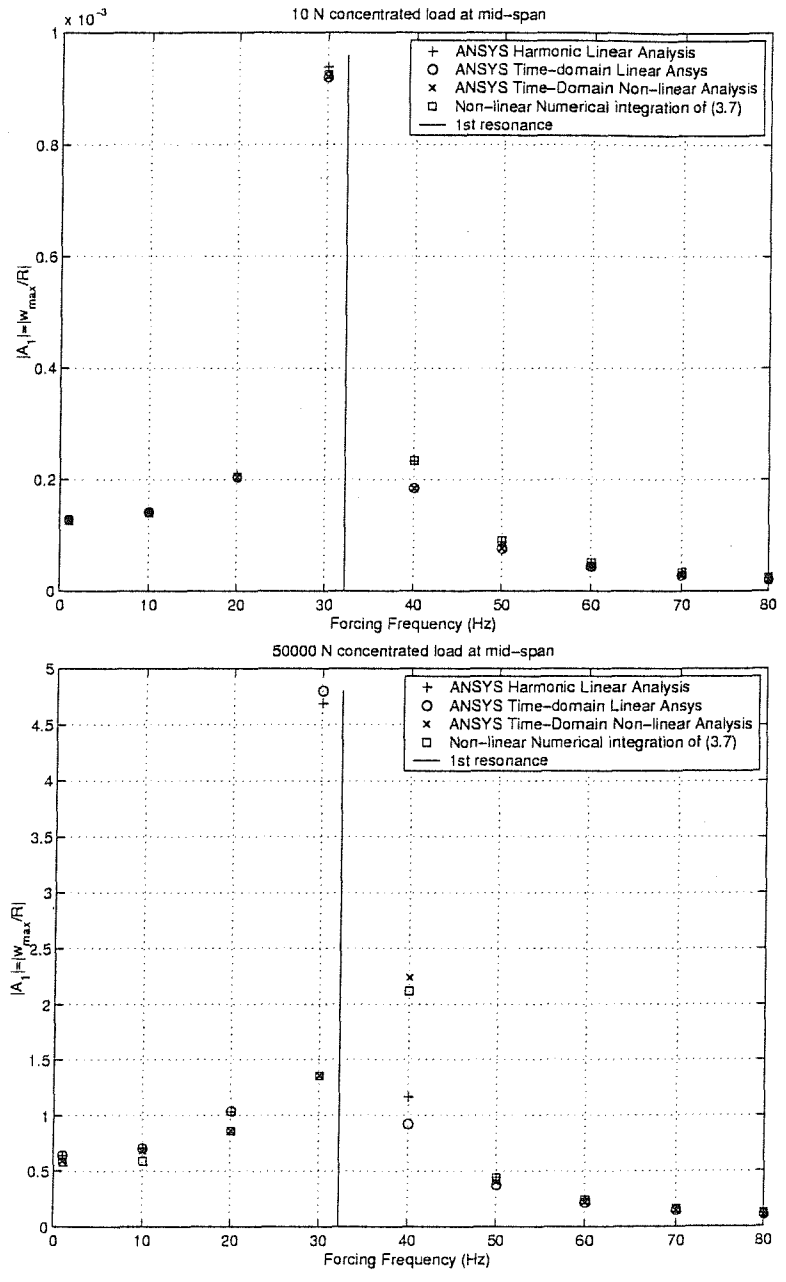

Figure 3.8: Non-linear Displacement Response at Selected Forcing Frequencies to Harmonic Concentrated Loads

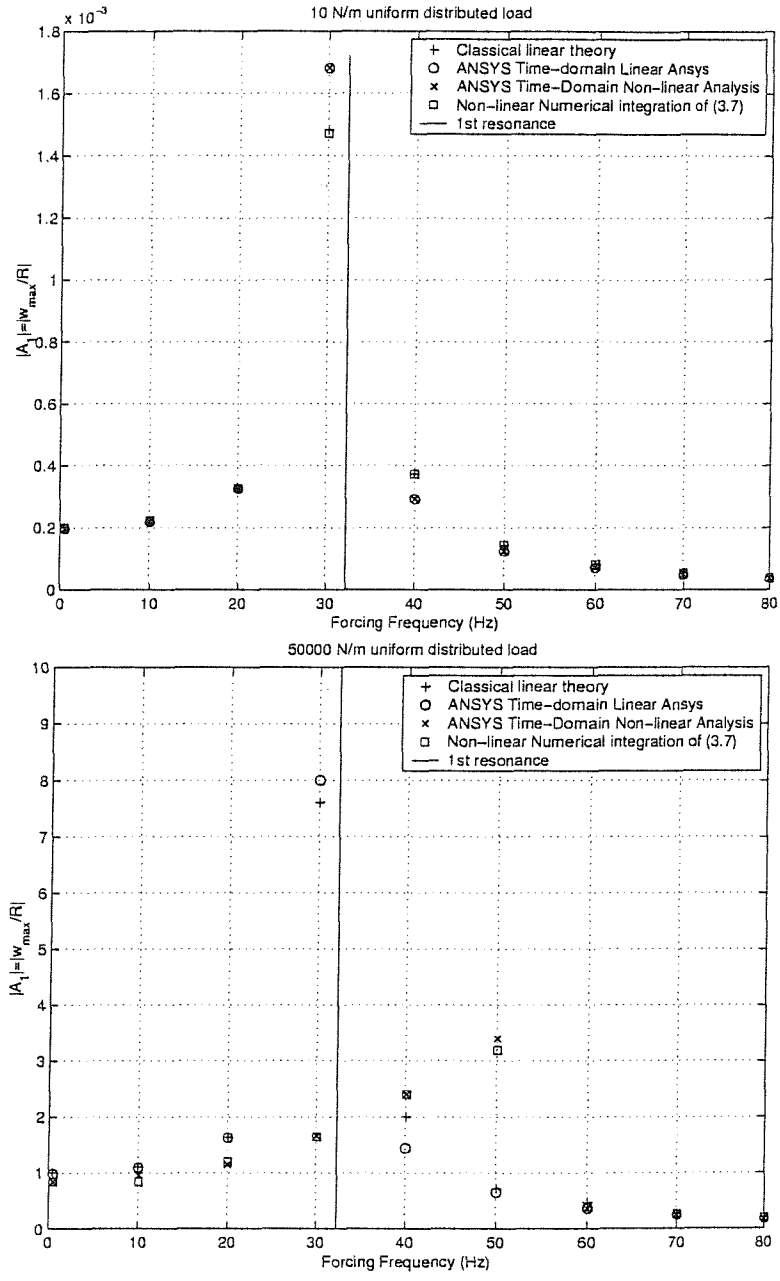

Figure 3.9: Non-linear Displacement Response at Selected Forcing Frequencies to Harmonic Uniformly Distributed Loads

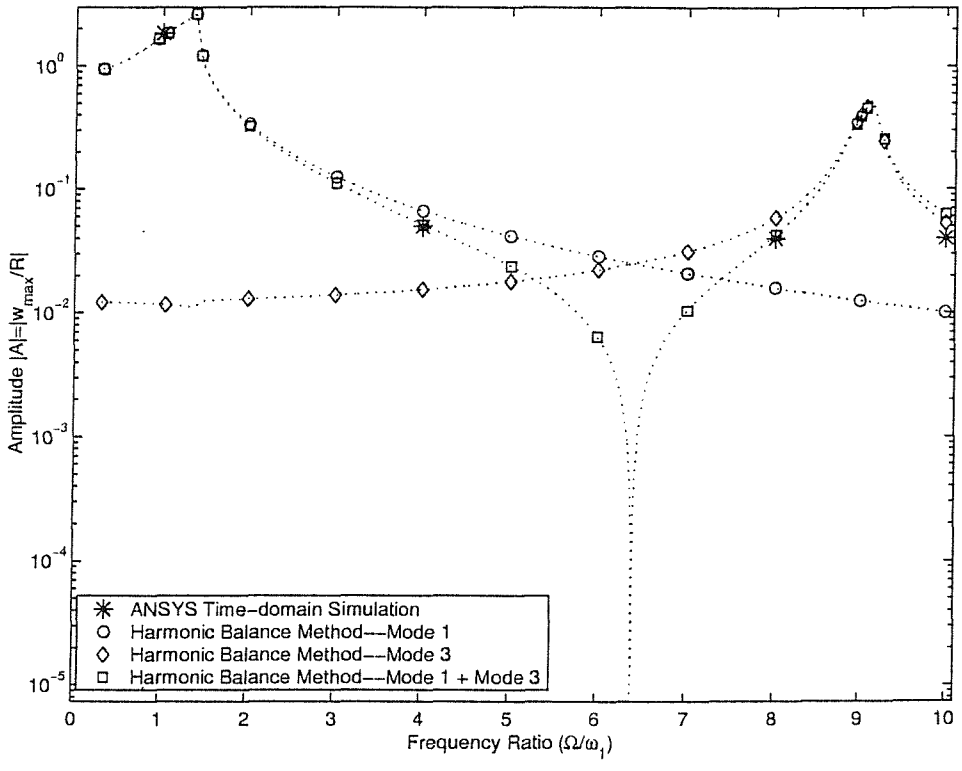

Figure 3.10: Frequency Response of the First and Third Coupled Modes for a Simply-supported Beam with Immovable End Conditions by Harmonic Balance Method, with Results by ANSYS® at Selected Frequency Ratios ($\overline{F_{01}^c}$=1)

first and the third modes, and the results agree well with ANSYS® solutions. Moreover, the total coupled response (mode 1 + mode 3) reveals that the first mode is dominant when the forcing frequencies are near to the first natural frequency. This agrees with previous findings obtained by the time-domain numerical methods. However, the total response is dominated by the third mode when the forcing frequencies are close to the third natural frequency.

It can be deduced that the uncoupled equations can give good approximations to the total response of the beam when the forcing frequencies are near to the natural frequency. In other words, when Ω is near to ω_1, the uncoupled SDOF Duffing's equation including only the first mode (equation (3.7)) can be used. When Ω is near to ω_3, the corresponding SDOF Duffing's equation including only the third mode can be employed. However, for Ω which is between the resonances of the two modes, e.g. $5 < \Omega/\omega_1 < 7$ in Figure 3.10, the equations including coupling of the modes should be used in order to obtain a valid overall response.

3.3 Chapter Summary and Conclusions

Non-linear transverse displacement response of a simply-supported beam with immovable end conditions when subjected to a harmonically varying excitation has been calculated using a linearisation technique called the Harmonic Balance Method. Two cases have been studied, a concentrated load at mid-span and a uniformly distributed pressure across the span.

Published results utilising several other approaches, namely the elliptical solutions, the perturbation solutions and the solutions by a Finite Element Method (F.E.M.) formulation [98] which has included the effects of longitudinal deformation and longitudinal inertia, are compared with solutions by the present harmonic balance method. All but the F.E.M. solutions [98] are based on the single-mode Duffing's equation (3.7). The solutions have also been obtained by the numerical integration of the single-mode Duffing's equation. Simulation of the vibration problem using the ANSYS® time-domain Finite Element Analysis has also been carried out. The harmonic balance solutions have

been compared with both the ANSYS® Finite Element solutions and solutions by the numerical integration of the single-mode Duffing's equation.

The closeness of the HBM response to the time-domain numerical-integration response implies that the linearisation technique in harmonic balance does give good approximation to the solution of the Duffing's equation.

The difference between the solutions based on the Duffing's equation and the ANSYS® ones may be explained by the fact that ANSYS® analysis does not solve the vibration problem based on the governing equation of motion (3.1), with the negligence of the longitudinal and rotary inertia. The ANSYS® Finite Element Approach simulates the entire beam when subjected to the prescribed excitation, thus taking into account of all the physical characteristics of the beam. Nevertheless, when comparing the two time-domain solutions, their closeness to each other indicates that equation (2.13) is an acceptable representation of the beam-vibration problem under investigation.

Finally, in the case of a simply-supported beam with immovable end conditions subjected to a symmetric loading with forcing frequencies lower than and well away from the third response mode, the non-linear response is predominantly due to the first resonance, and mode-coupling effects on the dominant first mode due to responses by subsequent modes are insignificant. As a result, the single-degree-of-freedom Duffing's equation is a good model to study the geometrically non-linear deflections of a simply-supported beam.

Chapter 4

RANDOM VIBRATIONS OF NON-LINEAR BEAM

In aerospace applications, excitation by jet or rocket engine noise and convected turbulence flow ought to be treated by probabilistic methods. The structures in the vicinity of jet or rocket engine exhaust are excited dynamically by acoustic pressure. The unfavourable outcome of this excitation are acoustic fatigue and possible damage or malfunction of operating electronic equipment placed on the excited structure.

4.1 Damped Large-deflection Beam Equations

When there is no axial prestressing, the governing equation of motion of an axially restrained beam subjected to transverse vibration, where large deflections are accounted for, has been presented in Chapter 2 by equation (2.13) which is replicated here.

$$EI\frac{\partial^4 w}{\partial x^4} - \left[\frac{EA}{2l}\int_0^l \left(\frac{\partial w}{\partial x}\right)^2 dx\right]\frac{\partial^2 w}{\partial x^2} + \mu\frac{\partial^2 w}{\partial t^2} + \beta\frac{\partial w}{\partial t} = f(x,t)$$

This forth-order partial differential equation can be represented by a set of second-order ordinary differential equations with cubic non-linearity, in the form of equation (2.24) which is restated here:

$$\frac{d^2u_m}{dt^2} + \xi_m \frac{du_m}{dt} + \omega_m^2 u_m + \Gamma_m = \frac{f(t)}{G_m} = F_{0m}(t)$$

The symbols in the equations have been defined previously in Chapter 2. Moreover in equation (2.24), the damping coefficient ξ_m is related to the damping factor ζ by the expression $\zeta = \xi_m/2\omega_m$. The damping factor is the ratio of the actual damping to the critical damping [7].

4.2 Response to Non-linear Random Excitation

4.2.1 Solution Based upon the Equivalent Linearisation Technique

When the excitation is a stationary and ergodic random function of time, and has a zero mean, an approximation to find the solution of equation (2.24), called the Direct Equivalent Linearisation Technique [29, 76] can be used. The approximated solution will also be stationary and ergodic. Moreover, it will be assumed that only the displacement term, Γ_m, is non-linear.

Equation (2.24) is a set of non-linear coupled equations and represents a multiple-degree-of-freedom non-linear system of the form

$$\overline{g}\left(\ddot{\vec{u}}, \dot{\vec{u}}, \vec{u}\right) = \vec{F}(t) \tag{4.1}$$

where $\vec{u}$ is the generalised displacement vector, $\overline{g}_i\left(\ddot{\vec{u}}, \dot{\vec{u}}, \vec{u}\right)$ is the total internal force acting in the i-th degree-of-freedom direction and $\vec{F}(t)$ is the stationary Gaussian random excitation vector, with zero mean.

It will be assumed that a stationary Gaussian solution to (4.1) exists.

Replace equation (2.24) by a linearised second-order ordinary differential equation:

$$\frac{d^2u_m}{dt^2} + \xi_m \frac{du_m}{dt} + k_m^2 u_m = \frac{f(t)}{G_m} = F_{0m}(t) \tag{4.2}$$

where k_m is the equivalent linear natural angular frequency, and defining the following set of linear equations

$$\overline{M}\ddot{\vec{u}} + \overline{C}\dot{\vec{u}} + \overline{K}\vec{u} = \vec{F}(t) \tag{4.3}$$

where the matrices $\overline{M}, \overline{C}$ and $\overline{K}$ are arbitrary mass, damping and stiffness matrices to be determined such that the solution of (4.3) will give an approximate solution to (4.1). Since the non-linear equation (4.1) has been replaced by the linear equation (4.3), there will be an error which can be written as

$$\overline{e} = \overline{g}\left(\ddot{\vec{u}}, \dot{\vec{u}}, \vec{u}\right) - \overline{M}\ddot{\vec{u}} + \overline{C}\dot{\vec{u}} + \overline{K}\vec{u} \tag{4.4}$$

The criterion to obtain a good approximation is that the mean-square value of the error is a minimum. The necessary conditions will be

$$\overline{m}_{ij} = E\left[\frac{\partial g_i\left(\ddot{\vec{u}},\dot{\vec{u}},\vec{u}\right)}{\partial \ddot{\vec{u}}_j}\right]$$

$$\overline{c}_{ij} = E\left[\frac{\partial g_i\left(\ddot{\vec{u}},\dot{\vec{u}},\vec{u}\right)}{\partial \dot{\vec{u}}_j}\right]$$

$$\overline{\kappa}_{ij} = E\left[\frac{\partial g_i\left(\ddot{\vec{u}},\dot{\vec{u}},\vec{u}\right)}{\partial \vec{u}_j}\right] \tag{4.5}$$

$E[\ldots]$ represents the expectation operator. Applying equation (4.5) on (2.24), provided that,

$$\overline{m}_{mj} = \begin{cases} 1 & \text{if } m = j; \\ 0 & \text{if } m \neq j. \end{cases}$$

$$\bar{c}_{mj} = \begin{cases} \xi_m & \text{if } m = j; \\ 0 & \text{if } m \neq j. \end{cases}$$

$$\bar{\kappa}_{mj} = E\left[\frac{\partial}{\partial u_j}(\omega_m^2 u_j + \Gamma_m)\right] = E\left[\frac{\partial \omega_m^2 u_j}{\partial u_j}\right] + E\left[\frac{\partial \Gamma_m}{\partial u_j}\right] \tag{4.6}$$

for $m, n, p, q, j = 1, 2, 3, \ldots$.

$$\bar{\kappa}_{mj} = \omega_m^2 \delta_{mj} + E\left[\frac{EAR^2}{2lM_m}\frac{\partial}{\partial u_j}\left(\sum_{n,p,q=1}^{\infty} K_{mn}K_{pq}u_n u_p u_q\right)\right]$$

$$\bar{\kappa}_{mj} = \omega_m^2 \delta_{mj} + \frac{EAR^2}{2lM_m}\left(\sum_{n,p,q=1}^{\infty} E\left[\frac{\partial K_{mn}K_{pq}u_n u_p u_q}{\partial u_{j=n}}\right]\right) +$$

$$\frac{EAR^2}{2lM_m}\left(\sum_{n,p,q=1}^{\infty} E\left[\frac{\partial K_{mn}K_{pq}u_n u_p u_q}{\partial u_{j=p}}\right]\right) + \frac{EAR^2}{2lM_m}\left(\sum_{n,p,q=1}^{\infty} E\left[\frac{\partial K_{mn}K_{pq}u_n u_p u_q}{\partial u_{j=q}}\right]\right)$$

$$\bar{\kappa}_{mj} = \omega_m^2 \delta_{mj} + \frac{EAR^2}{\mu l^2}\left(\sum_{p,q=1}^{\infty} K_{mj}K_{pq}E[u_p u_q] + 2\sum_{n,p=1}^{\infty} K_{mn}K_{pj}E[u_n u_p]\right) \tag{4.7}$$

The Kronecker delta $\delta_{mj} = 1$ for $m = j$, otherwise, $\delta_{mj} = 0$.

Since $K_{mn} = 0$ when $m \neq n$, $K_{pq} = 0$ when $p \neq q$ and $K_{pj} = 0$ when $p \neq j$,

$$\bar{\kappa}_{mj} = \omega_m^2 \delta_{mj} + \frac{EAR^2}{\mu l^2}\left(\sum_{p=1}^{\infty} K_{mj}K_{pp}E[u_p^2] + 2K_{mm}K_{jj}E[u_m u_j]\right) \tag{4.8}$$

The linearised equations have modal coupling as the term $E[u_m u_j] \neq 0$. This term will become zero when $E[u_m]$ and $E[u_j]$ are statistically independent from each other.

4.2.2 Random Vibrations: Uniform Acoustic Pressure

In the response of linear systems, there is generally low modal overlapping. Hence, the mass, damping and stiffness matrices are completely uncoupled. In the following analysis, the non-linear response is assumed to have low modal overlapping as well. In consequence, equation (4.3) is completely uncoupled in the mass, damping and stiffness matrices.

Let the beam be subjected to an acoustic pressure. The load is a stationary band-limited white-noise random pressure with zero mean and has a deterministic spatial distribution which is uniformly distributed across the span. Therefore, the spectral density function is independent of the forcing frequency and can be denoted by the magnitude, S_0. The mean square response of each mode can thus be expressed in terms of the spectral density function $S_f(\Omega)$ of the random load $f(t)$,

$$E[u_m^2] = \int_0^\infty S_f(\Omega)|H_m(\Omega)|^2\, d\Omega \simeq \frac{\pi S_f(k_m)}{4G_m^2\xi_m k_m^2} = \frac{\pi S_0}{4G_m^2\xi_m k_m^2} = \sigma_{um}^2 \tag{4.9}$$

If k_m is replaced by ω_m, equation (4.9) represents the m-th mode linear mean square response. The frequency response function, $H_m(\Omega)$, is given by

$$H_m(\Omega) = \frac{1}{G_m(k_m^2 - \Omega^2 + i\Omega\xi_m)} \tag{4.10}$$

With $m = j$, equation(4.8) becomes

$$\overline{\kappa_{mm}} = \omega_m^2 + \frac{EAR^2}{\mu l^2}\left(\sum_{p=1}^{N} K_{mm}K_{pp}E\left[u_p^2\right] + 2K_{mm}K_{mm}E\left[u_m^2\right]\right) \tag{4.11}$$

Here, as the distribution is uniform, even modes are not excited, i.e. p = odd. For the case where $m = 1$,

$$\overline{\kappa}_{11} = \omega_1^2 + \tfrac{EAR^2}{\mu l^2}\left\{K_{11}K_{11}E\left[u_1^2\right] + K_{11}K_{33}E\left[u_3^2\right] + \ldots + K_{11}K_{NN}E[u_N^2] + 2K_{11}^2E[u_1^2]\right\}$$

$$\overline{\kappa}_{11} = \omega_1^2 + \frac{\omega_1^2}{4}\left(3E\left[u_1^2\right] + 9\left[u_3^2\right] + \ldots + N^2\left[u_N^2\right]\right) \tag{4.12}$$

Denoting $k_1^2 = \overline{\kappa}_{11}$, the mean square displacement, σ_{u1}^2, is thus given by:

$$\sigma_{u1}^2 = E\left[u_1^2\right] = \frac{\pi S_0}{4G_1^2\xi_1 k_1^2} \tag{4.13}$$

Substituting equation (4.12) into equation (4.13) and tidying up give the following polynomial in terms of the variance σ_{u1}^2,

$$\frac{3}{4}(\sigma_{u1}^2)^2 + \left[1 + \frac{1}{4}\left(9\sigma_{u3}^2 + 25\sigma_{u5}^2 + \ldots + N^2\sigma_{nN}^2\right)\right]\sigma_{u1}^2 - S_{1o} = 0 \tag{4.14}$$

where $S_{1o} = \pi S_0/(4G_1^2\xi_1\omega_1^2)$.

In the same manner, as shown for the first mode, the mean square deflection for subsequent modes can be determined by the general format in equation (4.15).

$$\frac{3}{4}m^4\left(\sigma_{um}^2\right)^2 + m^4\sigma_{um}^2 + \frac{m^2}{4}\sum_{N=1,2,3,\ldots,N\neq m}^{\infty} N^2\sigma_{uN}^2 - S_m = 0 \tag{4.15}$$

where,

$$S_m = \frac{\pi S_0}{4G_m^2\xi_m\omega_1^2} \quad m = \text{mode number.}$$

Since there is coupling in the coefficients of the polynomial, the mean square deflections have to be solved for by using an iterative method. First the quadratic equations (in σ_{um}^2) are solved for σ_{um}^2 by neglecting the coupling in the coefficients. These values are used as the starting values for subsequent iterations. The iteration process is completed when a convergence criterion is met. Convergence is considered achieved for each mode, whenever $|[(\sigma_{um})_i - (\sigma_{um})_{i-1}]/(\sigma_{um})_i| \leq 10^{-5}$, where i is the iteration number.

The total mean square deflection can be expressed as:

$$\sigma_w^2(x,t) = R\sum_{m=1}^{\infty}\Phi_m^2(x)\sigma_{um}^2(t) \tag{4.16}$$

If only the first mode is considered, $m = 1$, the single-mode Duffing's equation can be derived from equation (2.24) and is given in equation (4.17).

$$\frac{d^2u_1}{dt^2} + \xi_1\frac{du_1}{dt} + \omega_1^2 u + \Pi_{1111}u_1^3 = \frac{f(t)}{G_1} = F_{01}(t) \tag{4.17}$$

The equivalent linear natural frequency can be derived from equation (4.8) and is given by:

$$k_1 = \sqrt{\omega_1^2 + 3\Pi_{1111}\sigma_{u1}^2} \tag{4.18}$$

Substituting equation (4.18) into equation (4.13), the non-linear mean square displacement for the first mode can be obtained and is given by:

$$\sigma_{u1}^2 = \frac{\sqrt{1 + 12\frac{\Pi_{1111}}{\omega_1^2}\sigma_{u01}^2} - 1}{6\frac{\Pi_{1111}}{\omega_1^2}} \tag{4.19}$$

where σ_{u01}^2 is the corresponding linear mean square displacement response of the first mode.

4.2.3 A Particular Example: S-S Beam with Immovable End Conditions

An isotropic beam which is rectangular in cross section is used in this example. Its properties are shown in Table 4.1. A uniformly distributed pressure as described in section 4.2.2 is applied on the beam with immovable simply-supported end conditions. Figure 4.1 should be referred to. The beam is subjected to five overall sound pressure levels (SPL) of 60, 70, 80, 90, 100, 110, 120 and 130 dB (Ref. $2 \times 10^{-5}\ N/m^2$). The corrected sound spectrum level, SSL is related to the SPL by the expression $SPL = SSL - 10\log(DW)$, where DW is a finite bandwidth and is equal to 250 Hz. Only linear structural damping will be considered.

As loading is symmetrically applied and the beam is simply supported, all even-numbered modes do not respond. Moreover, only the first mode will be included in the study.

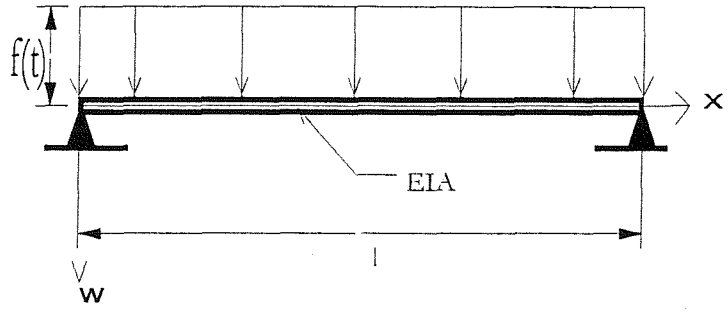

Figure 4.1: Simply-supported Beam with Immovable End Conditions Subjected to Uniformly Random Loading

Young's modulus E	70.395 GPa	Length of beam l	0.3048 m
Beam thickness h	0.001626 m	Width of beam b	0.0508 m
Density of beam ρ	2765.7606 kg/m^3	Damping factor $\zeta = \xi_1/2\omega_1$	0.01

Table 4.1: Dimensions and material properties of beam used in section 4.2.3

Here, $\Phi_1(x) = \sin\frac{\pi x}{l}$, hence the root-mean-square (r.m.s.) displacement response $\sigma_w(x,t)$ is:

$$\sigma_w(x,t) = R\sigma_{u_1}(t)\sin\frac{\pi x}{l} \tag{4.20}$$

For this loading condition,

$$G_1 = \frac{\pi R\mu}{4} \tag{4.21}$$

To relate the specified SSL in dB with spectral density function $S_f(\Omega)$, equation (4.22) can be used, provided that $\Omega_l \leqslant \Omega \leqslant \Omega_u$, where Ω_l and Ω_u is the lower and upper cut-off frequencies respectively [92, 101, 102]. S_f is zero for all values of Ω outside this range.

$$p^2_{r.m.s.} = p^2_{ref}10^{(\frac{SSL}{10})} = S_f(\Omega)\triangle\Omega \tag{4.22}$$

Here, p_{ref} is the pressure corresponding to the "zero" noise level, i.e., $SSL = 0$ dB. It is usually assumed that $p_{ref} = 2\times10^{-5}N/m^2$. The resulting r.m.s. pressure, $p_{r.m.s.}$ is simply the square root of the value $S_f(\Omega)\cdot\Delta\Omega$. Readers should seek further details from reference [101].

The linear and non-linear r.m.s deflections due to the response of the first mode will be obtained. The equivalent linear natural frequencies and the mean square displacement can be obtained from equations (4.18) and (4.19). The response spectrum of the displacement σ_{u1} is given by

$$S_{u1}(\Omega) = S_f(\Omega)\cdot|H_1(\Omega)|^2 = \frac{S_f(\Omega)}{G_1^2|(k_1^2-\Omega)+i\Omega\xi_1|^2} \tag{4.23}$$

4.2.4 Numerical Results and Discussions

It is possible to obtain non-linear solutions in virtually all cases by the step-by-step time-domain Monte-Carlo numerical integration scheme, provided that the nature of

the excitation and the equations of motion are known. It is therefore generally accepted to consider the solutions by the Monte-Carlo numerical scheme to be the benchmark when assessing the accuracy of solutions obtained by approximate analytical methods.

In order to assess both the accuracy and the efficiency of using the Direct Equivalent Linearisation as an approximation method, the analytical linear and non-linear solutions of random beam vibrations by this linearisation method have been compared with solutions obtained by the time-domain Monte-Carlo numerical method. Both the analytical and numerical approaches are based on solving the SDOF non-linear Duffing's equation.

As the input random load is a uniformly distributed band-limited stationary and Gaussian white noise, the technique of Inverse Fast Fourier Transform can be adopted to simulate it in the time domain. The procedures can be found in Appendix C.2.

The random input loads were simulated using parameters shown below in Table 4.2. Figure 4.2 shows time history of a 90 dB input pressure.

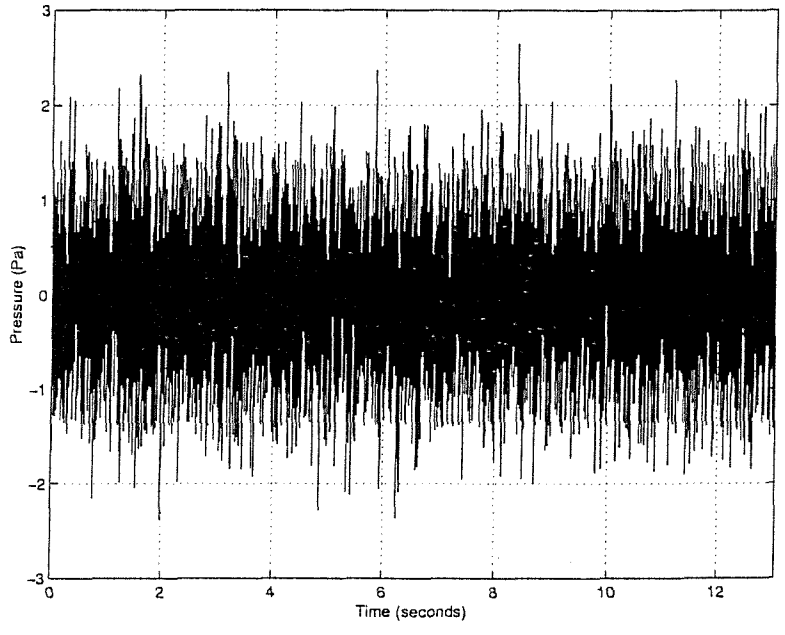

Figure 4.2: Time history of input pressure $SPL = 90dB$

The modal frequencies of the simply-supported beam are $\omega_1 = 251.57rad/s$ (40.04 Hz) and $\omega_3 = 2264.15rad/s$ (360.52Hz) . The frequency bandwidth of the input has

Overall SPL (dB)	90
Selected frequency bandwidth DW (Hz)	250 (1 to 251)
Input SSL (dB)	66.02
PSD $S_f(Pa^2/Hz)$	1.6×10^{-3}
Area under spectrum density graph (Pa^2), [I]	0.40012
Calculated r.m.s. pressure $prms(Pa)$, [II]	0.63245
Number of simulated points, M	262144
Frequency sampling interval $dw(Hz)$	0.07660
Length of Time history (s)	13.0550
Time interval (s)	4.9801×10^{-5}
Mean square value of simulated pressure (Pa^2), [III]	0.40003
R.M.S. value of simulated pressure (Pa), [IV]	0.63248
% difference between [I] and [III]	0.02
% difference between [II] and [IV]	0.005

Table 4.2: Parameters for one digital simulation of white noise

been chosen so as not to excite the third mode. Once the white-noise excitation has been simulated, the displacement response of the beam can be obtained in the time domain. This correspond to the centre of the beam, i.e., $x/l = 0.5$ This has been done by a step-by-step numerical analysis of the SDOF Duffing's equation (4.17)

For linear numerical analysis, the cubic non-linear coefficient Π_{1111} is set to equal zero. The Newmark-Beta time integration method [99, 100] is used. For non-linear analysis, the Newton-Ralphson method is used in conjunction with the Newmark-Beta method [99, 100]. To check convergence, the response is obtained with a certain time-step. Then the size of the time-step is halved and the response is obtained. Convergence of the solution is attained when the resulting response time-histories do not vary with further decrease of time-step size.

The displacement response time histories have been developed from the random input pressure. The time histories of the non-linear displacement responses for excitations of 70 dB, 90 dB, 110 dB and 130 dB are shown in Figure 4.3 and Figure 4.4. The numerical values of the steady-state r.m.s. solutions by different methods in the linear and non-linear cases are presented in Table 4.3. Note that the first 1.0 second has been omitted in retrieving these r.m.s. values as only steady-state solutions are required.

In reference to Table 4.4, the parameter F1 shows that the use of only one single mode can give excellent predictions in the linear case, which is a well-known fact. Parameter F2 indicates that the time-domain Newmark-Beta scheme has successfully been implemented to evaluate the r.m.s. value of the 1st mode displacement response in the linear case. It validates the accuracy of the time-domain solutions when compared to the frequency-domain solutions in the linear case.

In Table 4.4, parameter F3 gives the ratio of the non-linear r.m.s. response given by the Equivalent Linearisation to the corresponding linear r.m.s response. As the excitation magnitude increase, the value of F3 decreases. For the case of 60 dB, non-linearity effects are not expected to be severe, and the non-linear system should behave like a linear system. Non-linearity effects becomes quite significant as the excitation increases to 90 dB. At 130 dB, the non-linear r.m.s. response is approximated to be only about 16 % of its predicted linear counterpart. A check using the numerical solutions is given by parameter F4.

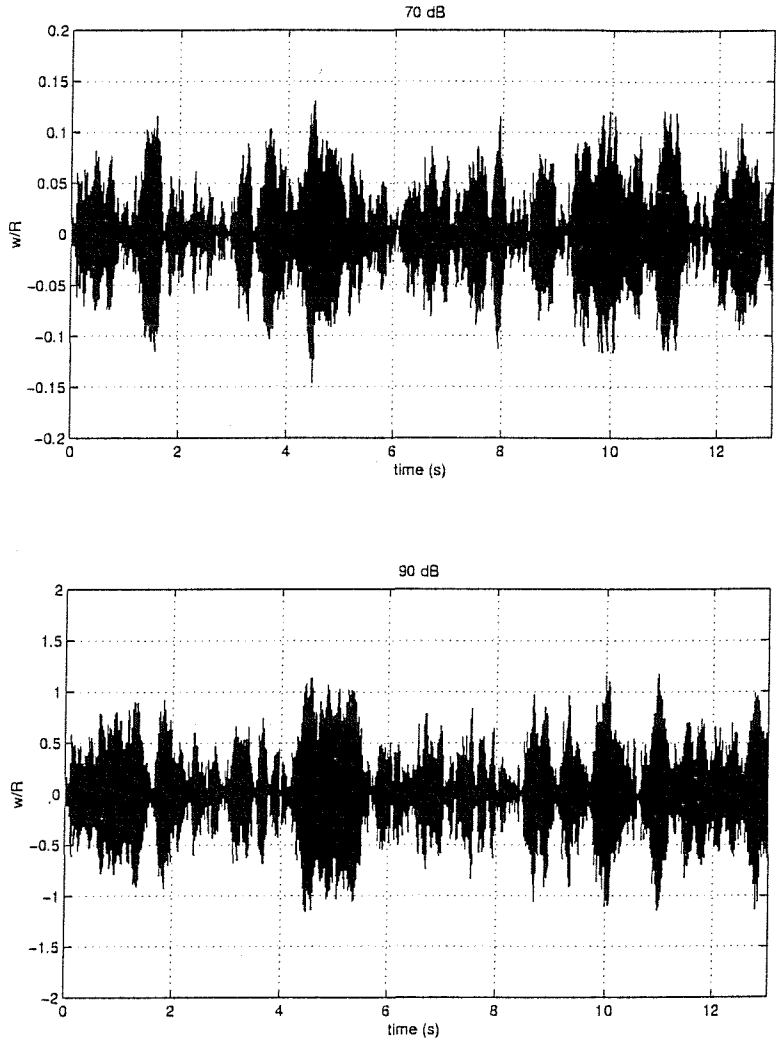

Figure 4.3: Non-linear Displacement Response Time Histories for overall sound pressure levels of $70dB$ and $90dB$ overall

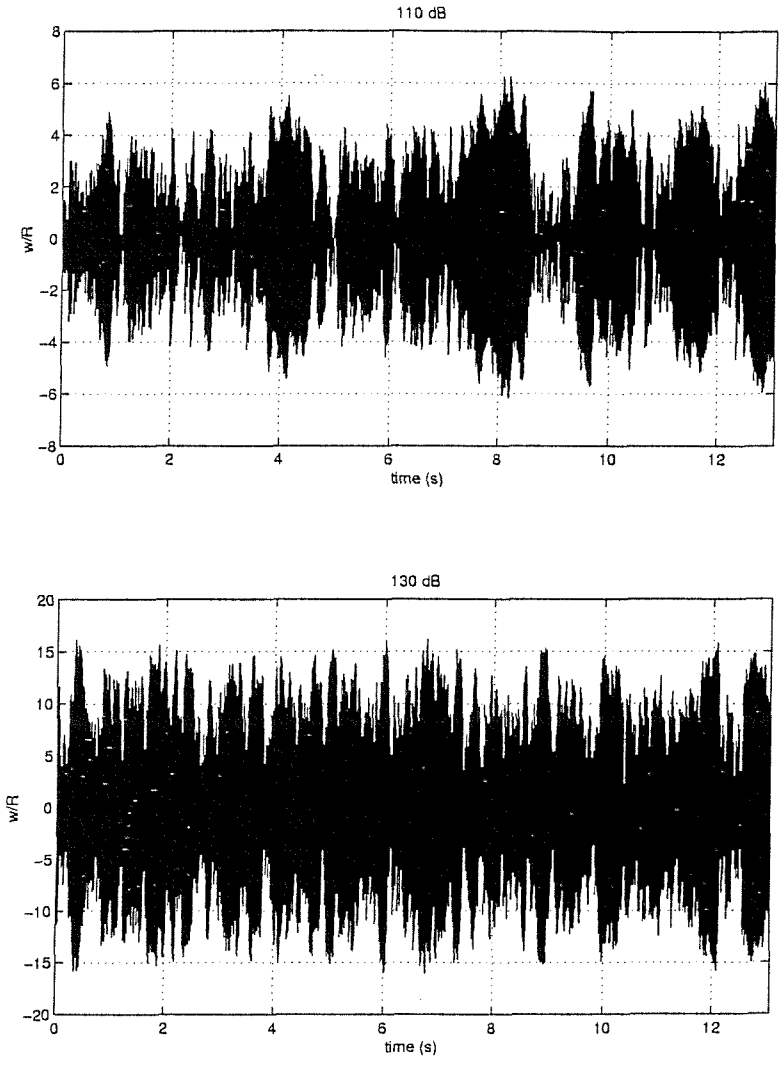

Figure 4.4: Non-linear Displacement Response Time Histories for overall sound pressure levels of $110dB$ and $130dB$ overall

SPL	LINEAR FRM (1 mode), [I]	LINEAR SA, [II]	LINEAR $N-\beta$ (1 mode), [III]	NON-LINEAR EL (1 mode), [IV]	NON-LINEAR $N-\beta$ (1 mode),[V]
60 dB	0.01331	0.01332	0.01330	0.01331	0.01330
70 dB	0.04208	0.04211	0.04205	0.04205	0.04198
80 dB	0.1331	0.1332	0.1330	0.1322	0.1327
90 dB	0.4208	0.4211	0.4205	0.3979	0.3848
100 dB	1.331	1.332	1.330	1.004	0.9577
110 dB	4.208	4.211	4.205	2.059	2.308
120 dB	13.31	13.32	13.30	3.836	3.969
130 dB	42.08	42.11	42.05	6.923	6.840

Table 4.3: Comparison of r.m.s w/R at eight selected SPL levels. FRM: Frequency Response Method; SA: ANSYS® "Spectrum analysis"; $N-\beta$: Newmark-Beta time-domain integration; EL: Direct Equivalent Linearisation

SPL (dB)	F1=% difference between [I] and[II]	F2=% difference between [I] and [III]	F3= [IV]/[I]	F4= [V]/[III]	F5= % difference between F3 and F4
60	0.08	0.08	0.9999	1.0	0.01
70	0.08	0.07	0.9993	0.9983	0.10
80	0.08	0.08	0.9935	0.9977	0.42
90	0.08	0.07	0.9455	0.9151	3.22
100	0.08	0.08	0.7546	0.7201	4.57
110	0.08	0.07	0.4892	0.5489	10.88
120	0.08	0.08	0.2882	0.2984	3.42
130	0.08	0.07	0.1645	0.1627	1.11

Table 4.4: Analysis of r.m.s. values of w/R presented in Table 4.3

By using parameter F5 to compare parameters F3 and F4, it can be shown how the technique of the Equivalent Linearisation performs in the approximation of non-linear response of the displacement. The Direct Equivalent Linearisation method would give good predictions for highly non-linear situations, when solving the SDOF Duffing's equation.

The fraction of the mean-square value of the non-linear response to that of the linear response, i.e., the squared values of parameter F5, are plotted for various input sound pressure levels in Figure 4.5.

It is shown that a single-mode solution is sufficient to provide reasonably accurate displacement responses.

Figures 4.6 to 4.9 show some snapshots of the time-domain displacement responses of the beam when the simulated white noises, with overall pressure levels of 70 dB, 90 dB, 110 dB and 130 dB respectively, act uniformly across the span. It can be confirmed again, by careful examination, that for a relatively weak loading (70 dB), the non-linear system basically behaves like a linear system, as the response oscillates with the

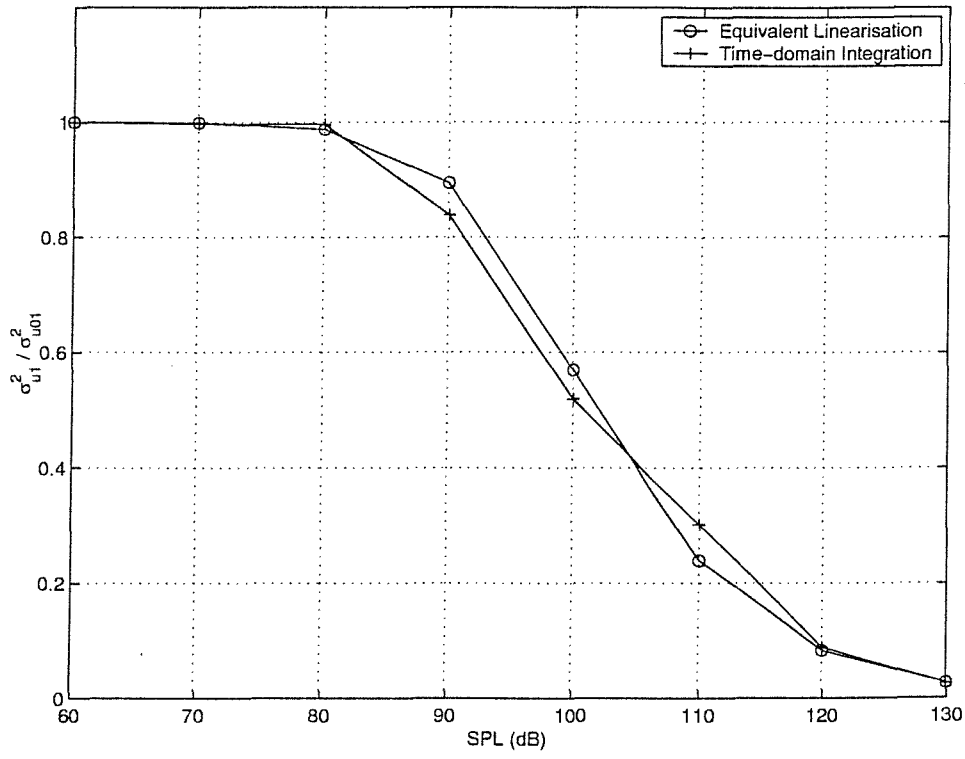

Figure 4.5: Fraction of Non-linear Mean-square Displacement Response (σ^2_{u1}) to Linear Mean-square Displacement Response (σ^2_{u01}) at Different SPLs

linear resonant frequency of the system. For a moderate level of excitation (90 dB), non-linearity effect becomes more apparent and the non-linear system starts to behave differently when compared to its linear counterpart. This can be seen by the fact that the response oscillates with a frequency different from the linear resonant frequency of the system. For a strong excitation (130 dB), the non-linear response time histories are completely different from the linear ones. Note that although Figures 4.6 to 4.9 share the same scale in the horizontal axis, the scales on the vertical axes are different to accommodate the different response magnitude.

The frequencies of oscillations in the non-linear response time histories can be retrieved from its frequency spectrum. The equivalent linearisation method calculates what is known as the "equivalent natural frequencies" which is the resonance frequencies of the equivalent linear differential equations (4.2). The first-mode resonance frequencies of the non-linear system at different sound pressure levels, are obtained by the equivalent linearisation solutions and from the frequency spectra of the time-domain displacement response. The fractions of the equivalent linear frequencies, k_1 to the fundamental linear frequencies, ω_1 are are reported in Figure 4.10. From this graph, it can be deduced that, unlike the linear case where the resonance frequency remains the same regardless of the change in the input excitation, the non-linear stiffness has the effect of shifting the resonance frequency to higher values as the level of sound pressure increases.

As non-linearity increases with the rising SPL level, the amount of the shift increases, together with the increase in the response. This phenomenon can be seen in Figures 4.11 and 4.12. The graphs compare the power spectral densities of the non-linear displacement response obtained by equivalent linearisation and from the time domain response time-histories. As it can also be seen from the charts in Figure 4.11, the frequency-response curves given by the time-domain integration solutions drop suddenly at 250 Hz, since this is the upper cut-off frequency of the band-limited white-noise excitation where its pressure spectral density drops to zero. However, this drop in power spectral density cannot be found in the response curves obtained by equivalent linearisation, described by equation (4.23), since the pressure spectral density is assumed to be constant at all frequencies in this case.

At higher excitation levels, the equivalent linearisation predicts that the frequency

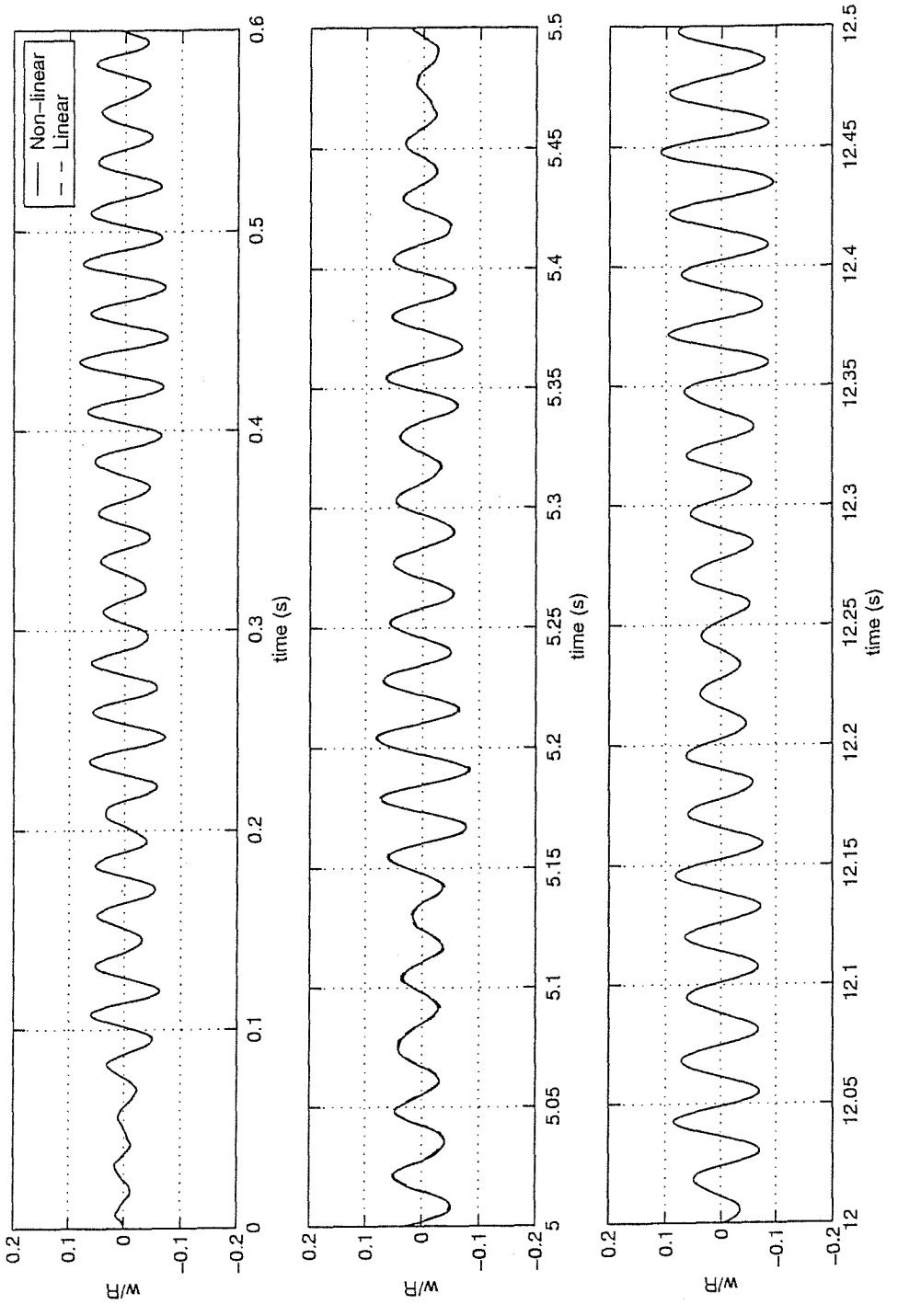

Figure 4.6: Snapshots of Response Time Histories at 70 dB overall

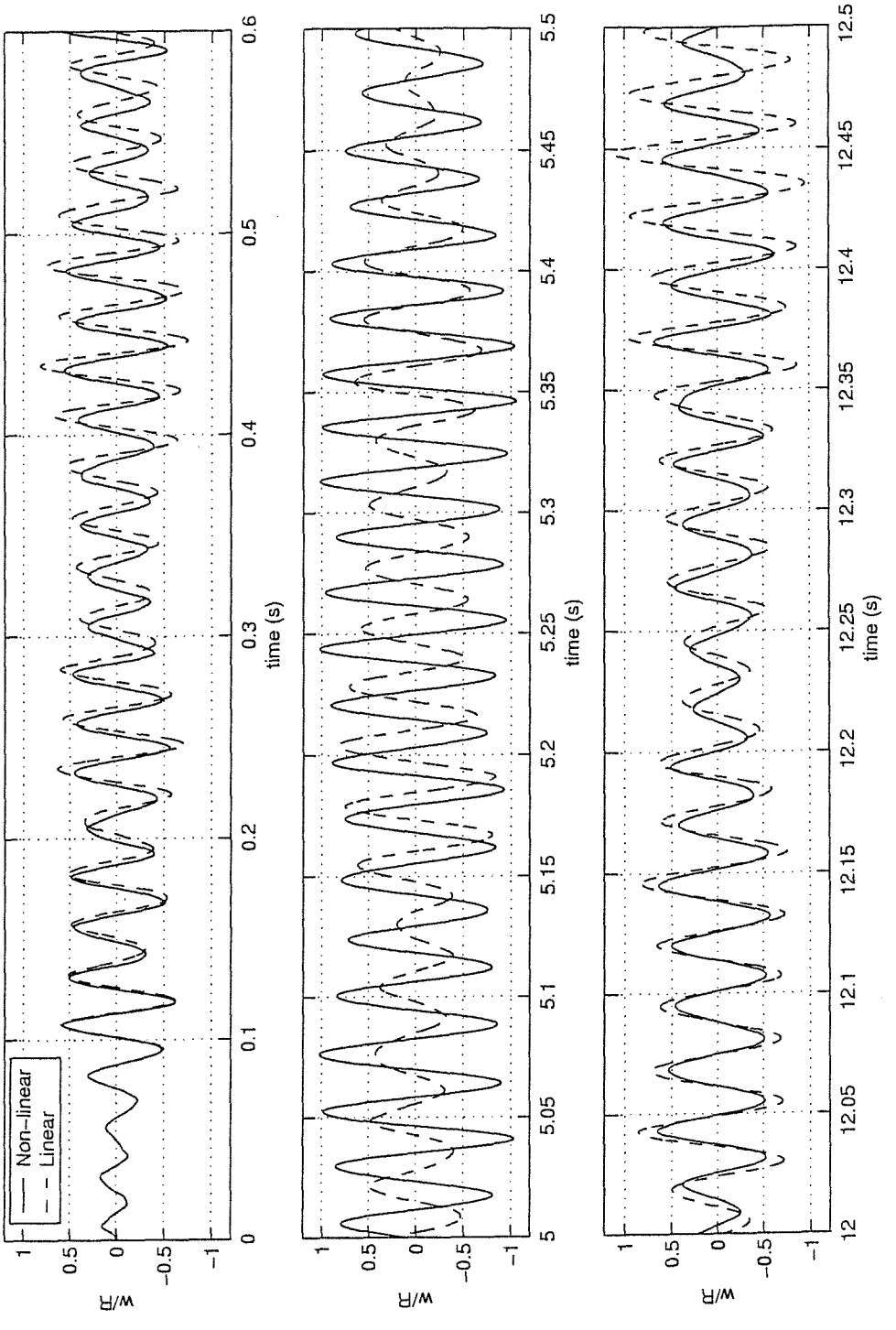

Figure 4.7: Snapshots of Response Time Histories at 90 dB overall

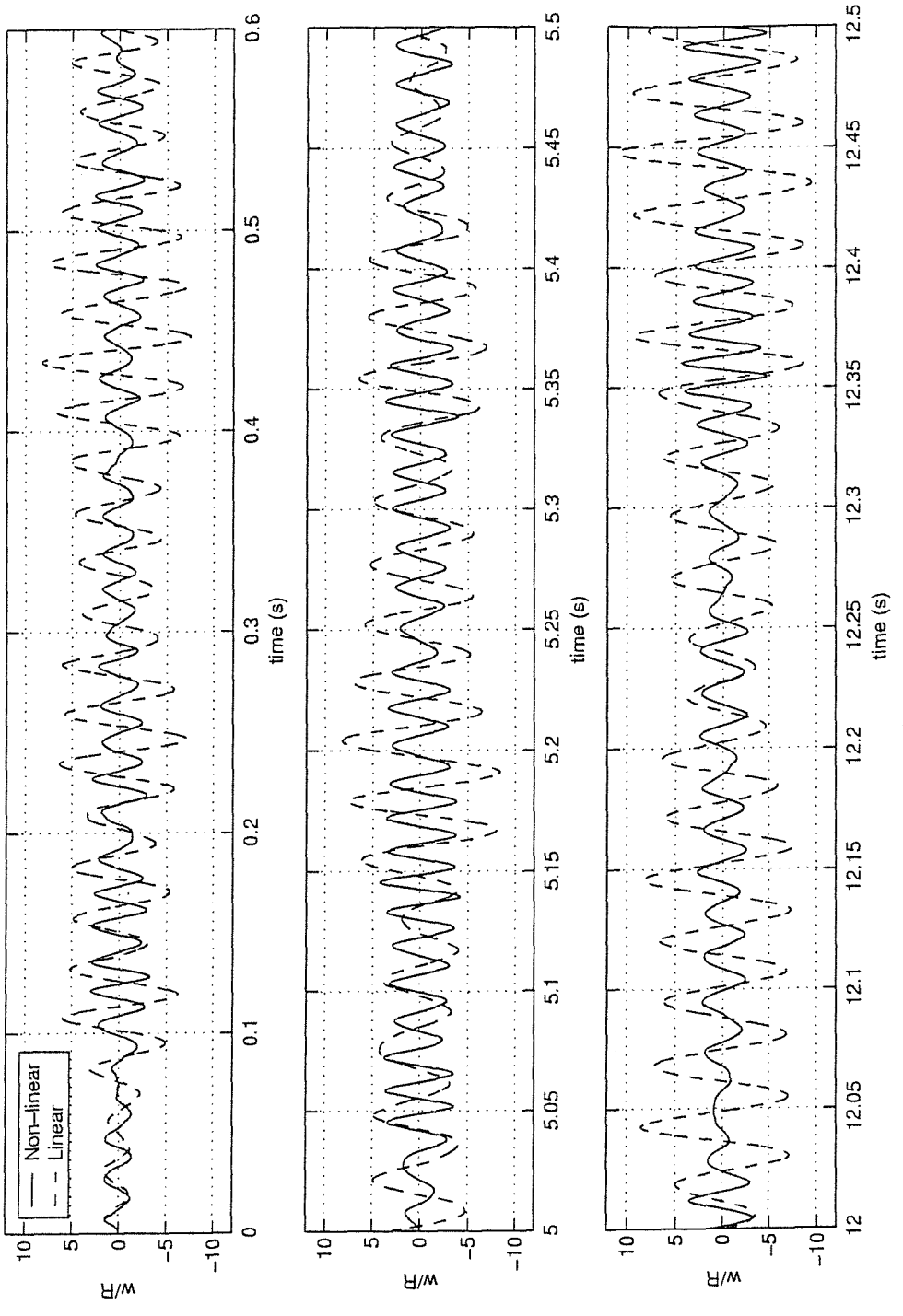

Figure 4.8: Snapshots of Response Time Histories at 110 dB overall

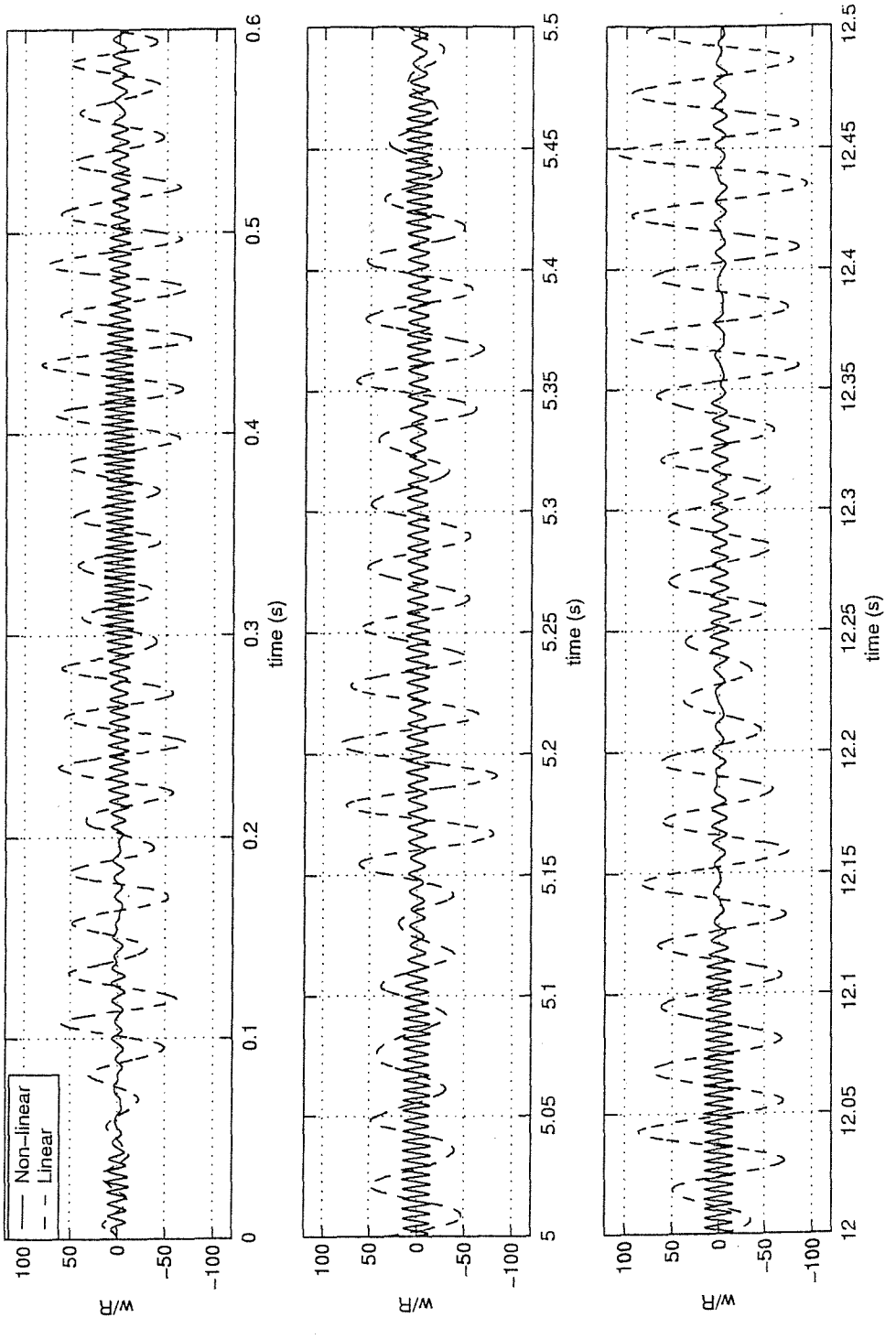

Figure 4.9: Snapshots of Response Time Histories at 130 dB overall

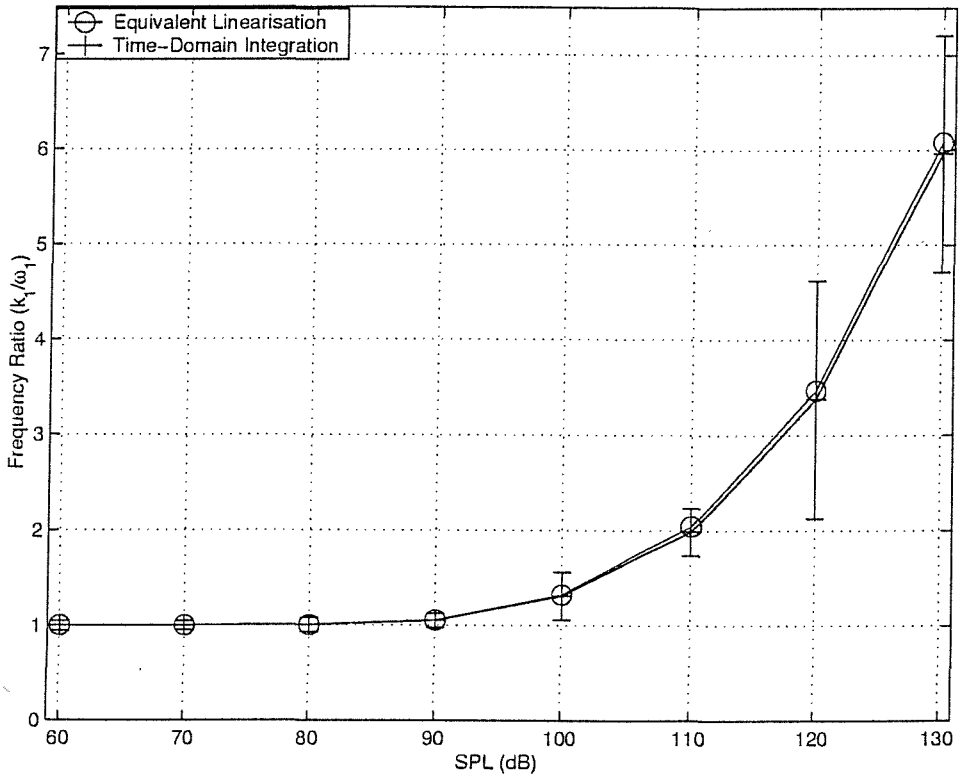

Figure 4.10: Fraction of Equivalent Linear Frequencies (k_1) to Fundamental Linear Frequencies (ω_1) at Different SPLs

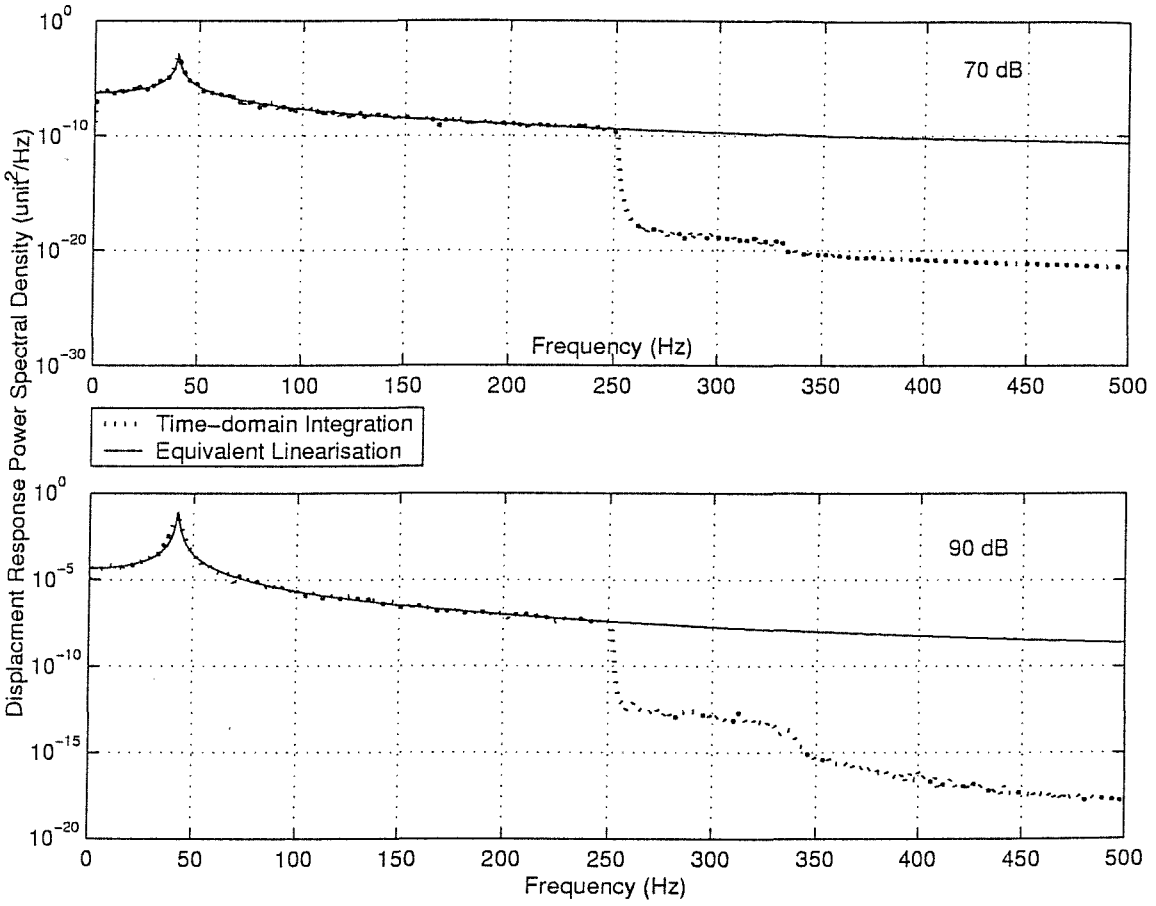

Figure 4.11: Response Power Spectral Density obtained by Equivalent Linearisation and from Random Response Time Histories: 70 dB and 90 dB

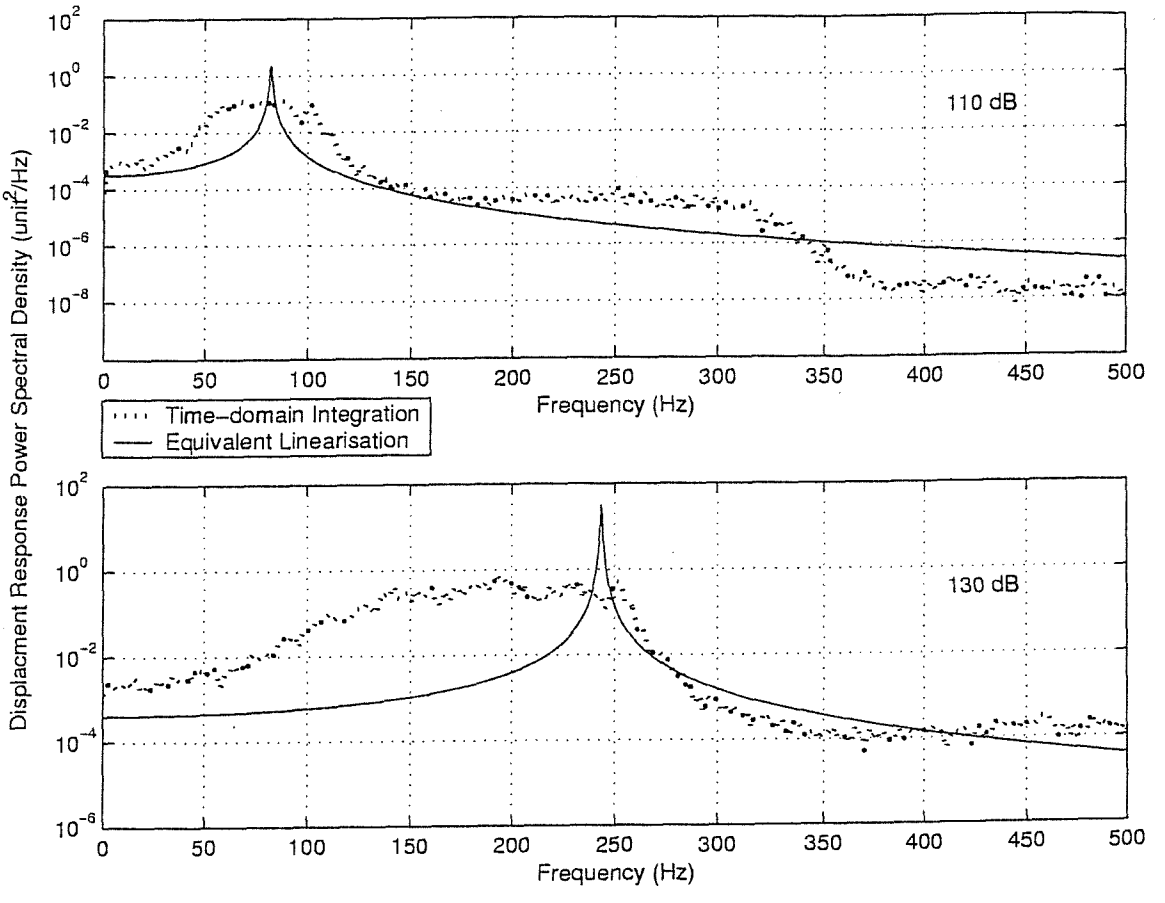

Figure 4.12: Response Power Spectral Density obtained by Equivalent Linearisation and from Random Response Time Histories: 110 dB and 130 dB

response of non-linear systems would have distinct peaks like those in linear systems. This contradicts to the time-domain integration results which show that sharp peak characteristics of linear vibrations are no longer evident. The characteristic distinct peaks merge into one broader peak which tends to flatten. As a result, the values of the equivalent linear frequencies obtained from the frequency spectrum of the time-domain displacement response are only approximations, and the range of uncertainty on where exactly the resonance peak occurs grows with increasing non-linearity. The graphs in Figures 4.11 and 4.12 clearly illustrate the phenomena.

For the time-domain integration results, a reason for the broadening of the resonance peak at highly non-linear regimes may be due to the leakage of energy. With small non-linearity, the energy of the response is concentrated at the natural frequency. As non-linearity increases dramatically to a high level, the energy concentration is distorted and energy starts to leak to the neighbouring frequency domain. Hence responses are being picked by the neighbourhood of the resonance, and a flat peak response is resulted.

Due to the different shape and character of the response spectra predicted by the two methods, different values would result in the prediction of resonance frequency of a structure when severely excited by random load.

4.3 Chapter Summary and Conclusion

In the vibrations of aircraft panels induced by jet noise, the major damage to the panels is known to occur during takeoff, when the jet engines are operated at maximum power. During the maximum engine power run, the generated acoustic pressure measured at a given point on the structure can be assumed to be a white noise which exhibits a weakly stationary pattern [92].

Based on the equations of motion developed from Chapter 2 for large deflections of simply-supported beam with immovable end conditions subjected to external load, the solution for the non-linear random response has been formulated by an approximate method called the Direct Equivalent Linearisation Technique. The loading type under

consideration is a uniformly distributed white noise excitation. For the special case of a uniformly distributed random surface pressure, the non-linear response solutions are known to be dominated by a single mode. Root-mean-square non-linear displacements at the mid-span have been obtained for a single-degree-of-freedom system. The results by equivalent linearisation have been compared with those obtained by numerical analysis. A good agreement of the root-mean-square response has been obtained between the Direct Equivalent Linearisation and the time-domain step-by-step numerical integration approach for severely exciting situations. Moreover, when the excitation is so large that the vibration problem becomes non-linear, non-linear stiffness shifts the resonance frequency to higher values. The amount of shift increases with the increase of non-linearity due to the rising sound spectrum level, and the peak of the resonance broadens.

The equivalent linearisation solutions have been able to demonstrate the characteristics of the non-linear r.m.s. displacement response predicted by the time-domain numerical solutions even at high levels of excitations. Hence, it is believed that the application of the Direct Equivalent Linearisation to a SDOF Duffing's equation to obtain the large-deflection displacement response of a simply-supported beam with immovable end conditions due to a uniformly distributed white noise can indeed give reasonably good results.

The non-linear response spectrum obtained by the Direct Equivalent Linearisation method predicts that the characteristic distinct peaks in linear vibrations would be retained in the non-linear system even at high excitation. This differs from the results obtained from the time-domain numerical integration solutions, in which the peaks in the spectrum are relatively flat. This has concern for the prediction of fatigue life of the structure. This is because for two responses having the same r.m.s. value but different response power spectral densities, their fatigue lives will be different.

Finally, it has been shown that classical linear theory of vibrations can be an over-conservative means to predict the random response of beam vibration. To obtain a more factual description of the non-linear beam response under intensive acoustic pressure, non-linear theory of vibrations should be employed.

Chapter 5

ASSESSMENT OF MODE-COUPLING EFFECTS IN NON-LINEAR BEAM VIBRATIONS

From previous studies in non-linear harmonic vibrations, it has been shown that the single-degree-of-freedom Duffing's equation is a good tool to describe the geometrically non-linear vibrations of simply-supported beams with immovable end conditions. It has also been shown that mode-coupling effects are insignificant when the external harmonic excitation is a uniformly distributed pressure or a symmetrically applied point load. In those cases, the spatial distribution of excitation has excited all odd-numbered modes of response, whilst the forcing frequencies have been chosen to excite mainly the first mode of response only.

However, the aerodynamic loading may excite the panel structure in such a way that typical frequencies of excitation caused by large-scale turbulence are close to some of the natural frequencies of the structure. At the same time the pressures over the

surface of the structure are spatially matched to the linear mode shapes of some other vibration responses of the structure. It is interesting to see which modes of response will prevail over the others. Blevins [5] has studied the multiple-mode response of panel-type structures subjected to surface pressures associated with sound and turbulence. However, the study was limited to the linear case.

In this chapter, the non-linear vibration of a simply-supported beam which has the properties given Table 4.1 is studied. The spatial distribution of the load and the frequency content to match and excite different modes of response. For example, the spatial distribution of the load has a shape which matches the first linear mode shape of the beam whilst the forcing frequency is equal to the third-mode natural frequency of the beam. Moreover, only non-linear responses to loads which are symmetrically applied across the beam are considered here. The damped two-degree-of-freedom (2DOF) Duffing's equations including the first two symmetric modes (1^{st} and 3^{rd}) will be employed to study the non-linear vibrations of simply-supported beams with immovable end conditions. By considering the 2DOF Duffing's equations with and without mode-coupling terms, the significance of the phenomenon of "coupling resonance" due to non-linear coupling is investigated in various loading conditions.

5.1 The Damped Two-degree-of-freedom Duffing's Equation under Symmetric Loads

With reference to equations (2.24 to 2.28), the non-linear coupled differential equations including the first and third modes can be expressed by equations (5.1) and (5.2) as:

$$\frac{d^2u_1}{dt^2} + \xi_1\frac{du_1}{dt} + \omega_1^2 u_1 + \Pi_{1111}u_1^3 + \Pi_{1133}u_1u_3^2 = \frac{f_1 f_1(t)}{G_1} = F_{01}(t) \tag{5.1}$$

$$\frac{d^2u_3}{dt^2} + \xi_3\frac{du_3}{dt} + \omega_3^2 u_3 + \Pi_{3333}u_3^3 + \Pi_{3311}u_3u_1^2 = \frac{f_3 f_3(t)}{G_3} = F_{03}(t) \tag{5.2}$$

In this work, these will be referred to as the 2DOF damped Duffing's equations with coupling. The coupling terms in these two simultaneous ordinary differential equations

are $\Pi_{1133}u_1u_3^2$ and $\Pi_{3311}u_3u_1^2$. By neglecting these coupling terms, the resulting equations (5.3, 5.4) in this work will be referred to as the 2DOF damped Duffing's equation without coupling.

$$\frac{d^2u_1}{dt^2} + \xi_1\frac{du_1}{dt} + \omega_1^2u_1 + \Pi_{1111}u_1^3 = \frac{f_1f_1(t)}{G_1} = F_{01}(t) \tag{5.3}$$

$$\frac{d^2u_3}{dt^2} + \xi_3\frac{du_3}{dt} + \omega_3^2u_3 + \Pi_{3333}u_3^3 = \frac{f_3f_3(t)}{G_3} = F_{03}(t) \tag{5.4}$$

5.2 Non-linear Response to Spatially and Temporally Harmonic Excitation

With a symmetrically distributed harmonic pressure acting across the span of the simply-supported beam with immovable end conditions, the mid-span displacement response time histories of the beam are obtained by the step-by-step time-domain numerical integration of the equations of motion (5.1, 5.2) and (5.3, 5.4), with the harmonic pressure simulated in the time domain. The results are observed and the steady-state solutions are retrieved by ommitting the first 1.0 second of the time history. Different types of harmonic pressure are studied and analysed. The cases under investigations are summarised in Figure 5.1.

5.2.1 Load Case 1: Pressure Distribution Matching One Particular Response Linear Mode Shape

In this case study, two scenarios will be looked at. In the first scenario, the external pressure which varies sinusoidally with time has a forcing frequency (Ω) which is equal to ω_3 whilst its spatial distribution is spatially matched to the first linear mode shape of the system, so that the generalised force in all other modes is zero. The pressure with this type of spatial distributed will be denoted by the symbol $P1$ and its amplitude

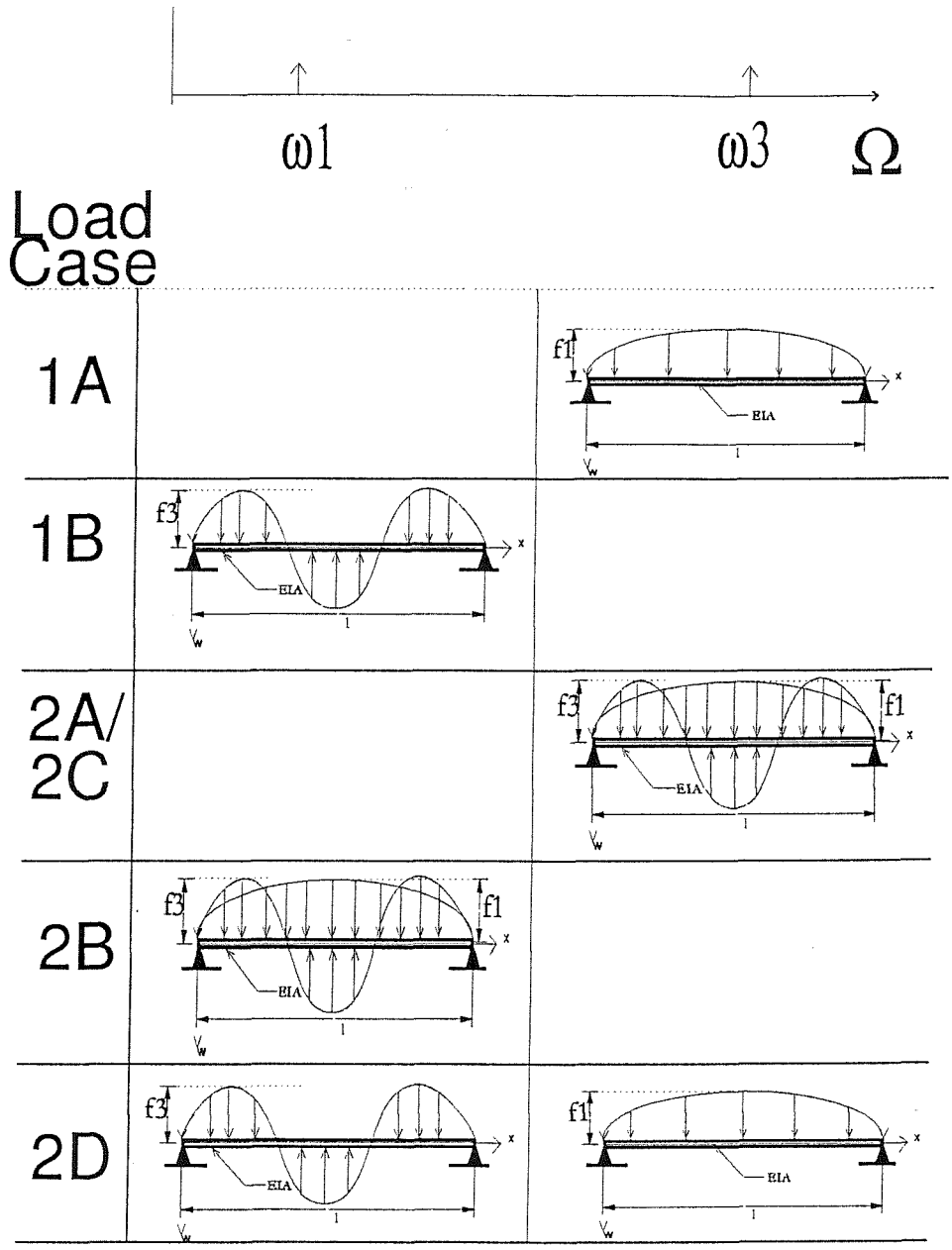

Figure 5.1: Simply-supported Beam with Immovable End Conditions Subjected to Different Types of Harmonic Pressure

by f_1. In the second scenario, the forcing frequency is set to equal the first natural frequency and the spatial distribution coincides with the linear mode shape of the third-mode response, so that the generalised force in all but the third mode is zero. The pressure with this type of spatial distributed will be denoted by the symbol $P3$ and its amplitude by f_3.

Load Case 1A: $\Omega = \omega_3$

The spatial distribution of the pressure matches exactly the function of the first-mode response in the space domain. However, the harmonic excitation has a forcing frequency equal to the natural frequency of the third mode of the system. In other words, the forcing function can be expressed in the form of $f_0 sin(\frac{\pi x}{l}) sin(\omega_3 t)$, where f_0 is the magnitude of excitation.

It can be deduced from equation (2.27) that F_{01} and F_{03} on the right-hand side of equations (5.1, 5.2, 5.3 and 5.4) are equal to $\frac{f_1}{R\mu} sin(\omega_3 t)$ and 0 respectively. The magnitude of excitation, $f_1 = 100Pa$, has been selected so that significant non-linearity should be present when the beam is excited. A graphical representation of the loading can be seen from Figure 5.2.

It is well-known, and thus expected, that when the mode-coupling terms in the coupled Duffing's equations are neglected in this type of excitation, the steady-state displacement response of the third mode will be zero. This is the result obtained when the uncoupled Duffing's equations (5.3) and (5.4) are solved.

Now, the coupled equations (5.1) and (5.2) are solved numerically with different initial conditions. Observations are made and the results are summarised in Table 5.1.

As expected, under this loading condition, the steady-state displacement response consists of only the contribution from the first mode, as seen in Table 5.1. For instance, the steady-state root-mean-square (r.m.s.) displacement responses ($u = w/R$) of the first and third modes with zero initial displacement and velocity at mid-span are 0.1317 and 0 respectively.

State	Initial Displacements	Initial Velocities	Behaviour of Displacement Response
I	$u_{1_0} = 0; u_{3_0} = 0$	$\dot{u}_{1_0} = 0; \dot{u}_{3_0} = 0$	1^{st} mode:Steady-state oscillates with frequency of ω_3; 3^{rd} mode: stays zero
II	$u_{1_0} = 0; u_{3_0} = 1$	$\dot{u}_{1_0} = 0; \dot{u}_{3_0} = 0$	1^{st} mode:Steady-state oscillates with frequency of ω_3; 3^{rd} mode: decays exponentially to zero.
III	$u_{1_0} = 0; u_{3_0} = 10$	$\dot{u}_{1_0} = 0; \dot{u}_{3_0} = 0$	As in State II
IV	$u_{1_0} = 0; u_{3_0} = 10$	$\dot{u}_{1_0} = 0; \dot{u}_{3_0} = 1$	As in State II
V	$u_{1_0} = 1; u_{3_0} = 1$	$\dot{u}_{1_0} = 1; \dot{u}_{3_0} = 1$	1^{st} mode: as in State I;3^{rd} mode: as in State II

Table 5.1: Effects of Mode-coupling and Initial Conditions on Behaviour of Non-linear Harmonic Response of a Simply-supported Beam with Immovable End Conditions (Load Case 1A)

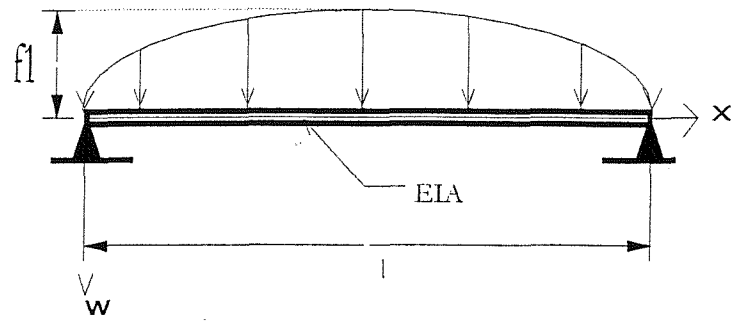

Figure 5.2: Simply-supported Beam with Immovable End Conditions Subjected to Excitation in Load Case 1A

Following the above study, it is reasonable to suggest that, in the case of a sinusoidal load with spatial distribution matching only the linear mode shape of the first mode and with forcing frequency equal to any other higher natural frequencies, the steady-state non-linear displacement response would have a shape equal to the linear mode shape of the first mode. Its frequency would equal to that of the applied load. The steady-state non-linear responses of any other modes would be zero.

It may also be deduced that if the spatial distribution of the pressure matched exactly the linear mode shape of the third resonance of the system, and that if the forcing frequency of the excitation were equal to the first natural frequency, only the third mode would respond in the steady-state condition. In fact, this second deduction can be confirmed by carrying out a similar analysis to that in Load Case 1A. This situation is investigated in Load Case 1B which follows in the next section.

Load Case 1B: $\Omega = \omega_1$

The right-hand side of equations (5.1) and (5.2) are now equal to 0 and $\frac{f_3}{R_\mu} sin(\omega_1 t)$ respectively, with $f_3 = 100Pa$. The loading can be represented in Figure 5.3.

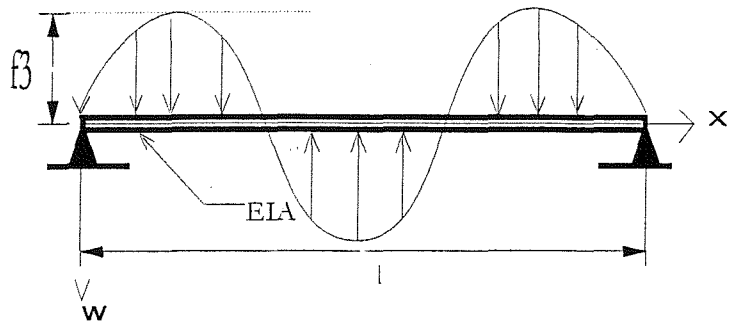

Figure 5.3: Simply-supported Beam with Immovable End Conditions Subjected to Excitation in Load Case 1B

The steady-state r.m.s. displacement responses ($u = w/R$) of the first and third modes with zero initial displacement and velocity at mid-span are 0 and 0.12952 respectively.

As a result, it can be concluded that the general behaviour of the coupled system is the same as the corresponding uncoupled system under the stated types of loading. In the presence of large excitation effecting non-linearity in the mode-coupled Duffing's equations, the unexcited modes do not respond under the influence of the excited mode due to the presence of the coupling terms. If the spatial distribution of the excitation just matches the linear mode shape of one particular resonance, only that mode will be excited and its steady-state response will oscillate at the forcing frequency of excitation.

5.2.2 Load Case 2: Pressure Distribution Matching The First and Third Linear Mode Shapes of The Beam

In this case, the pressure of the excitation will be modelled in such a way that it aims to excite both the first and third-mode responses of the system. The pressure can be

described by the forcing function $[f_1 sin(\frac{\pi x}{l}) + f_3 sin(\frac{3\pi x}{l})]sin(\Omega t)$, where f_1 and f_3 are magnitudes of excitation. A graphical interpretation of the loading is shown in Figure 5.4.

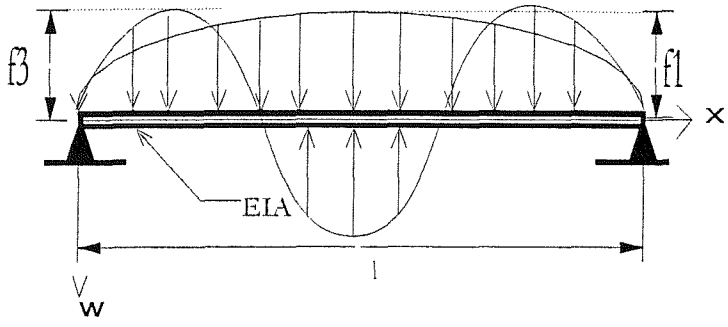

Figure 5.4: Simply-supported Beam with Immovable End Conditions with Load Case 2

Load Case 2A: $\Omega = \omega_3$; fixed f_1, varying f_3

In Load Case 1A, it was shown that the third mode of the beam had no response due to the absence of an excitation with pressure which matched only the third linear mode shape of the beam, $P3$. Hence an increasing amount of the pressure level of $P3$ ($f_3 = 1, 10, 100, 1000$ and $10000Pa$) is now introduced. The pressure of a fixed magnitude of $f_1 = 100Pa$ which only excited the first spatial response mode of the system in Load Case 1A, $P1$, is retained. Moreover, the two harmonic pressures, $P1$ and $P3$, oscillate in phase with each other at exactly the same forcing frequency ($\Omega = \omega_3$).

From equation (2.27), it can be shown that the terms F_{01} and F_{03} on the right-hand side of equations (5.1– 5.4) are now equal to $\frac{f_1}{R\mu} sin(\omega_3 t)$ and $\frac{f_3}{R\mu} sin(\omega_3 t)$ respectively.

The two sets of 2DOF equations (5.1, 5.2) and (5.3, 5.4) are solved numerically. The non-linear r.m.s. displacement responses at mid-span for values of $f_3/f_1 = 0.01, 0.1, 1, 10$

and 100, together with the percentage difference between the coupled responses and the uncoupled ones, are presented in Table 5.2. The results are expressed in the graphs in Figure 5.5. The first graph shows the steady-state non-linear r.m.s. displacement responses, and the second one reflects the difference between the coupled and uncoupled responses in percentage.

f_3/f_1	0.01	0.1	1.0	10	100
Uncoupled (u_1)[I]	0.1317	0.1317	0.1317	0.1317	0.1317
Uncoupled (u_3)[II]	0.06432	0.3134	0.6983	1.487	2.923
Uncoupled $(u_1 + u_3)$[III]	0.1452	0.2107	0.5694	1.358	2.812
Coupled (u_1)[IV]	0.1318	0.1321	0.1340	0.1441	0.2264
Coupled (u_3)[V]	0.06424	0.3116	0.6973	1.487	2.923
Coupled $(u_1 + u_3)$[VI]	0.1445	0.2087	0.5657	1.343	2.726
% Difference [I] and [IV]	0.08	0.30	1.7	9.4	72
% Difference [II] and [V]	0.12	0.57	0.14	0.00	0.00
% Difference [III] and [VI]	0.48	0.95	0.65	1.1	3.1

Table 5.2: Comparison of Coupled and Uncoupled Non-linear R.M.S. Displacement Responses $u = (w/R)$ for Selected Ratios of f_3/f_1 (Load Case 2A)

In both cases, the steady-state responses oscillates at the forcing frequency which is equal to the third-mode natural frequency, ω_3. Except for $f_3/f_1 = 0.01$ where the loading introduced to excite the third mode is small, the dominating response comes

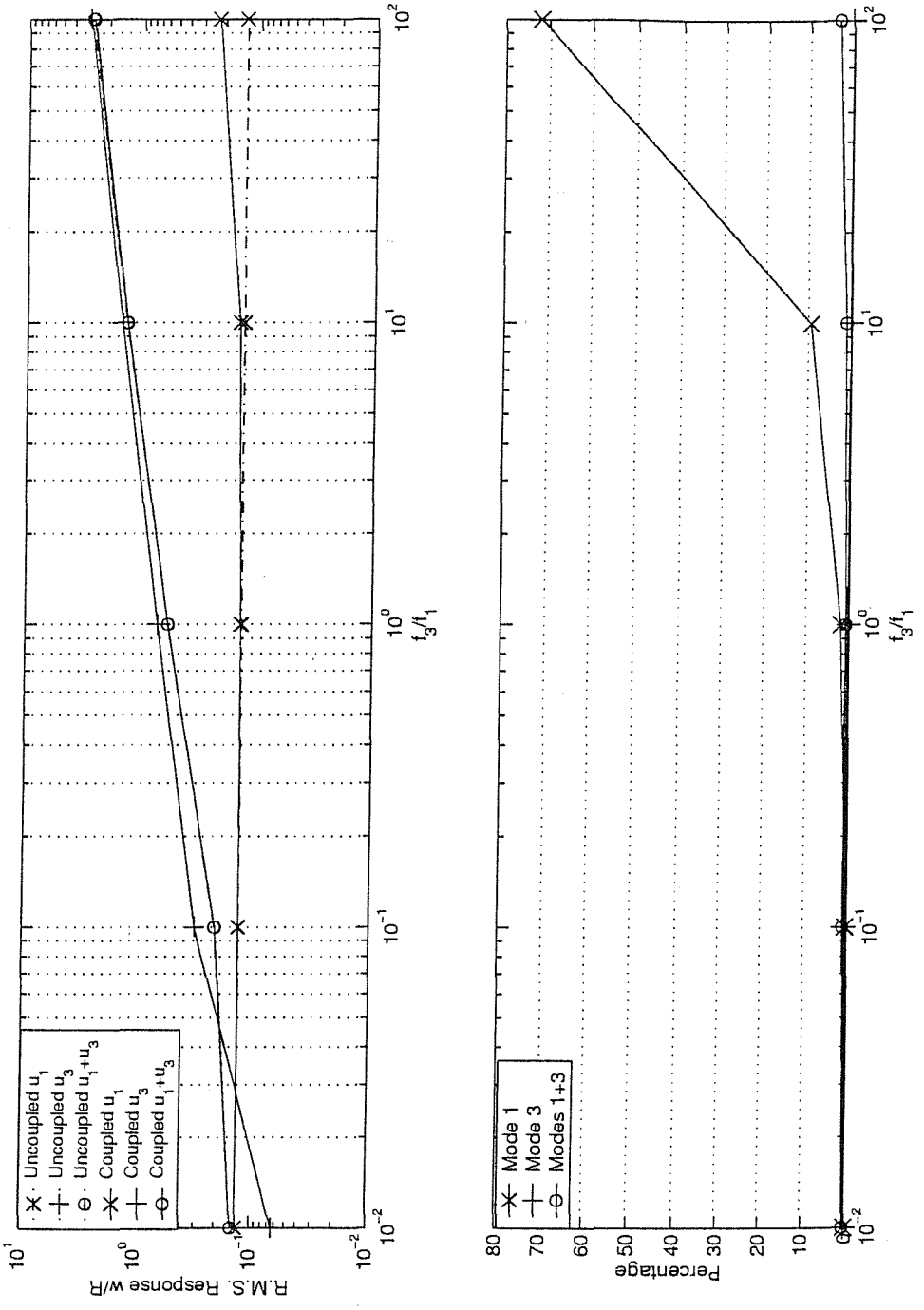

Figure 5.5: Non-linear Coupled and Uncoupled R.M.S. Displacement Responses and Percentage Differences of Coupled Response Relative to Uncoupled Responses at Selected f_3/f_1 (Load Case 2A).

from the contribution of the third-mode response.

In the case without mode-coupling, the r.m.s. values of u_1 remain the same regardless of the value of f_3. This is simply because the amplitude of the input loading into the first mode, f_1, remains constant. However, there is an increase in the r.m.s. value of u_3 due to the increase in the magnitude of the force into the third mode, f_3. As expected from previous studies in non-linear harmonic vibrations, the increase in u_3 is not linearly proportional to that in f_3.

When comparing the uncoupled first-mode response in this case and that in Load Case 1A, it is interesting to see that they are in fact identical. This confirms again that mode-coupling in the stiffness term in fact has no influence on the response of the unexcited modes in Load Case 1A.

With mode-coupling terms now included, an increase in f_3 causes both u_1 and u_3 to build up. The increase in coupled u_1 can be explained by examining the coupled terms in equations (5.1) and (5.2). As the third mode response is increasing with the input $P3$, the coupling term in equation (5.1) is more and more dominated by u_3. Hence the extra response adds to the original uncoupled first-mode response.

Furthermore, when comparing the r.m.s. responses with and without coupling, it can be seen that values of u_3 with coupling are always less than those without coupling. As when the third mode is dominant ($u_3 \gg u_1$), the coupled equation (5.2) can be viewed as a system which has got a higher stiffness ($\approx \omega_3^2 + \Pi_{3311}$) than has the uncoupled equation (5.4). This in turn explains why the third-mode-dominant total coupled responses ($u_1 + u_3$) are less than the uncoupled ones at all times.

By looking at the percentage difference between the coupled and uncoupled responses, it can be seen that the dominant response, i.e., the third mode, is quite unaffected by the presence of the first mode. However, as far as the subordinate first-mode response is concerned, it becomes progressively affected by the coupling of the third-mode response as u_3 is gaining increasing significance with increasing f_3/f_1, and the behaviour of the coupled equation (5.1) deviates from that of the uncoupled equation (5.3). The degree of overestimation in the resultant displacement by the uncoupled system when compared to the coupled one also increases with f_3/f_1. Nevertheless, as

stated again, since the resultant response mainly consists of the third-mode response, this percentage difference remains small.

In short, the response of the dominant mode is less affected than that of the subordinate mode by the coupling terms. These findings agree with those obtained in Chapter 3 when the excitation is a uniformly-distributed pressure where all odd-numbered modes are excited.

Results in Load Case 2A shows that mode-coupling does not play an important role. The most likely reason for this behaviour is the fact that the forcing frequency is above that of the resonating modes, i.e, the first mode. In this case, the response is mass-dominated, as opposed to stiffness-dominated when the forcing frequency is below the resonance frequency. It is suspected that as mode-coupling arises from the stiffness components of the system, its effect would be more significant when the excited system were stiffness-dominated. Hence, the forcing frequency is set to equal the natural frequency of the first mode, i.e., $\Omega = \omega_1$.

Load Case 2B: $\Omega = \omega_1$; fixed f_3, varying f_1

The beam is now excited so that the response is stiffness-dominated. Moreover, as seen in Load Case 1B, the first mode of the beam did not respond to the pressure which was not spatially matched to the first linear mode shape of the beam. Hence an increasing amount of pressure load of $f_1 = 1, 10, 100, 1000$ and $10000Pa$ is now added, of which the spatial distribution aims to excite specifically the first mode of the system. The pressure of a fixed magnitude of $f_3 = 100Pa$ which excited just the third mode of the system in Load Case 1B, $P3$, will remain to act on the beam. The pressures $P1$ and $P3$ oscillate in phase with each other at exactly the same forcing frequency $\Omega = \omega_1$. The procedure of the numerical analysis is repeated in a likewise manner as in Load Case 2A and the results are presented in Table 5.3 and Figure 5.6. The differences, in percentage, between the coupled displacement responses and the uncoupled responses are also included.

The r.m.s. value of the uncoupled u_3 stays the same for all ratios of f_1/f_3 whilst that of u_1 increases with f_1/f_3. The total uncoupled displacement response is dominated by

f_1/f_3	0.01	0.1	1.0	10	100
Uncoupled (u_1)[I]	0.64951	1.3887	2.7742	6.8348	14.578
Uncoupled (u_3)[II]	0.12952	0.12952	0.12952	0.12952	0.12952
Uncoupled $(u_1 + u_3)$[III]	0.77819	1.5181	2.8919	6.9458	14.692
Coupled (u_1)[IV]	0.57529	1.3589	2.7594	6.8855	14.547
Coupled (u_3)[V]	0.12780	0.12030	0.10166	0.078236	0.054380
Coupled $(u_1 + u_3)$[VI]	0.70208	1.4789	2.8428	6.9313	14.565
% Difference [I] and [IV]	11	2.2	0.53	0.74	0.21
% Difference [II] and [V]	1.3	7.1	21	40	58
% Difference [III] and [VI]	9.8	2.6	1.7	0.21	0.86

Table 5.3: Comparison of Coupled and Uncoupled Non-linear R.M.S. Displacement Responses $u = (w/R)$ for Selected Ratios of f_1/f_3 (Load Case 2B)

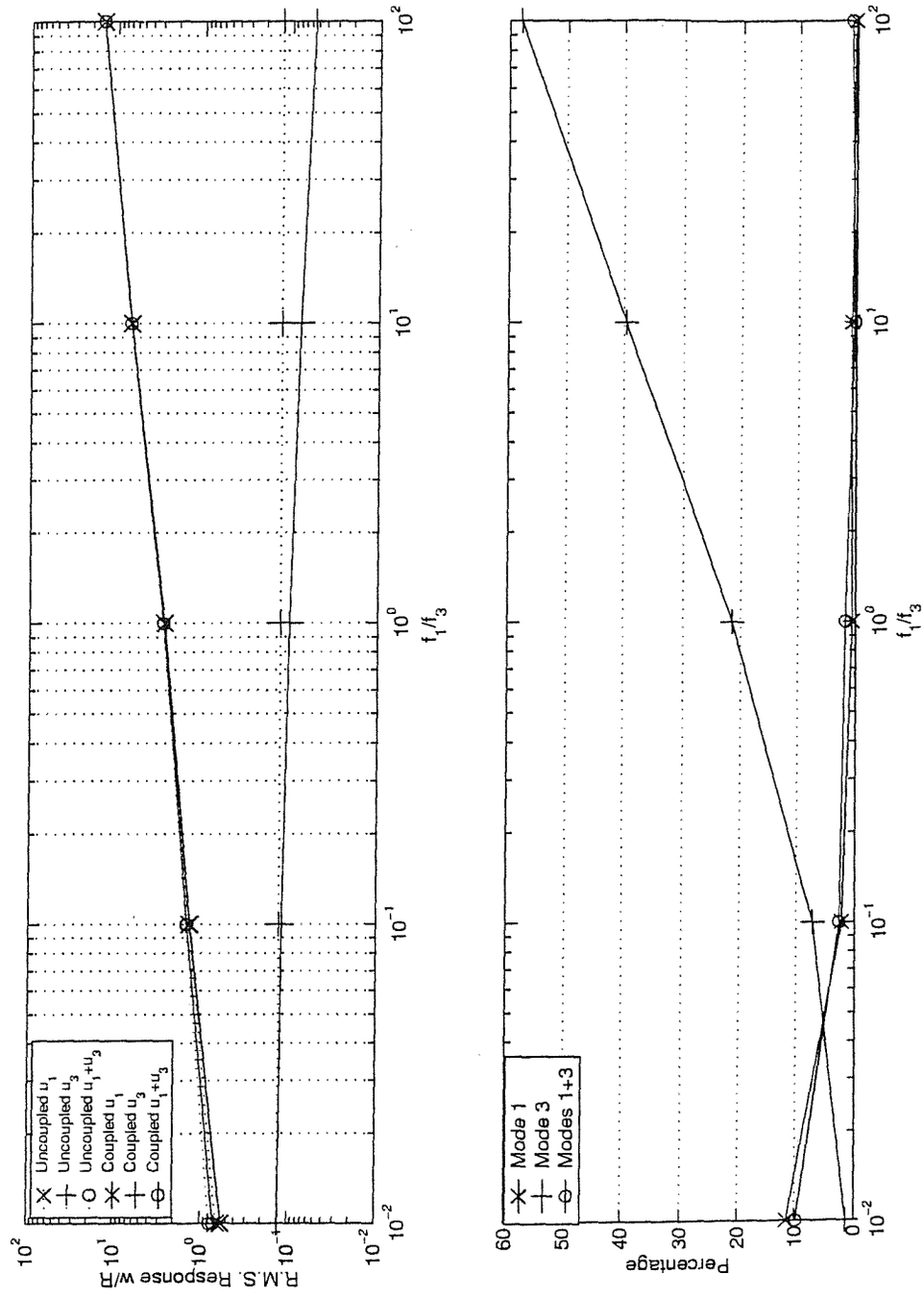

Figure 5.6: Non-linear Coupled and Uncoupled R.M.S. Displacement Responses and Percentage Differences of Coupled Response Relative to Uncoupled Responses at Selected f_3/f_1 (Load Case 2B).

the first mode at all times. Again, when comparing the uncoupled third-mode responses with those in Load Case 1B, their same values confirms once again that mode-coupling in the stiffness term in fact has little contribution to the characteristics of the system in that case.

However, for the coupled system into which the input excitation f_1 is increasing, the third-mode response starts to fall off and deviates progressively from its uncoupled counterpart. As the first-mode response becomes more and more significant relative to that of the third mode, u_1 dominates the coupling term in equation (5.2). As the contribution of the coupling term in equation (5.2) becomes increasingly significant, its behaviour would deviate more and more away from that of the uncoupled system governed by equation (5.4).

With decreasing influence of u_3 over the coupled term $\Pi_{1133}u_1u_3^2$ in equation (5.1), the mode-coupling effects in this equation decrease. Thus, as f_1 increases, the coupled system governed by equation (5.1) would start to behave as if it were an uncoupled system represented by equation (5.3) as the third-mode response gives way to the first-mode response. Hence the percentage difference between the coupled and uncoupled u_1 falls.

The non-linear first-mode coupled response builds up but is still smaller than the uncoupled u_1. This is due to an addition stiffness contribution from the mode-coupling term $\Pi_{1133}u_1u_3^2$ in equation (5.1). Here, u_1 is of first order but dominant, and u_3 is of second order but very small. As equation (5.1) defines a system which has a higher stiffness than that characterised by equation (5.3), one would expect that the coupled responses be smaller than the uncoupled ones.

Finally, the coupled total displacement response consists of mainly the first-mode contribution. It is interesting to note that the degree of overestimation varies for the two scenarios studied. In the mass-dominated excited system in Load Case 2A, the increase in mode-coupling effect would cause an increase in the level of overestimation. In the stiffness-dominated excited system in Load Case 2B, however, this severity of response overestimation tends to decrease with increase in mode-coupling effect.

From the second graph of Figure 5.6, it can be seen that a significant difference between the uncoupled and the coupled total displacement response arises at $f_1/f_3 =$

0.01. It may be interesting to see if an increasing non-linearity effect would change the phenomenon of resonance-coupling in this situation when the amplitude of the excitation with the first linear mode shape of the beam is maintained at one-tenth that of the excitation with the third linear mode shape. This can be done by increasing amplitudes of both f_1 and f_3, whilst keeping $f_1/f_3 = 0.01$.

Results show that the percentage difference between the coupled and uncoupled u_3 response hardly changes with increasing non-linearity. The third mode is in general playing a more significant role in the contribution to the total displacement response. However, as non-linearity increases, the contribution by the first mode to the total response increases. At the same time, mode-coupling has a growing effect on the response u_1. As a result, very high non-linearity effects, with the influence of mode-coupling is likely to have an impact on the total response of the beam.

Load Case 2C: $P1$ oscillating 90^o out of phase with $P3$

So far, when the two harmonic pressures, $P1$ and $P3$, excited the beam simultaneously, they were oscillating in phase with each other at exactly the same forcing frequency, even if they had different spatial distributions. The phenomenon of resonance coupling is further investigated when the pressures are oscillating with a phase difference of 90^o with each other.

The generalised forces $F_{01}(t)$ and $F_{03}(t)$ on the right-hand side of equations (5.1— 5.4) now become $f_0 sin(\frac{\pi x}{l}) sin(\omega_3 t)$ and $f_3 sin(\frac{\pi x}{l}) sin(\omega_3 t + \pi/2)$ respectively. Here, the magnitude of the pressure $P1$ is set to equal that of $P3$, i.e, $f_3/f_1 = 1$.

From the numerical solutions of the Duffing's equations (5.1— 5.4), it is shown in Table 5.4 that when the two pressures are 90^0 out of phase with each other, the coupling effects on the r.m.s. displacement response will decrease significantly. Moreover, from Table 5.5, it can be predicted that the differences between the r.m.s. coupled and r.m.s. uncoupled displacement responses are insignificant, even when the level of non-linearity is high.

	Mode 1 (%)	Mode 3 (%)	Total (%)
In phase	1.7	0.14	0.65
90^o out of phase	0.038	0.046	0.35

Table 5.4: Load Case 2C: Percentage Difference between Non-linear Coupled and Uncoupled R.M.S. Displacement Responses $u = (w/R)$ — Effects of Phase Difference of Excitation on Non-linear Coupling ($f_1 = f_3 = 100Pa$)

Level of Non-linearity	$f_1(Pa)$	$f_3(Pa)$	Mode 1 (%)	Mode 3 (%)	Total (%)
Low	100	100	0.038	0.046	0.35
High	100000	10000	1.9	24	2.7

Table 5.5: Load Case 2C: Percentage Difference between Non-linear Coupled and Uncoupled R.M.S. Displacement Responses $u = (w/R)$ — Effects of Non-linearity (Phase difference=90^o)

Load Case 2D: $\Omega_1 = \omega_3, \Omega_3 = \omega_1$

This loading situation can be viewed as a combination of Load Case 1A and Load Case 1B. In other words, the harmonic pressure $P1$ excites the beam with a forcing frequency, Ω_1, at the third natural frequency whilst at the same time $P3$ excites it with a frequency, Ω_3, at the first natural frequency. The amplitudes of the non-linear uncoupled displacement responses u_1 and u_3 are predefined in this study. The level of excitation of the pressures $P1$ and $P3$ has been chosen so that the resulting uncoupled u_1 is of the same order of magnitude as the corresponding uncoupled u_3. Only two levels of excitation are studied here, one of which would produce a small amount of non-linearity in the system whilst another would cause a strong non-linear effect. As before, both the coupled and uncoupled Duffing's equations are solved numerically and the solutions are studied.

The results of the displacement response show that when the magnitude of the load does not produce a significantly non-linear response, the difference between the coupled and uncoupled displacement responses is minimal. With high non-linearity effect, the

difference between the coupled and uncoupled dominant first-mode responses is relatively small whilst that between the coupled and uncoupled subordinate third-mode responses is much more significant. Nonetheless, this difference for the total displacement response is still not noteworthy. The percentage differences are tabulated in Table 5.6.

Level of Non-linearity	$f_1(Pa)$	$f_3(Pa)$	Mode 1 (%)	Mode 3 (%)	Total (%)
Low	100	100	0.46	0.043	0.057
High	100000	10000	1.8	2.4	1.8

Table 5.6: Percentage Difference between Non-linear Coupled and Uncoupled R.M.S. Displacement Responses $u = (w/R)$ at Two Levels of Non-linearity (Load Case 2D)

Conclusion of Studies in Load Case 2

Various types of harmonic excitation across the non-linear beam have been studied. Under certain circumstances, the mode-coupling terms in the Duffing's system can cause noticeable effects in the total displacement response of the beam in highly non-linear harmonic vibrations. This especially concerns the loading conditions when the forcing frequencies of the pressures are equal to the lowest natural frequency of the beam, and the pressures are in phase with one another. With a comparatively large excitation which only excites a subordinate mode of a system with mode-coupling, the response of the dominant mode of this system can be significantly different from what is predicted by a Duffing's system without mode-coupling. In general, the Duffing's system without mode-coupling terms would overestimate the resultant response in harmonic vibrations.

5.3 Non-linear Response to Spatially Harmonic and Temporally Random Excitation

In this study, the distribution across the span of the beam is the same as that of Load Case 2 studied in section 5.2.2. In other words, the pressure has a spatial distribution

which matches only and exactly the first and third linear mode shapes of the beam, so that the generalised force in all other modes is zero. This pressure is applied with a time history which corresponds to a band-limited temporal white noise. Two loading scenarios with two different input pressure spectra are studied. First, as an extension to Load Case 2B, the frequency content of the excitation is centred around the natural frequency of the first mode of the beam. Then, another type of band-limited white-noise random pressure of which the frequency contents cover frequencies including the first and the third natural frequencies will be employed. Figure 5.7 should also be referred to. In both cases, the non-linear mid-span coupled and uncoupled displacement response time histories will be obtained from the equations of motion (5.1, 5.2) and (5.3, 5.4) by the step-by-step numerical integration scheme. The steady-state solutions are then retrieved by ommitting the first 1.0 second of the time history. The non-linear coupled and uncoupled r.m.s. responses are obtained, and any differences between the two responses will be studied.

5.3.1 Load Case 3: Forcing Frequency Contents Covering the First Natural Frequency

For an overall sound pressure level of $SPL_3 = 90dB$, the input band-limited white-noise pressure simulated and used earlier in Chapter 4 has been adopted and used in this loading scenario. The frequency range was between $1Hz$ and $251Hz$. However, the spatial fluctuation of the input pressure, $P3$, has a distribution matching the third linear mode shape of the beam, so that the generalised force in all other modes is zero. The load is also characterised by parameters such as the sound pressure level ($SPL_3 = 90dB$), the r.m.s. pressure (r.m.s. $f_3 = 0.6325Pa$) and the frequency sampling interval ($dw = 0.0766Hz$). Data concerning $P3$ can be found in section 4.2.4 of Chapter 4.

The pressure with spatial distribution matching the first linear mode shape of the beam, $P1$, has a similar time history as that of $P3$. This pressure $P1$ is implemented here to aim to excite the first-mode response of the beam and its pressure level is increasing

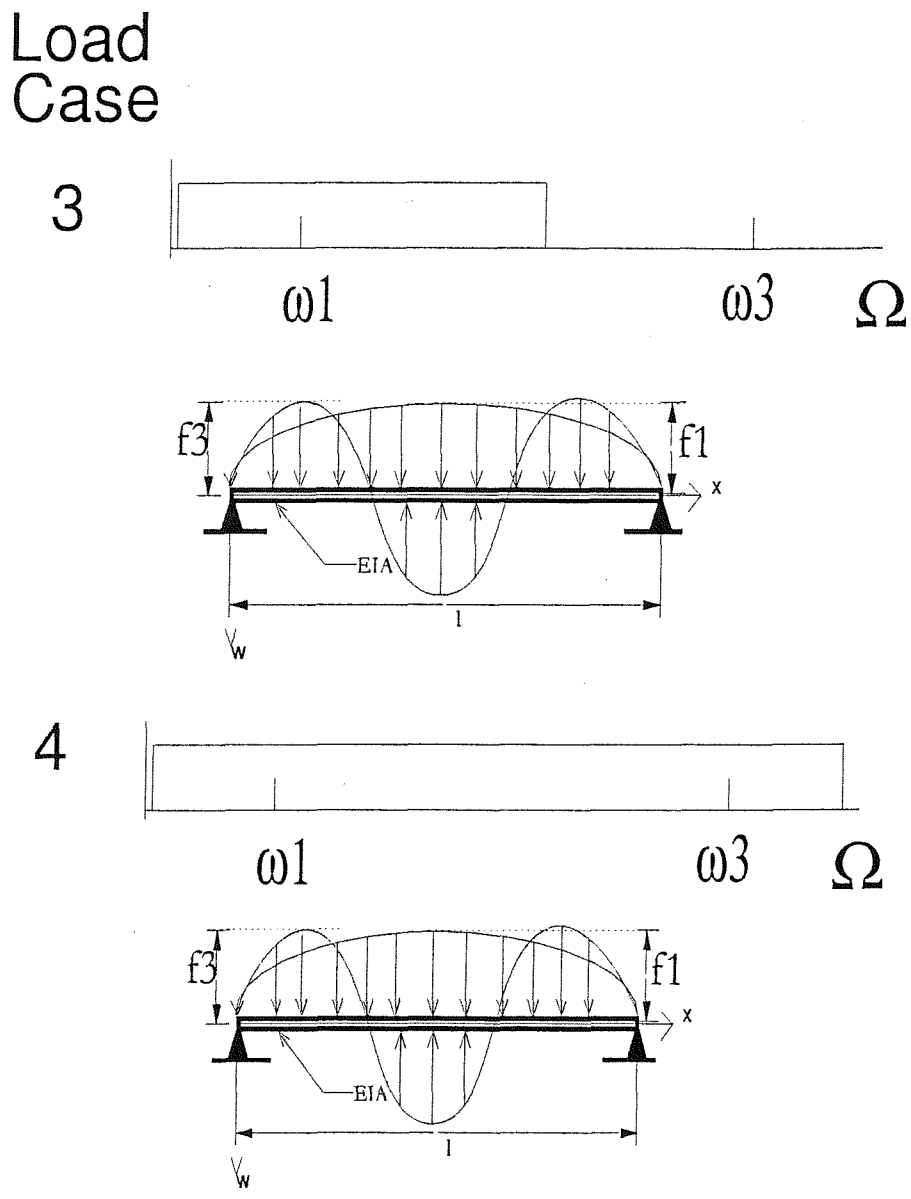

Figure 5.7: Simply-supported Beam with Immovable End Conditions Subjected to Different Types of Random Pressure

according to the sound pressure levels, $SPL_1 = 50, 70, 90, 110$ and $130dB$, whereas the pressure amplitude, f_3, of $P3$ is always kept to have a pressure level of $90dB$. The ratio of their r.m.s. value is denoted by f_1/f_3.

After the two sets of 2DOF equations (5.1, 5.2) and (5.3, 5.4) have been solved numerically, the non-linear r.m.s. values of the displacement responses at mid-span for various f_1/f_3 are presented in Table 5.7. These results, together with the percentage differences between the coupled displacement responses and the uncoupled responses, are also given for various values of f_3/f_1 in this table and in Figure 5.8.

Based on the results in Table 5.7 and Figure 5.8, and by referring to Table 5.3 and Figure 5.6, some similarities regarding both the uncoupled and coupled r.m.s. responses, u_1, u_3 and $(u_1 + u_3)$, can be identified between the solutions of random response and those of harmonic response as seen in Figure 5.6. Like the case of non-linear harmonic vibrations without mode-coupling, the non-linear random r.m.s. uncoupled response u_1 increases whilst the uncoupled u_3 remains constant with increase in f_1/f_3. Moreover, the first mode dominates in the resultant displacement response. With mode-coupling effects considered, the trend of the change of the non-linear coupled response u_1 with increasing f_1/f_3 is similar to that of the corresponding uncoupled response. The dominant mode in the resultant displacement response is still the first mode. The coupled response u_3 deviates from its uncoupled counterparts with increasing levels of excitation f_1.

However, in contrary to that in harmonic vibrations in Load Case 2B of section 5.2.2, the coupled response u_3 increases at higher levels of excitation f_1. In addition, the degree of overestimation by a system without mode-coupling intensifies with increasing f_1/f_3, as opposed to that observed in Load Case 2B. This distinction in the behaviour of the responses may be due to the different type of excitation concerned.

In harmonic vibration (Load Case 2B), due to non-linearity effect, the resonance of the first mode moved away from the forcing frequency with the increase of the ratio f_1/f_3. Overall, the coupled response u_1 increased by roughly 25 times whilst f_1/f_3 increased by 10000 times, with f_3 held constant. Due to the coupling effect, the stiffness controlling the coupled response of u_3, as explained above, causes it to decrease with increasing f_1/f_3.

f_1/f_3	0.01	0.1	1.0	10	100
Uncoupled (u_1)[I]	3.3056 $\times 10^{-3}$	3.3020 $\times 10^{-2}$	3.3321 $\times 10^{-1}$	1.8136	6.2190
Uncoupled (u_3)[II]	1.4546 $\times 10^{-3}$	1.4546 $\times 10^{-3}$	1.4546 $\times 10^{-3}$	1.4546 $\times 10^{-3}$	1.4546 $\times 10^{-3}$
Uncoupled $(u_1 + u_3)$[III]	3.6165 $\times 10^{-3}$	3.3058 $\times 10^{-3}$	3.3321 $\times 10^{-1}$	1.8136	6.2191
Coupled (u_1)[IV]	3.3056 $\times 10^{-3}$	3.3020 $\times 10^{-2}$	3.3320 $\times 10^{-1}$	1.8641	6.0265
Coupled (u_3)[V]	1.4546 $\times 10^{-3}$	1.4545 $\times 10^{-3}$	1.4488 $\times 10^{-3}$	1.5274 $\times 10^{-3}$	3.2462 $\times 10^{-3}$
Coupled $(u_1 + u_3)$[VI]	3.6165 $\times 10^{-3}$	3.3056 $\times 10^{-2}$	3.3320 $\times 10^{-1}$	1.8641	6.0266
% Difference [I] and [IV]	0.0	0.0	4.5 $\times 10^{-3}$	2.8	3.1
% Difference [II] and [V]	0.0	4.6 $\times 10^{-3}$	0.40	5.0	123
% Difference [III] and [VI]	0.0	4.6 $\times 10^{-3}$	4.5 $\times 10^{-3}$	2.8	3.1

Table 5.7: Comparison of Coupled and Uncoupled Non-linear R.M.S. Displacement Responses $u = (w/R)$ for Selected Ratios of f_3/f_1 (Load Case 3)

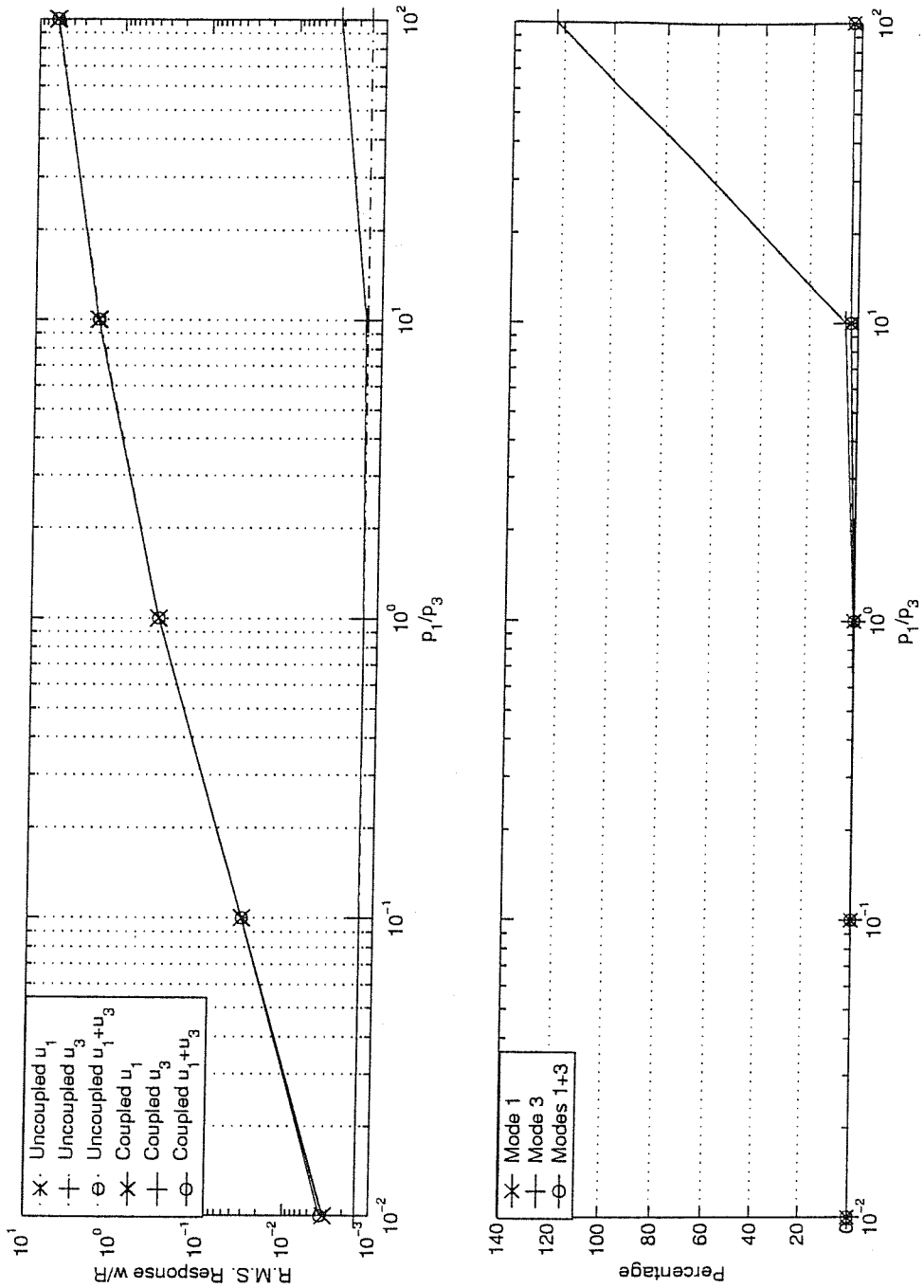

Figure 5.8: Non-linear Coupled and Uncoupled R.M.S. Displacement Responses and Percentage Differences of Coupled Response Relative to Uncoupled Responses at Selected f_3/f_1 (Load Case 3).

Now in random vibration (Load Case 3) with increasing f_1/f_3, the first mode is always being excited, as the equivalent linear frequencies, even if increasing, are still within the frequency content of excitation. The response u_1 now increases by nearly 2000 times with f_1/f_3 increasing by 10000 times. Although the argument on the increase in stiffness in the third mode and its tendency to lower u_3 is still valid, the enormous amount of contribution due to the first mode into the third mode through the mode-coupling terms has an effect of overriding this tendency and causes u_3 to amplify.

Nevertheless, the dominant mode is the first mode and the total displacement response is very little affected by this different behaviour of the response of the third mode.

5.3.2 Load Case 4: Forcing Frequency Contents Covering the First and the Third Natural Frequencies

The coupling effect on the non-linear random vibration of the beam is further studied when the frequency content of the input random pressure spectrum includes both the first and the third natural frequencies. The pressure in the time domain, P, is digitally simulated and has an r.m.s. magnitude f. This corresponds to a band-limited Gaussian white-noise random pressure of which the characteristics can be found in Table 5.8 and Figure 5.9.

The pressure which possesses a spatial distribution matching that linear mode shape of the third-mode resonance of the system, $P3$, has an r.m.s. magnitude f_3. The r.m.s. magnitude of the pressure $P1$, which has a spatial distribution matching the linear mode shape of the first resonance of the system, is chosen so that the resulted non-linear uncoupled r.m.s. u_1 is of the same order of magnitude as the corresponding uncoupled r.m.s. u_3. This would give the value of f_3 which is bigger than f_1, and $f_3/f_1 = \sqrt{1000} \approx 32$. The sound pressure level of the pressure P is also selected so that significant non-linearity is present in the response.

The non-linear r.m.s. displacement responses are obtained, again from the numerical solutions of the coupled and uncoupled equations (5.1, 5.2) and (5.3, 5.4). The solutions

Overall SPL (dB), $ref.2 \times 10^{-5}$	140
Selected frequency bandwidth DW (Hz)	800 (1 to 801)
Input SSL (dB)	111
PSD $S_f(Pa^2/Hz)$	50
Area under spectrum density graph (Pa^2), [I]	40006
Calculated r.m.s. pressure (Pa), [II]	200
Number of simulated points, M	524288
Frequency sampling interval $dw(Hz)$	0.1222
Length of Time history (s)	8.1818
Time interval (s)	1.5605×10^{-5}
Mean square value of simulated pressure (Pa^2), [III]	40004
r.m.s. value of simulated pressure, f (Pa^2), [IV]	200.0089
% difference between [I] and [III]	0.0064
% difference between [II] and [IV]	0.0044

Table 5.8: Parameters for One Digital Simulation of Input Pressure P

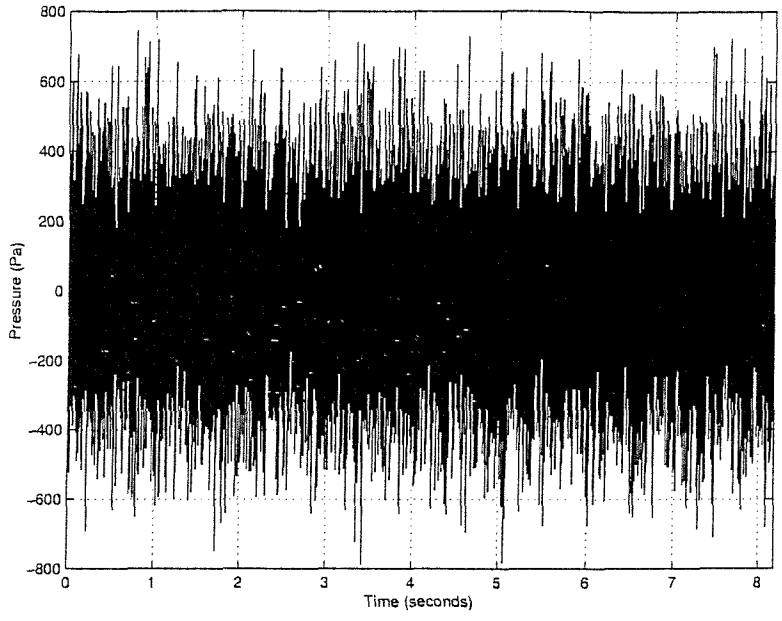

Figure 5.9: Time Histories of Simulated Random Pressure P, overall $SPL = 140$

are shown in Table 5.9.

	Mode 1	Mode 3	Modes 1+3
Uncoupled	1.1823	1.4186	1.8463
Coupled	1.2230	1.4273	1.8801
Percentage Difference	3.4	0.61	1.8

Table 5.9: Coupled and Uncoupled Non-linear R.M.S. Displacement Responses ($u = w/R$) and Percentage Difference of Coupled Response Relative to Uncoupled Response (Load Case 4)

The non-linear coupled r.m.s. first-mode response, u_1, is of the same order of magnitude as the corresponding r.m.s. third-mode response, u_3. By comparing the coupled and uncoupled r.m.s. responses, it is found the percentage differences between the two responses are small. Hence, it can be deduced that in this type of excitation, the effect of mode-coupling under large non-linearity does not have a large influence over the total response of the vibration of the beam.

The non-linear coupled r.m.s. displacement responses are greater than the corresponding uncoupled ones. This behaviour could not been found in any of the case in which the excitation was harmonic in the time domain. However, based on the findings regarding the increase in the third mode response in random vibrations (Load Case 3 of section 5.3.1), explanations can be sought. Here, the resonances of both modes 1 and 3 are always within the frequency content of excitation. Even though the tendency of response reduction as a result of stiffening due to mode-coupling still exists, the greater amount of the response addition through the coupling term will overpower. Unlike in non-linear harmonic vibrations, the uncoupled Duffing's equation would underestimate the displacement response of the beam when subjected to a broad-band random pressure.

5.4 Chapter Summary and Conclusion

The non-linear forced vibrations of simply-supported beams with immovable end conditions have been studied. The 2DOF Duffing's equations with and without coupling terms have been solved numerically. The steady-state non-linear displacement response of the beam when subjected to different types of symmetrically distributed pressure has been obtained. Only the first two symmetric modes have been included in the response of the beam. The findings are summarised in Table 5.10.

From studies in Load Cases 1A and 1B, the harmonic pressure has a spatial distribution matching one of the linear mode shapes of the beam and has a frequency equal to the natural frequency of the other mode. It has been shown that the shape of the displacement response is the same as that linear mode shape being matched by the spatial distribution of the pressure. The response oscillates at the frequency of excitation.

In Load Case 2A, the beam is excited by two harmonic pressures in phase with each other at its third natural frequency. One of the pressures, $P1$, has spatial distribution matching the first linear mode shape of the beam whilst the other one, $P3$, is spatially matched to the third linear mode shape. The amplitude of excitation of the former pressure is fixed and that of the latter varying. In Load Case 2B, the beam is excited

Load Cases	Excitation Types	Effects of Mode-coupling in Non-linear R.M.S. Displacement Responses
1A	Harmonic, $P1$ at ω_3	Response due to mode 1 only
1B	Harmonic, $P3$ at ω_1	Response due to mode 3 only
2A	Harmonic, $P1+P3$ at ω_3, f_1 fixed, f_3 varying	Coupling has large effect on u_1 which has small contribution
2B	Harmonic, $P1+P3$ at ω_1, f_3 fixed, f_1 varying	Coupling has large effect on u_3 which has small contribution
2C	Harmonic, $P1 + P3$ at ω_3, 90^o out of phase, $f_3/f_1 = 1$	Coupling has small effect on both u_1 and u_3
2D	Harmonic, $P1$ at ω_3; $P3$ at ω_1, $f_3/f_1 = 1$	Coupling has large effect on u_3 which has small contribution
3	Random white-noise containing ω_1, $P1 + P3$, f_3 fixed, f_1 varying	Coupling has large effect on u_3 which has small contribution
4	Random white-noise containing $\omega_1 + \omega_3$, $P1 + P3$, $f_3/f_1 = \sqrt{1000}$	Coupling has small effect on both u_1 and u_3

Table 5.10: Summary of Results in Studies Outlined in Figure 5.1 and Figure 5.7

by the pressures $P1$ and $P3$ in Load Case 2A. The forcing frequency, however is equal to the first natural frequency of the beam. The amplitude of excitation of $P3$ is fixed and that of $P1$ varying.

A similar study to Load Case 2A has been carried out. In this case, referred to as Load Case 2C, the pressures $P1$ and $P3$ are 90^o out of phase and their amplitudes are the same. In another study, designated as Load Case 2D, the pressure $P1$ excites the beam at its third natural frequency. The other pressure $P3$ has a frequency equal to the first natural frequency of the beam. The amplitudes of the two loads are equal to each other.

In all these cases, results have indicated that mode-coupling can cause large effects on one of the modes, but the effects on the overall beam displacement response are small.

Two further cases have been studied, which concentrates on the mode-coupling on the non-linear vibrations of S-S beams with immovable end conditions subjected to acoustic pressure. In Load Case 3, the beam is subjected to the pressures $P1$ and $P3$. The frequency content of excitation is centred around the first natural frequency of the beam. With the amplitude of $P1$ varying whilst keeping that of $P3$ fixed, the non-linear beam displacements have been obtained. Furthermore, a similar study has been carried out in Load Case 4, in which the random white-noise load contains both the first and the third natural frequencies. The amplitudes of $P1$ and $P3$ have also been selected so that the non-linear uncoupled first- and third-mode displacement responses are of the same order of magnitude. It has been discovered that there are only small effects caused by non-linear coupling.

The SDOF Duffing's equation has been known to be a reliable tool to describe the behaviour of a simply-supported beam with immovable end conditions in geometrically non-linear vibrations. Through the current studies, it has been confirmed that in many cases, negligence of mode-coupling in the Duffing's system does not cause significant effects in the total displacement response. Nevertheless, the absence of coupling terms will overestimate the response. Moreover, it has been found that severe non-linearity can cause noticeable coupling effects in the overall beam response. As a result, the Duffing's

equation without mode-coupling should be treated with care when it is intended for describing beam vibrations in very non-linear situations.

Chapter 6

CONCLUSIONS AND FURTHER WORK

6.1 Background of Current Work

A variety of problems regarding the structural strength of thin panels which arise in modern aircraft constructions cannot be adequately analysed on the basis of the classical linear theory of vibration. Since the panel deflections experienced are not small in comparison with the size of the panel and in particular its thickness, the basic assumptions of the linear theory are violated. Therefore, the development of a structural response prediction model which would take into account the non-linear response behaviour in the treatment of panel vibration is necessary. Moreover, the phenomenon of "coupling-resonance" due to the coupling of modes has been known for some time. Its effect, however, has very often been neglected in the study of beam vibration problems.

The objective of the study is to improve the understanding of the vibration behaviour of non-linear response of thin aircraft beam structures subject to different loads in flight by several different approaches, with effects of mode-coupling taken into account. The study will serve as a background for the development of the prediction of non-linear vibrations of aircraft panel-type structures.

6.2 Summary and Conclusions of Current Work

A literature review in the field of non-linear vibrations of slender beams and thin panels has been presented. A review in the topic of non-linear free vibrations of these structures has also been reported. The survey has focused on the non-linear forced response of beams and plates. The types of excitation are harmonic and random loads.

The focus of this study has been on the behaviour of the response in the geometrically non-linear forced vibration of simply-supported isotropic slender beams. The geometrically non-linear response of the forced vibration of a slender beam with simply-supported end conditions has been analysed. The Duffing's equation has been derived and utilised to study the motion of non-linear beam vibrations. The types of excitation are concentrated mainly on uniform harmonic load and white-noise random pressure

Harmonic Vibrations

Two cases have been studied, in one of which a point force is applied at the mid-span of the beam. In the second case, a uniformly distributed pressure is applied across the span of the beam. In either case, the load is varying harmonically with time and has forcing frequencies around the first natural frequency but well separated from the next higher resonance. Approximated solutions by the analytical Harmonic Balance Method (HBM) have been compared against results obtained through the time-domain numerical integration of the SDOF Duffing's equation, those through ANSYS® Finite Element Analysis, as well as several published analytical results.

1. The Finite Element Analysis has indicated that the non-linear mode-coupling effects due to higher resonating modes are minor in this case.

2. The SDOF Duffing's equation has shown to be capable of describing the large-deflection forced vibration motion of the beam.

3. The analytical technique Harmonic Balance Method has been found to give satisfactory approximation and that it can be used efficiently in analysing large-deflection harmonic vibrations of a simply-supported beam.

Random Vibrations

The non-linear vibration of simply-supported beams has been further analysed. The study aimed to determine the suitability of applying the Direct Equivalent Linearisation Technique in the analysis of highly non-linear response of the beam when subjected to a uniformly distributed band-limited white-noise pressure. In this case, only a SDOF system has been investigated and the SDOF Duffing's equation was employed. The solutions by the equivalent linearisation method have been compared with those obtained by the numerical time-domain Monte-Carlo approach.

1. From the comparison of the root-mean-square displacement beam response, it has been shown that the Direct Equivalent Linearisation approximation agrees well with the solutions by the Monte-Carlo approach, even with the presence of a high level of non-linearity.

2. The phenomenon of the rise in resonance frequency with increase of non-linearity has been observed by using both the Direct Equivalent Linearisation and time-domain Monte-Carlo methods.

3. In high levels of non-linearity due to intense excitation, results obtained by the time-domain Monte-Carlo approach indicate that resonance peaks of the displacement response merge into one flat peak. However, solutions from equivalent linearisation show that the non-linear system would have the characteristic distinct peaks of a linear system regardless of the level of non-linearity.

Mode-coupling Effects on Non-linear Vibrations

Using the two-degree-of-freedom Duffing's equations with only the first and the third modes included, the impact of different excitation on mode-coupling effects in the non-linear vibrations of simply-supported beams has been assessed.

1. Under symmetric harmonic loads across the span of the beam, the crucial factor governing which modes of response are to be excited is the shape of the spatial

distribution possessed by pressure fluctuations. For example, if the pressure is spatially matched to the first linear mode shape, so that the generalised force in all other modes is zero, only the first mode of the beam will respond. The forcing frequencies have only effect of controlling the frequency content of the excited response.

2. A Duffing's oscillator without coupling would overestimate the total displacement response in harmonic excitation, when compared to one with mode-coupling terms accounted for.

3. For a harmonically excited non-linear Duffing's system which is stiffness-dominated, the level of overestimation decreases with increasing mode-coupling effects, whilst for one which is mass-dominated, the level increases with the mode-coupling effects.

4. When the beam is subjected to a random band-limited white-noise pressure of which the frequency spectrum is centred around the first resonance, the non-linear Duffing's equations predicts that the beam would respond in a similar fashion as one being harmonically excited.

5. In the case when the frequency spectrum of the random pressure covers both the first and third resonances, the overall random response behaviour is different from the total response in harmonic excitation. A system without coupling underestimates the total displacement response in random excitation, when compared to one including mode-coupling terms.

6.3 General Conclusions

In the study of non-linear vibrations of simply-supported slender beams, the Duffing's equation has been proved to be a reliable tool to describe the vibration behaviour. Among the various approaches to obtain the non-linear response due to external excitation, the time-domain numerical methods can almost always give solutions with high

levels of accuracy and thus may act as a benchmark. However, the employment of such methods should be restricted to relatively simple systems because when a more physically complex aircraft structure is to be analysed, where a lot of degrees of freedom is required or when high accuracy is paramount, the cost of the heavy computational workload could be extremely large. Even for simpler structures such as beams, the amount of resources spent in computation might still be significant. Less complicated but reliable approximate analytical techniques are attractive and should be considered, as they are very often able to capture the key features of the behaviour of the response.

It has been shown that, in general, mode-coupling effects on the non-linear forced response of simply-supported beams under symmetric loads are relatively small. This means that the use of a SDOF uncoupled Duffing's equation is valid for approximation, but when very high accuracy is required, or when the excitation has more complicated characteristics, its use should be treated with care.

6.4 Recommendations for Further Work

The Duffing's equation has been investigated by numerous researchers over the past few decades. However, the forcing functions which have been used to simulate the actual acoustic load on aerospace structures are mainly restricted to stationary Gaussian white noise with a deterministic spatial distribution across the surface of the beam. Moreover, as a white noise with uniform spatial distribution is not a very good reflection of the excitation concerned in reality the random process of the non-linear analysis of response of aircraft panel-type structures due to acoustic loading which is uncorrelated in both time-wise and space-wise should be investigated. The excitation can be visualised as an aircraft skin exposed to a turbulence flow (a convected pressure) and acoustic pressures simultaneously.

Certainly, the employment of some numerical Monte-Carlo approaches can obtain very accurate solutions in the non-linear response of beams. Nevertheless, the usefulness of the application of approximation schemes as an analytical tool should not be

undervalued, and their use to understand the non-linear response behaviour of beams subjected to more complex random loads should be investigated.

The cases when severe mode-coupling effects are present in highly non-linear vibrations of various panel-type structures under different types of excitation need to be investigated. For instance, the severity of mode-coupling effects in a non-linear beam with multiple supports under random excitation could be studied analytically or numerically. This can simulate a stiffened aircraft panel in rigorous flight conditions.

List of References

[1] H F WOLFE, C A SHROYER, D L BROWN, and L W SIMMONS. An experimental investigation of nonlinear behavior of beams and plates excited in high levels of dynamic response. Technical report WL-TR-96-3057, Wright Laboratory, Wright Patterson AFB, Ohio, 1995.

[2] J MILES. On structural fatigue under random loading. *Journal of Aeronautical Sciences*, 21:753–762, 1954.

[3] A POWELL. On the fatigue failure of structures due to vibrations excited by random pressure fields. *The Journal of the Acoustical Society of America*, 30(12):1130–1135, 1958.

[4] B L CLARKSON. Stress in skin panels subjected to random acoustic loading. *The Aeronautical.Journal of the Royal Aeronautical. Society*, 72(695), November 1968.

[5] R D BLEVINS. An approximation method for sonic fatigue analysis of plates and shells. *Journal of Sound and Vibration*, 129(1):51–71, 1989.

[6] C ZIENKIEWICZ. *The Finite Element Method.* McGraw-Hill, New York, 1977.

[7] E J RICHARDS and D J MEAD. *Noise and Acoustic Fatigue in Aeronautics.* John Wiley and Sons Ltd, 1968.

[8] S H CRANDALL. *Random Vibration.* The M.I.T. Press, Massachusetts, 1958.

[9] S H CRANDALL. *Random Vibration*, volume 2. The M.I.T. Press, Massachusetts, 1963.

[10] W J TRAPP and D M FORNEY , JR. *Acoustical Fatigue in Aerospace Structures.* Syracuse University Press, Syracuse, New York, 1965.

[11] A H NAYFEH and D T MOOK. *Nonlinear Oscillators.* John Wiley and Sons New York, 1979.

[12] M. SATHYAMOORTHY. Nonlinear vibration analysis of plates: A review and survey of current developments. *Applied Mechanics Review*, 40:1553–1561, 1987.

[13] R A IBRAHIM. Nonlinear random vibration experimental results and research needs. In *Proceedings of the 4th International Conference on Recent Advances in Structural Dynamics*, pages 58–83, 1991.

[14] H CHALLIS and C STANTON. Non-linear vibration in thin panels. In *Research in Noise and Vibration.* Swindon P.O. Box 18, Swindon SN2 1ET : The Council, 1979.

[15] J J STOKER. *Nonlinear Vibrations in Mechanical and Electrical Systems.* Interscience Publishers, Inc., New York, 1950.

[16] T K CAUGHEY. Derivation and application of the fokker-planck equation to discrete nonlinear dynamic systems subjected to white random excitation. *The Journal of the Acoustical Society of America*, 35(11):1683–1692, 1963.

[17] J M T. THOMPSON and H B STEWART. *Nonlinear dynamics and chaos: geometrical methods for engineers and scientists.* Wiley, 1986.

[18] D E NEWLAND. *An Introduction to Random Vibrations and Spectral Analysis.* Longman, New York, second edition, 1984.

[19] P D SPANOS. Stochastic linearization in structural dynamics. *Applied Mechanics Reviews*, 34(1):1–8, 1981.

[20] S H CRANDALL. Perturbation techniques for random vibration of nonlinear systems. *The Journal of the Acoustical Society of America*, 35(11):1700–1705, 1963.

[21] J HE. A new perturbation technique which is also valid for large parameters. *Journal of Sound and Vibration*, 229(5):1257–1263, 2000.

[22] T K CAUGHEY. Nonlinear theory of random vibrations. *Advances in Applied Mechanics*, 11:209–253, 1971. New York, Academic Press.

[23] C MEI and D B PAUL. Nonlinear multimode response of clamped rectangular plates to acoustic loading. *AIAA Journal*, 24(4):643–648, 1986.

[24] G AHMADI, I TADJBAKHSH, and M FARSHAD. On the response of nonlinear plates to random loads. *Acustica*, 40(5):316–322, 1978.

[25] Y K LIN. Recent advances in nonlinear random vibration. In *Proceedings of the 3rd International Conference on Recent Advances in Structural Dynamics*, volume 2, pages 717–732, 1988.

[26] T K CAUGHEY. Equivalent linearization techniques. *The Journal of the Acoustical Society of America*, 35(11):1706–1711, 1963.

[27] N KRYLOV and N BOGOLIUBOV. Introduction à la méchanique nonlinearization: les méthodes approachées et asymptotiques. Technical report, Ukrainskaya Akaademia Nauk. Inst. de la Méchanique,Chaire de Phys. Math. Ann., 1937. (S. Lefshetz, translator), 1947 in Annals of Mathematics Studies, Vol.11. Princeton, NJ: Princeton University Press.

[28] R C BOOTON JR. Nonlinear control systems with random inputs. *IRE Transactions Circuit Theory 1*, pages 32–34, 1954.

[29] T SELCUK ATALIK and S UTKU. Stochastic linearization of multi-degree-of-freedom non-linear systems. *Earthquake Engineering and Structural Dynamics*, 4:411–420, 1976.

[30] F DINCĂ and C TEODOSIU. *Nonlinear and Random Vibrations.* New York: Academic Press, 1973.

[31] I ELISHAKOFF, J FANG, and R CAIMI. Random vibration of a nonlinearly deformed beam by a new stochastic linearization technique. *International Journal of Solids and Structures*, 32(11):1571–1584, 1995.

[32] H R BUSBY JR and V I WEINGARTEN. Response of nonlinear beam to random excitation. *ASCE Journal Engineering Mechanics*, pages 55–68, 1973.

[33] R E HERBERT. Random vibrations of a nonlinear elastic beam. *The Journal of the Acoustical Society of America*, 36(11):2090–2094, 1964.

[34] R S LANGLEY. Stochastic linearisation of geometrically non-linear finite element models. *Computers and Structures*, 27(6):721–727, 1987.

[35] I SIMULESCU, T MOCHIO, and M SHINOZUKA. Equivalent linearization method in nonlinear fem. *Journal of Engineering Mechanics*, 115(3):475–492, March 1989.

[36] I ELISHAKOFF and P COLOMBI. Successful combination of the stochastic linearization and monte carlo methods. *Journal of Sound and Vibration*, 160(3):554–558, 1993.

[37] R. VAICAITIS. Recent advances of time domain approach for nonlinear response and sonic fatigue. In *Proceedings of the 4th International Conference on Recent Advances in Structural Dynamics*, pages 84–103, 1991. plates,stiffened plates, composites, forced vibrations.

[38] M SHINOZUKA and C M JAN. Digital simulation of random processes and its applications. *Journal of Sound and Vibration*, 25(1):111–128, 1972.

[39] M SHINOZUKA and G DEODATIS. Simulation of multi-dimensional gaussian stochastic fields by spectral representation. *Applied Mechanics Review*, 49(1):29–53, 1996.

[40] A BLAQUIÈRE. *Nonlinear System Analysis.* Academic Press Inc, New York, 1966.

[41] A.W. LEISSA. *Vibration of Plates.* Springfield, Va. : National Technical Information Service, 1969.

[42] A.W. LEISSA 1984. Non-linear analysis of plates and shell vibrations. In *Proceedings of the 2nd International Conference on Recent Advances in Structural Dynamics, University of Southampton*, volume 1, pages 84–103, 1984. plates,stiffened plates, shells, forced vibrations.

[43] J N REDDY. A review of the literature on finite element modeling of laminated composite plates. *Shock and Vibration Digest*, 17:3–8, 1985.

[44] S TIMOSHENKO. *Theory of Plates and Shells.* McGraw-Hill, 1959.

[45] S WOINOWSKY-KRIEGER. The effect of axial force on the vibration of hinged bars. *Journal of Applied Mechanics*, 17:35–36, 1950.

[46] JR. P H McDONALD and RALEIGH N C. Nonlinear dynamic coupling in a beam vibration. *Journal of Applied Mechanics*, 22:573–578, 1955.

[47] G SINGH, A K SHARMA, and G V RAO. Large amplitude free vibration of beams-discussion of various formulations and assumptions. *Journal of Sound and Vibration*, 142:77–85, 1990.

[48] R BENAMAR, M M K BENNOUNA, and R G WHITE. The effects of large vibration amplitudes on the fundamental mode shape of thin elastic structures, part i: simply supported and clamped-clamped beams. *Journal of Sound and Vibration*, 149:179–195, 1991.

[49] R BENAMAR, M M K BENNOUNA, and R G WHITE. The effects of large vibration amplitudes on the fundamental mode shape of thin elastic structures, part ii: Fully clamped rectangular isotropic plates. *Journal of Sound and Vibration*, 164:295–316, 1993.

[50] R BENAMAR, M M K BENNOUNA, and R G WHITE. The effects of large vibration amplitudes on the fundamental mode shape of thin elastic structures, part iii: Fully clamped rectangular isotropic plates - measurements of the mode shape amplitude dependence and the spatial distribution of harmonic distortion. *Journal of Sound and Vibration*, 175:377–395, 1994.

[51] B HARRAS, R BENAMAR, and R G WHITE. Geometrically non-linear free vibration of fully clamped symmetrically laminated rectangular composite plates. *Journal of Sound and Vibration*, 251(4):579–619, 2002.

[52] R BENAMAR, M M K BENNOUNA, and R G WHITE. The effects of large vibration amplitudes on the fundamental mode shape of a fully clamped, symmetrically laminated rectangular plate. In *Proceedings of the 4th International Conference on Recent Advances in Structural Dynamics, University of Southampton*, pages 749–760, 1990. plates,composites, free vibrations.

[53] M EL KADIRI, R. BENAMAR, and R.G. WHITE. The non-linear free vibration of fully clamped rectangular plates: second non-liner mode for various plate aspect ratios. *Journal of Sound and Vibration*, 228:333–358, 1999.

[54] S.R. RAO, A.H. SHEIKH, and M. MUKHOPADHYAY. Large-amplitude finite element flexural vibration of plates/stiffened plates. *Journal of the Acoustical society of America*, 93(6):3250–3257, 1993.

[55] R.Y.Y. LEE, Y SHI, and C. MEI. A finite element time domain modal method for large amplitude free vibration of composite pates. In *Proceedings of the 6th International Conference on Recent Advances in Structural Dynamics, University of Southampton*, volume 2, pages 1375–1392, 1990. plates,composites, free vibrations.

[56] F MOUSSAOUI, R BENAMAR, and R G WHITE. The effects of large vibration amplitudes on the mode shapes and natural frequencies of thin elastic shells,part i: Coupled transverse-circumferential mode shapes of isotropic circular cylindrical shells of infinite length. *Journal of Sound and Vibration*, 232(5):917–943, 2000.

[57] 59. M M BENNOUNA and R G WHITE. The effects of large vibration amplitudes on the dynamic strain response of a clamped-clamped beam with consideration of fatigue life. *Journal of Sound and Vibration*, 96(3):281–308, 1984.

[58] C HAYASHI. *Nonlinear Oscillations in Physical Systems.* McGraw-Hill Book Company, 1964.

[59] C S HSU. On the application of elliptic functions in non-linear forced oscillations. *Quarterly of Applied Mathematics*, 17(4):393–407, 1960.

[60] A V SRINIVASAN. Non-linear vibrations of beams and plates. *International Journal of Non-linear Mechanics*, 1:179–191, 1966.

[61] J A BENNETT and J F EISLEY. A multiple degree-of-freedom approach to nonlinear beam vibrations. *AIAA Journal*, 8(4):734–739, 1970.

[62] L AZRAR, R BENAMAR, and R G WHITE. A semi-analytical approach to the non-linear dynamic response problem of s-s and c-c beams at large vibration amplitudes part 1: General theory and application to free and forced vibration analysis. *Journal of Sound and Vibration*, 224(2):183–207, 1999.

[63] M EL KADIRI, R BENAMAR, and R G WHITE. Improvement of the semi-analytical method, for determining the geometrically non-linear response of thin straight structures. part 1: Application to clamped-clamped and simply supported-clamped beams. *Journal of Sound and Vibration*, 249(2):263–305, 2002.

[64] 38. A Y T LEUNG and S.K. CHUI. On the non-linear vibration of the von karman square plate by the ihb method. *Journal of Sound and Vibration*, 204(2):239–247, 1997.

[65] H.A. SHERIF. Non-linear forced vibrations of a clamped circular unsymmetrical sandwich plate. *Journal of Sound and Vibration*, 182(3):495–503, 1995.

[66] N. YAMAKI, K. OTOMO, and M. CHIBA. Non-linear vibration of a clamped circular plate with initial deflection and initial displacement, part 1: Theory. *Journal of Sound and Vibration*, 79:23–42, 1981.

[67] H R BUSBY JR. and V I WEINGARTEN. Non-linear response of a beam to periodic loading. *International Journal of Non-Linear Mechanics*, 7:289–303, 1972.

[68] R Y Y. LEE, Y SHI, and C MEI. Nonlinear response of composite plates to harmonic excitation using the finite element time domain modal method. In *Proceedings of the 6th International Conference on Recent Advances in Structural Dynamics, University of Southampton, U.K.*, volume 2, pages 1423–1436, 1997.

[69] C K CHIANG, C MEI, and C E GRAY , JR. Finite element large-amplitude free and forced vibrations of rectangular thin composite plates. *Journal of vibration and Acoustics*, 113:309–315, 1991.

[70] P.RIBEIRO and M. PETYT. Non-linear vibration of beams with internal resonance by the hierarchical finite-element method. *Journal of Sound and Vibration*, 224(4):591–624, 1999.

[71] P RIBEIRO and M PETYT. Geometrical non-linear, steady state, forced, periodic vibration of plates, part i: model and convergence studies. *Journal of Sound and Vibration*, 226(5):955–983, 1999.

[72] P.RIBEIRO and M. PETYT. Geometrical non-linear, steady state, forced, periodic vibration of plates, part ii: stability study and analysis of multi-modal response. *Journal of Sound and Vibration*, 226(5):985–1010, 1999.

[73] R E HERBERT. Random vibrations of plates with large amplitudes. *Journal of Applied Mechanics*, 32:547–552, 1965.

[74] R E HERBERT. On the stresses in a nonlinear beam subject to random excitation. *International Journal of Solids and Structures*, 1:235–242, 1965.

[75] P SEIDE. Nonlinear stresses and deflections of beams subjected to random time dependent uniform pressure. *Journal of Engineering for Industry, Transactions of the ASME Paper No. 75-DET-23*, 1975.

[76] C B PRASAD and C MEI. Multiple-mode large deflection random response of beams with nonlinear damping subjected to acoustic excitation. *AIAA PAPER NO 8-2712-CP*, 1987.

[77] J.A. SCHUDT. The response of nonlinear systems to random excitation. Master's thesis, The Ohio University, Ohio, 1991.

[78] 53. C. MEI and C.K. CHIANG. A finite element large deflection random response analysis of beams and plates subjected to acoustic loading. In *AIAA 11th Aeroacoustic Conference Paper 87-2713*, 1987. Paper 87-2713.

[79] C HWANG and W S PI. Nonlinear acoustic response analysis of plates using the finite element method. *AIAA Journal*, 10:276–282, 1972.

[80] R S SRINIVASAN and P A KRISHNAN. Application of integral equation technique to nonlinear stochastic response of rectangular plates. *Journal of Acoustical Society of America*, 88(5):2277–2283, 1990.

[81] C MEI and K R WENTZ. Large-amplitude random response of angle-ply laminated composite plates. *AIAA Journal*, 20(10):1450–1458, 1982.

[82] C E GRAY JR., K DECHA-UMPHAI, and C MEI. Large deflection, large amplitude vibrations and random response of symmetrically laminated plates. *Journal of Aircraft*, 22(11):929–930, 1985.

[83] R VAICAITIS and P A KAVALLIERATOS. Nonlinear response of composite panels to random excitation. In *Proceedings of 34th Structures, Structural Dynamics and Material Conference,AIAA-93-1426-CP, Lajella, CA*, pages 1041–1049, 1993.

[84] R VAICAITIS and R R ARNOLD. Nonlinear response and sonic fatigue of metal and composite panels. In *13th Aeroacoustics Conference, AIAA-90-3938, Tallahassee, FL.*, 1990.

[85] J DHAINAUT, B DUAN, C MEI, S SPOTTSWOOD, and H WOLFE. Non-linear response of composite panels to random excitations at elevated temperatures. In

Proceedings of the 7th International Conference on Recent Advances in Structural Dynamics, University of Southampton, U.K., volume 2, pages 769–784, 2000.

[86] V DOGAN and R VAICATIS. Nonlinear response of cylindrical shells to random excitation. *Nonlinear Dynamics*, 20:33–53, 1999.

[87] P D GREEN and A KILLEY. Time domain dynamic finite element modelling in acoustic fatigue design. In *Proceedings of the 6th International Conference on Recent Advances in Structural Dynamics, University of Southampton, U.K.*, volume 2, pages 1007–1025, 1997.

[88] M I McEWAN, J R WRIGHT, J E COOPER, and A Y T LEUNG. A combined modal/finite element analysis technique for the dynamic response of a non-linear beam to harmonic excitation. *Journal of Sound of Vibration*, 243(4):601–624, 2001.

[89] S C GALEA and R G WHITE. Effect of temperature on acoustically induced stresses in some cfrp plates. In *Proceedings of the 3rd International Conference on Recent Advances in Structural Dynamics, University of Southampton, U.K.*, volume 2, pages 629–640, 1988.

[90] R R CHEN, C MEI, and H F WOLFE. Comparison of finite element non-linear beam random response with experimental results. *Journal of Sound and Vibration*, 195(5):719–737, 1996.

[91] A STEINWOLF, N S FERGUSON, and R G WHITE. Variations in steepness of the probability density function of beam random vibration. *European Journal of Mechanics A–Solids*, 19(2):319–341, 2000.

[92] Y K LIN. *Probabilistic Theory of Structural Dynamics.* McGraw-Hill Book Company, 1969.

[93] M GHANBARI and J F DUNNE. An experimentally verified non-linear damping model for large amplitude random vibration of a clamped-clamped beam. *Journal of Sound and Vibration*, 215(2):343–379, 1998.

[94] S TIMOSHENKO, D H YOUNG, and JR. W WEAVER. *Vibration Problems in Engineering.* John Wiley and Sons, 4 edition, 1974.

[95] J PRESCOTT. *Applied Elasticity.* Dover Publications, Inc., New York, 1961.

[96] R S LANGLEY. The effect of linearization and longitudinal deformation on the predicted response of non-linear beams. *Journal of Sound and Vibration,* 116(2):390–393, 1987.

[97] G B WARBURTON. *The Dynamical Behaviour of Structures.* Pergamon Press Ltd., U.K., 2nd edition, 1976.

[98] C MEI and K DECHA-UMPHAI. A finite element method for non-linear forced vibrations of beams. *Journal of Sound and Vibration,* 102(3):369–380, 1985.

[99] A K CHOPRA. *Dynamics of Structures, Theory and Applications to Earthquake Engineering.* Prentice Hall, second edition edition, 2001.

[100] K-J BATHE. *Finite Element Procedures.* Prentice Hall, 1996.

[101] ESDU8396. *Engineering Science Data Item No 66018: The Relation between Sound Pressure Level and R.M.S. Fluctuating Pressure.* Martinus Nijhoff Publishers, The Hague, 1996.

[102] V V BOLOTIN. *Random Vibrations of Elastic Systems.* Martinus Nijhoff Publishers, The Hague, 1984.

[103] A BALFOUR and A J McTERNAN. *The Numerical Solution of Equations.* Heinemann Education Books Ltd, 1967.

Appendix A

THE MULTI-DEGREE-OF-FREEDOM FORM OF THE DUFFING'S EQUATION

A.1 Expansion of Modes

If equation (3.2) in Section 2.1.2 is expanded up to the first three modes, it becomes

$$\begin{aligned}
\frac{d^2u_1}{dt^2} + \omega_1^2 u_1 + \Gamma_1 &= F_{01} \\
\frac{d^2u_2}{dt^2} + \omega_2^2 u_2 + \Gamma_2 &= F_{02} \\
\frac{d^2u_3}{dt^2} + \omega_3^2 u_3 + \Gamma_3 &= F_{03}
\end{aligned} \tag{A.1}$$

The coefficients within the terms Γ_1, Γ_2 and Γ_3 contain coupling terms and can be evaluated from the second of equation (2.26). However, due to different boundary conditions, several of these coefficients are in fact zero.

A.1.1 The Case of Symmetric Forcing

In the case of a symmetric forcing, i.e., if a point force acts at the mid-span of the beam or if a distributed load acting across the beam has a symmetric distribution about the mid-span of the beam, the even numbered modes would not respond, so that the second equation of (A.1) will be zero.

The term $\int_0^l \Phi_m \frac{d^2\Phi_n}{dx^2}\, dx$ in equation (2.20) of Section 2.1.2 governs the nth mode coupling in the mth equation. Hence, it can then be shown in equation (2.21) in that section that for all choices of $m \neq n$, this term is identically zero for the simply-supported boundary conditions. Thus, expanding (A.1) up to three modes, the following equations result:

$$\begin{aligned} \frac{d^2u_1}{dt^2} + \omega_1^2 u_1 + \Pi_{1111}u_1^3 + \Pi_{1133}u_1u_3^2 &= F_{01} \\ \frac{d^2u_3}{dt^2} + \omega_3^2 u_3 + \Pi_{3311}u_1^2u_3 + \Pi_{3333}u_3^3 &= F_{03} \end{aligned} \tag{A.2}$$

By the method of harmonic balance in section 3.2.1, the following equations are obtained.

$$\begin{aligned} -A_1\Omega^2 + \omega_1^2 A_1 + \frac{3}{4}\Pi_{1111}A_1^3 + \frac{3}{4}\Pi_{1133}A_1A_3^2 &= Q_{01} \\ -A_3\Omega^2 + \omega_3^2 A_3 + \frac{3}{4}\Pi_{3311}A_1^2A_3 + \frac{3}{4}\Pi_{3333}A_3^3 &= Q_{03} \end{aligned} \tag{A.3}$$

The harmonic response for the first two symmetric modes (mode one and mode three) under these specified conditions can be found by solving the equations in (A.3) by an iterative method such as the Newton's method [103].

A.1.2 The Case of Asymmetric Forcing

When the beam is asymmetrically excited, even-numbered modes enter into the response. Hence, in this case, all terms representing the even-numbered modes within

all three equations in (A.1) have to be considered. The three equations (A.1) for the simply-supported end conditions with asymmetric forcing conditions, expanded up to and including the third mode, would become:

$$\begin{aligned}
\frac{d^2u_1}{dt^2} + \omega_1^2 u_1 + \Pi_{1111}u_1^3 + (\Pi_{1122}u_2^2 + \Pi_{1133}u_3^2)u_1 &= F_{01} \\
\frac{d^2u_2}{dt^2} + \omega_2^2 u_2 + \Pi_{2222}u_2^3 + (\Pi_{2211}u_1^2 + \Pi_{2233}u_3^2)u_2 &= F_{02} \\
\frac{d^2u_3}{dt^2} + \omega_3^2 u_3 + (\Pi_{3311}u_1^2 + \Pi_{3322}u_2^2)u_3 + \Pi_{3333}u_3^3 &= F_{03}
\end{aligned} \tag{A.4}$$

A.2 Iterative Process in Harmonic Balance: Newton's Method

An iterative process such as the Newton's Method could be used when solving the coupled non-linear algebraic equations (A.3) when employing the Harmonic Balance Method. Reformulate equations (A.3) so that they become:

$$\begin{aligned}
-A_1\Omega^2 + \omega_1^2 A_1 + \frac{3}{4}\Pi_{1111}A_1^3 + \frac{3}{4}\Pi_{1133}A_1A_3^2 - Q_{01} &= \phi \\
-A_3\Omega^2 + \omega_3^2 A_3 + \frac{3}{4}\Pi_{3311}A_1^2A_3 + \frac{3}{4}\Pi_{3333}A_3^3 - Q_{03} &= \psi
\end{aligned} \tag{A.5}$$

From the equations in (A.5), set all the coupling terms to zero and solve for A_1 and A_3, namely $A_{1,0}$ and $A_{3,0}$ which are the initial guesses for the next approximated solutions $A_{1,1}$ and $A_{3,1}$. This is done by employing the expressions:

$$\begin{aligned}
A_{1,i} &= A_{1,i-1} - \left[\frac{\phi\psi'_{A_3} - \psi\phi'_{A_3}}{\phi'_{A_1}\psi'_{A3} - \phi'_{A3}\psi'_{A_1}}\right]_{A_1=A_{1,i-1},A_3=A_{3,i-1}} \\
A_{3,i} &= A_{3,i-1} - \left[\frac{\psi\phi'_{A_1} - \phi\psi'_{A_1}}{\phi'_{A_1}\psi'_{A3} - \phi'_{A3}\psi'_{A_1}}\right]_{A_1=A_{1,i-1},A_3=A_{3,i-1}}
\end{aligned} \tag{A.6}$$

where $\psi'_{A_1} = \partial\psi/\partial A_1$, $\psi'_{A_3} = \partial\psi/\partial A_3$, $\phi'_{A_1} = \partial\phi/\partial A_1$, $\phi'_{A_3} = \partial\phi/\partial A_3$ and $i = 1, 2, 3, \ldots$.

The values of the next approximated solutions $A_{1,2}$ and $A_{3,2}$ are then calculated by using the previous set of solutions ($A_{1,1}$ and $A_{3,1}$) as initial guesses. The process is terminated when $(\frac{A_{1,i}}{A_{1,i-1}}) - 1 \leq TOL$ and $(\frac{A_{3,i}}{A_{3,i-1}}) - 1 \leq TOL$, where TOL is a predefined tolerance and should be small. The resultant values will be the solutions of A_1 and A_3 in equations (A.3).

Appendix B

SOLUTION OF THE SDOF DUFFING'S EQUATION

B.1 Frequency Response of The Primary Resonance of The SDOF Duffing's Equation

Consider the SDOF Duffing's equation (3.7) which is reformulated with the subscripts dropped.

$$\frac{d^2u}{dt^2} = -\omega^2 u - \Pi u^3 + F_0(t) \tag{B.1}$$

The solutions of equation (B.1) can be described by the frequency-response curve known as the "backbone curve". It represents the frequency response in the non-linear cases and can be thought of as arising from the response curve for the linear case by bending it to the right for a hardening spring and to the left for a softening spring.

The solutions for the undamped frequency response can be obtained by using equation (3.9). With subscripts dropped, it is reformulated and given by equation (B.2).

$$\frac{\Omega}{\omega} = \sqrt{1 + \frac{3}{4}\frac{\Pi A^2}{\omega^2} - \frac{F_0(t)}{\omega^2 A sin(\Omega t)}} = \sqrt{1 + \frac{3}{4}\frac{\Pi A^2}{\omega^2} - \frac{Q_0}{\omega^2 A}} \tag{B.2}$$

A typical response curve or backbone curve is shown in Figure 3.2. The response curves for a linear spring ($\Pi = 0$) and for a hardening spring ($\Pi > 0$) with damping are shown in Figure B.1. The effect of damping controls the "peak" of the curve.

For particular values of frequency ratio (Ω/ω) there are three corresponding values of response amplitude $|A|$ on the backbone curve. However, only two of the three amplitudes are regarded as the stable solutions. These are the amplitudes which exists in reality. Moreover, which stable amplitude will exist at a particular (Ω/ω) depends on the initial conditions of excitation. The behaviour is known as "jump" phenomenon.

For instance, when the amplitude of excitation is held constant and its frequency (Ω) is far above the natural frequency (ω) and is monotonically decreasing, the response amplitude $|A|$ increases slowly and moves along the curve from point A towards point B, as indicated in Figure B.1. At a particular (Ω/ω) (point B), $|A|$ "jumps" spontaneously to the top curve. For further decrease in Ω, $|A|$ decreases slowly along that curve towards point D.

On the other hand, when the forcing frequency is initially far below ω and monotonically increasing, $|A|$ increases and moves from point D via point C towards point E. With damping, after passing the peak of the curve (point E), $|A|$ "drops" spontaneously to the bottom curve at point F. The amplitude $|A|$ continues to decrease slowly and moves towards point A. The sudden drop in amplitude from points E to F would be inexplicable on the basis of the corresponding backbone curve with no damping included [15]. The regions where the amplitude $|A|$ never exists in reality, bounded by the curves between points E and B, contain the unstable solutions of the Duffing's equation.

When the Duffing's equation including the first mode is solved numerically for $|A|$ at each value of Ω/ω_1, the backbone curve can also be constructed. The curves have been presented in Figures 3.6 and 3.7 for responses due to concentrated and distributed loads respectively. Observations of the graphs reveal that the values of $|A|$ at $\Omega/\omega_1 = 0.4243$ for the concentrated load case and at $\Omega/\omega_1 = 0.433$ for the distributed load case do

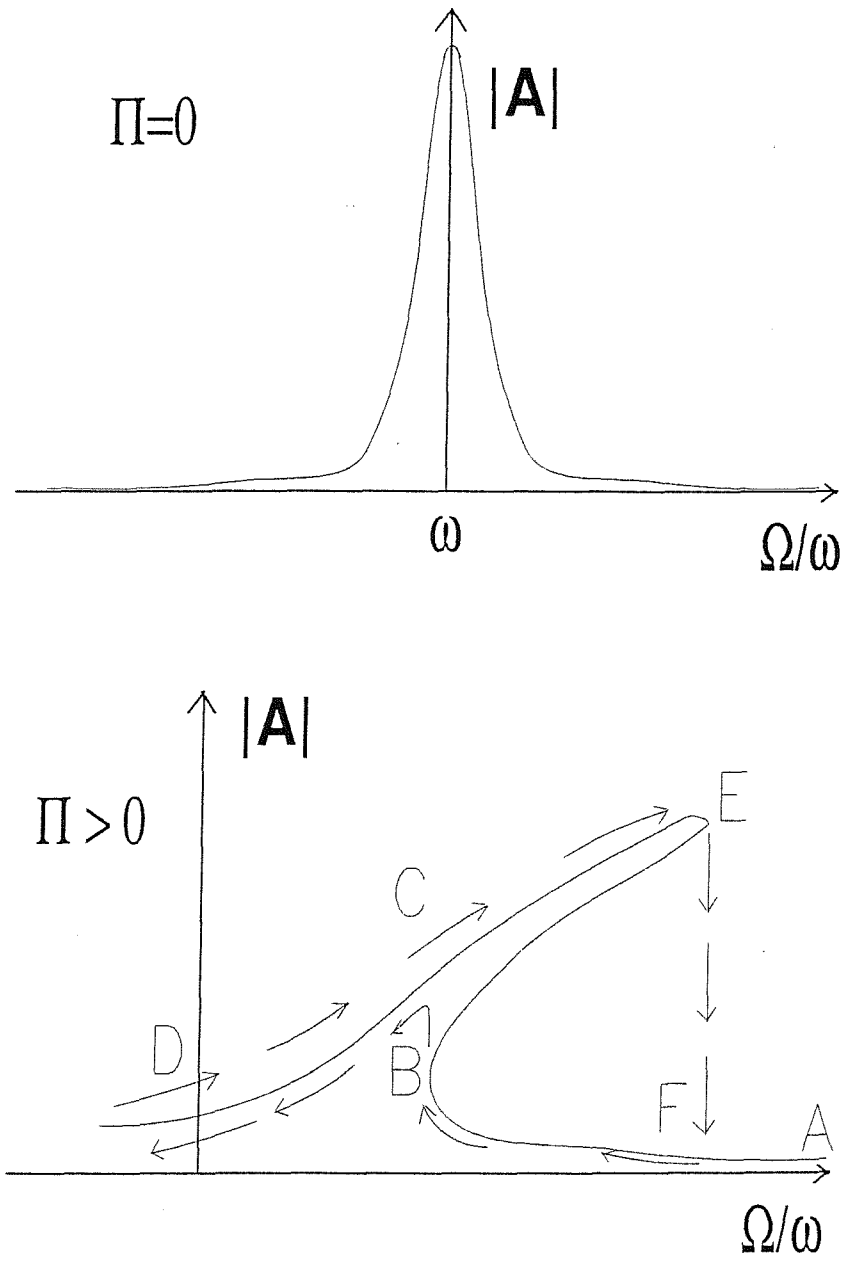

Figure B.1: Frequency-response curves for the Duffing's equation for a linear spring (top) and a hardening spring (bottom).

not agree with the corresponding Harmonic Balance and the ANSYS® solutions. As a result, equation (B.1) is solved numerically for $|A|$ at several values of Ω/ω_1 in the region concerned. The results are shown in Figures B.2 and B.3.

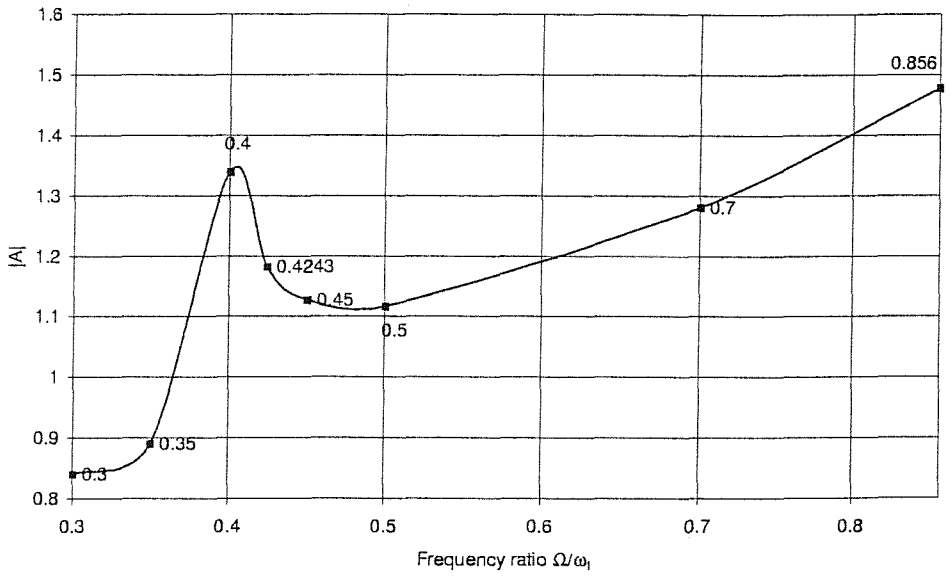

Figure B.2: Frequency-response curves obtained by the numerical integration of the Duffing's equation: concentrated load $\overline{F_0^c} = 1$

It is suggested that the peaks are due to a non-linear phenomenon called superharmonic resonance of the non-linear system [11]. This happens when the resonance frequency is about three times the forcing frequency. In a superharmonic oscillation, the overall steady-state response is a superposition of two components: the free-oscillation and the forced-oscillation responses. The steady-state forced-oscillation response has the same period as the external load, the behaviour of which is the same as that in a linear system. The free-oscillation response oscillates at a frequency which is three times the forcing frequency. However, unlike a linear system, the amplitude of the free-oscillation response in a non-linear system at superharmonic resonance does not decay to zero in spite of the presence of damping [15].

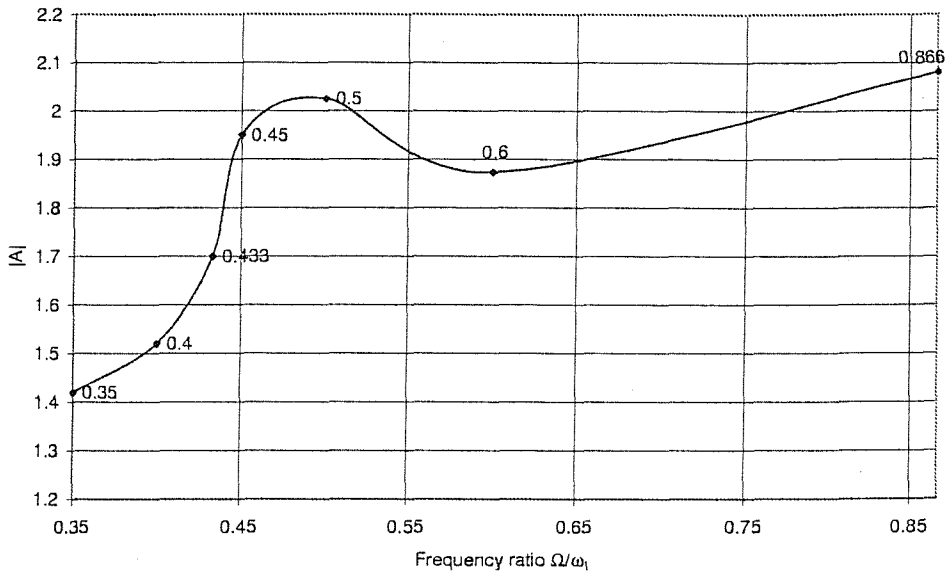

Figure B.3: Frequency-response curves obtained by the numerical integration of the Duffing's equation: distributed load $\overline{F_0^d} = 2$

To verify if the suggested reason is valid, the frequency spectra of the time histories of the displacement response are obtained. In particular, the time histories and power spectra of the non-linear responses for $\Omega/\omega_1 = 0.4$ in the concentrated load case and for $\Omega/\omega_1 = 0.45$ in the distributed load case are presented in Figures B.4 and B.5 respectively.

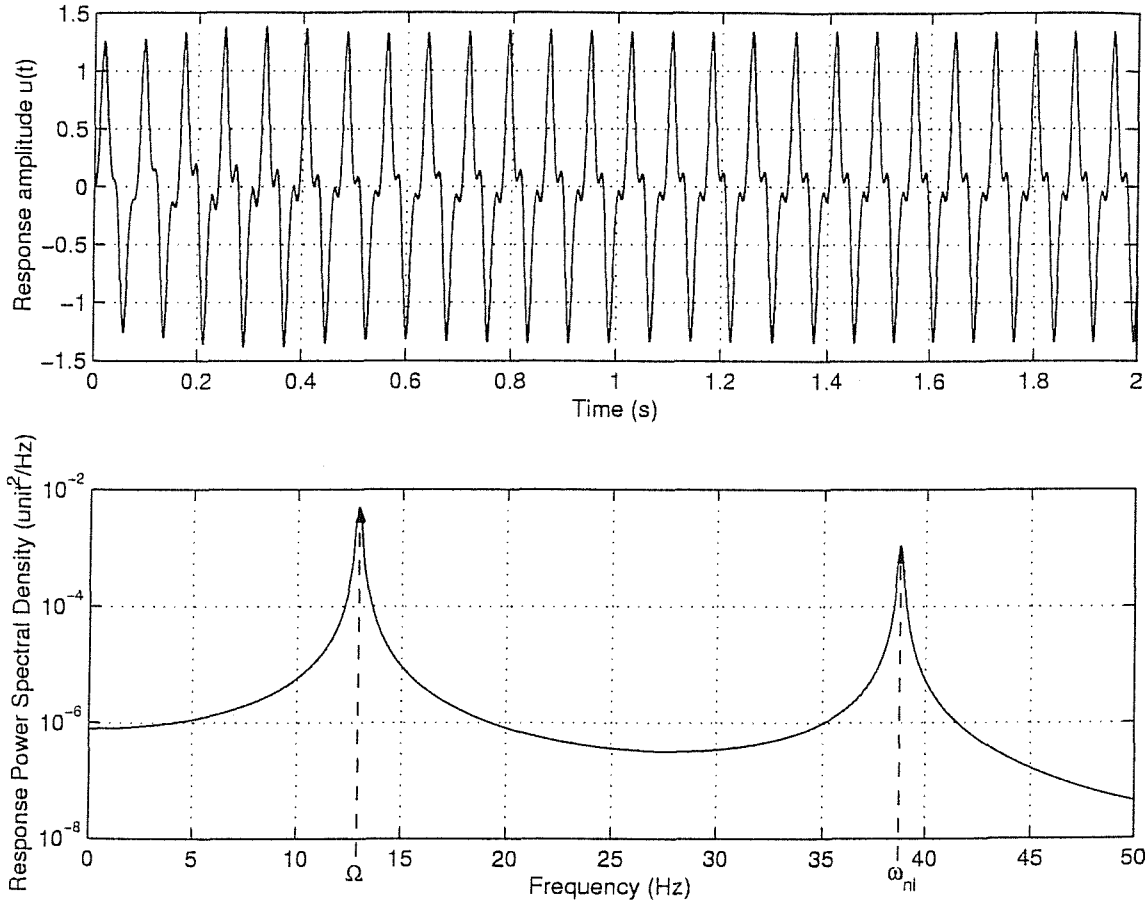

Figure B.4: Time Histories (top) and Power Spectrum (bottom) of Non-linear Displacement Response at $\Omega/\omega_1 = 0.4$: Concentrated Load $\overline{F_0^c} = 1$

From the resulted frequency spectra, it is found that besides a distinct peak at the forcing frequency, there is another peak at a higher frequency, denoted by w_{nl}, whose power spectral density (PSD) is significant relative to the PSD at Ω. By obtaining the ratio between the forcing frequency and w_{nl} at each Ω/ω_1 for the two loading cases, it

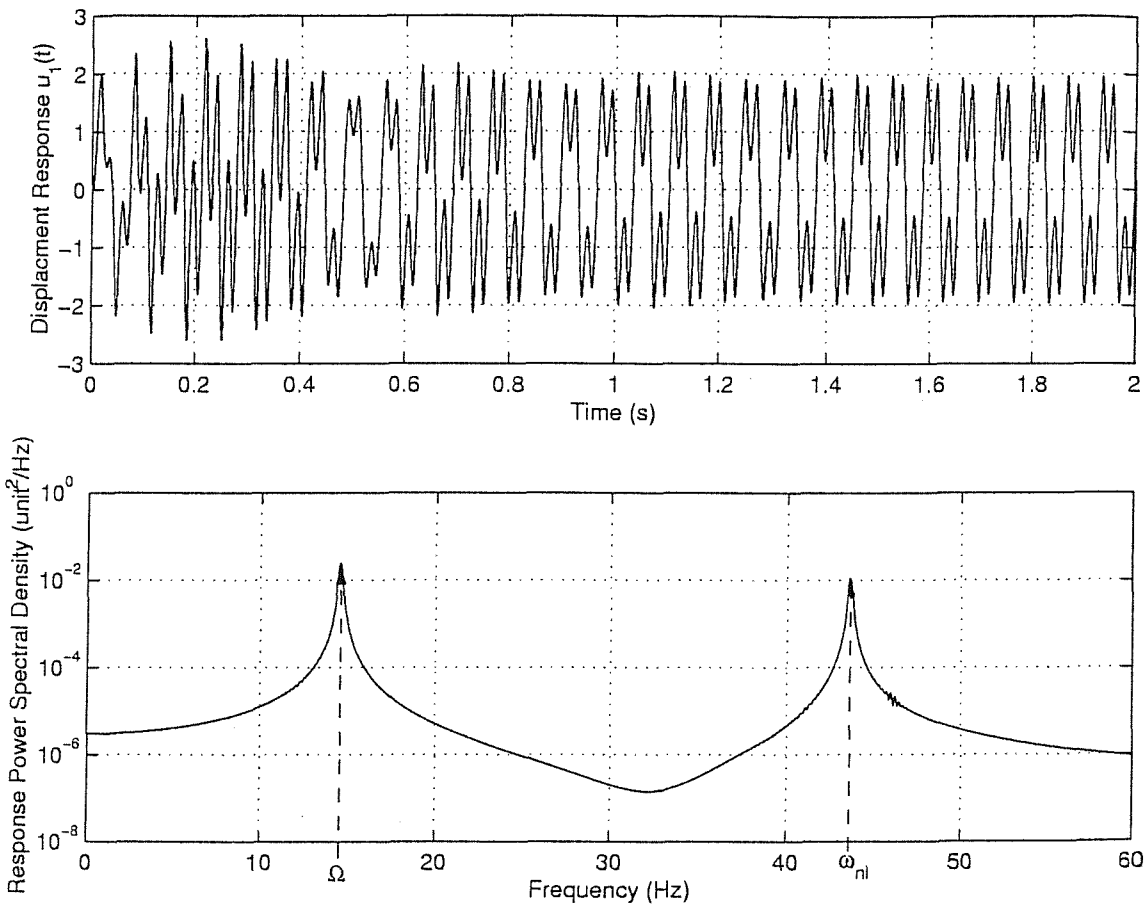

Figure B.5: Time Histories (top) and Power Spectrum (bottom) of Non-linear Displacement Response at $\Omega/\omega_1 = 0.45$: Distributed Load $\overline{F_0^d} = 2$

can be seen that these values of w_{nl} are about 3Ω. Hence the frequency w_{nl} is thought to be the frequency of the free-oscillation response in superharmonic resonance. It is also noticed that the value of w_{nl} increases with increasing Ω/ω_1 in this region of the curve. A comparison of different frequency ratios is given in Table B.1 and B.2.

Ω/ω_1	ω_{nl}/ω_1	ω_{nl}/Ω	Ω/ω_{nl}
0.35	1.05	3.000	0.333
0.4	1.20	3.000	0.333
0.4243	1.27	3.003	0.333
0.5	1.50	2.994	0.334

Table B.1: Comparison of Frequencies Ratios in The Concentrated Load Case

Ω/ω_1	ω_{nl}/ω_1	ω_{nl}/Ω	Ω/ω_{nl}
0.35	1.05	3.002	0.333
0.433	1.30	3.000	0.333
0.45	1.35	3.000	0.333
0.5	1.50	3.000	0.333

Table B.2: Frequencies Ratios in The Distributed Load Case

It is thus believed that the small peaks found on the backbone curves in Figures B.2 and B.3 are due to superharmonic resonance.

B.2 Approximation of the Temporal Responses for a SDOF Duffing's System

The time-dependent displacement response $u(t)$ in equation (B.1) can be obtained by numerical methods. However, an approximated method can also be obtained by many analytical methods, and the iteration method from reference [15] will be outlined here.

Note that this is valid when Π is small and when F_0 is of the same order of magnitude of Π. In theory, for weakly non-linear systems, the value of Π should be small. After rearranging and adding an extra term $\Omega^2 u$ to equation (B.1), it becomes:

$$\frac{d^2u}{dt^2} + \Omega^2 u = (\Omega - \omega^2)u - \Pi u^3 + \Pi F \sin \Omega t \tag{B.3}$$

Note in equation (B.3) that the value of ω need not be small and that $F_0 = \Pi F$. Now, the single mode analogy to equation (3.3) is

$$u_I(t) = A \sin \Omega t \tag{B.4}$$

The parameter u_I is the first approximation of the solution of u, and A is supposed to be given. Substituting the expression of $u_I(t)$ of (B.4) and its derivatives into the right hand side of (B.3), followed by the use of the identity $\sin^3 \Omega t = (3 \sin \Omega t - \sin 3\Omega t)/4$, gives the following differential equation:

$$\frac{d^2u_{II}}{dt^2} + \Omega^2 u_{II} = \left[(\Omega - \omega^2)A - \frac{3}{4}\Pi A^3 + \Pi F\right] \sin \Omega t + \frac{1}{4} A^3 \Pi \sin 3\Omega t \tag{B.5}$$

where u_{II} is the refined approximation to u.

To ensure that u_{II} is periodic, the coefficient of $\sin \Omega t$ has to be zero [15] so that:

$$\frac{\Omega}{\omega} = \sqrt{1 + \frac{3}{4}\frac{\Pi A^2}{\omega^2} - \frac{\Pi F}{\omega^2 A}} \tag{B.6}$$

This is analogous to equation (B.2), and $\Pi F = Q_0$. By integrating equation (B.5) and setting the constants of integration to zero, the next approximation of the solution of $u(t)$, which is harmonic with period $2\pi/\Omega$, will be:

$$u_{II}(t) = A \sin \Omega t + \frac{\Pi A^3}{36\Omega^2} \sin 3\Omega t \tag{B.7}$$

Making Ω^2 the subject of equation (B.6) and substituting it into (B.7), the following can be obtained:

$$u_{II}(t) = A\sin\Omega t + \frac{1}{36}\left[\frac{\Pi A^3}{\omega^2 + \frac{3}{4}\Pi A^2 - \left(\frac{\Pi F}{A}\right)}\right]\sin 3\Omega t \tag{B.8}$$

This is an analytical approximated value for the single-degree-of-freedom time-varying displacement $u_1(t)$.

Once the values of $u_m(t)$ are known, the maximum bending and the total axial (membrane) strains for a selected set of amplitudes, A_m and frequencies, Ω, can be obtained.

For a multiple-degree-of-freedom system, from equations (2.6) and (2.14), the average axial (membrane) strain, $\epsilon_a(t)$, is given by:

$$\epsilon_a(t) = \frac{\Delta l}{l} = \frac{1}{2l}\int_0^l \left(\frac{\partial w(x,t)}{\partial x}\right)^2 dx = \frac{R^2}{2l}\sum_{m,n=1}^{\infty} K_{mn}u_m(t)u_n(t) \tag{B.9}$$

The bending strain due to curvature has a maximum value at the top or bottom surfaces and occurs at the mid-span of the simply-supported beam. The maximum bending strain is denoted by $\epsilon_b(t)$ and is given by:

$$\epsilon_b(t) = \pm\frac{h}{2}\left[\frac{\partial^2 w}{\partial x^2}\right]_{x=l/2} = \pm\frac{Rh}{2}\left(\frac{\pi}{l}\right)^2\sum_{m=1}^{\infty} m^2 u_m(t) \tag{B.10}$$

The total strain is the sum of the two strains with the use of equations (B.9) and (B.10).

$$\epsilon_t(t) = \epsilon_a(t) + \epsilon_b(t) \tag{B.11}$$

For the one-mode case with simply-supported end conditions, $\Phi(x) = \sin(\pi x/l)$, and hence,

$$\epsilon_a(t) = \frac{\pi R^2}{2l}u_1(t)^2 \tag{B.12}$$

$$\epsilon_b(t) = \pm \frac{Rh}{2} \left(\frac{\pi}{l}\right)^2 u_1(t) \tag{B.13}$$

where $u_1(t)$ could be given in equation (B.8) as $u_{II}(t)$, or the displacement response time-histories obtained in a time-domain numerical analysis.

Appendix C

NOTES ON NUMERICAL ANALYSIS TECHNIQUES

C.1 Non-linear Analysis by Finite Element Software ANSYS®: Undamped Harmonic Vibrations

The non-linear displacement response of the beam due to a harmonic load can be obtained by building a finite element model of the beam and then carrying out "transient" analysis in ANSYS®. The procedure is outlined briefly here.

In the "Preprocessor" phase (/PREP7) in ANSYS®, a three-dimensional elastic beam element BEAM4 is used. The element BEAM4 is a uni-axial element with tension, compression, torsion, and bending capabilities. The element has six structural degrees of freedom at each node: three translational and three rotational. Stress stiffening and large deflection capabilities are included. A consistent tangent stiffness matrix option is available for use in large deflection (finite rotation) analyses. Shear deflection effects can be included.

The properties of the beam such as the cross-sectional area, the second moment of inertia, the beam thickness, the Modulus of Elasticity and the density are defined. The

model of the beam is then meshed into a finite number of elements along the length of the beam in such a way that the highest linear mode shape can be captured whilst at the same time the mesh is not too fine that computational resources are wasted. In the current study, eight elements have been found to be adequate to capture the third linear mode shape.

In the "Solution" phase (/SOLU), ANTYPE,TRANS is used. To account for the effects of geometrical non-linearity, the mode NLGEOM,ON should be present. The boundary conditions are then defined. A "loadstep-by-loadstep" approach is carried out to obtain the response due to an external sinusoidal load.

It should be noted that even when no damping is considered in the work, some damping has been carefully implemented in order to remove the "transients" in the results. As the current analysis type TRANS does not allow the use of a constant damping ratio, the proportional damping constants ALPHAD and BETAD are used. Damping attributed to stiffness-proportional damping (BETAD) increases with increasing frequency whilst damping attributed to mass-proportional (ALPHAD) damping decreases with increasing frequency.

Finally, the results are retrieved from the "Postprocessor" phase (/POST26).

C.2 Simulation of Input Random Loads

Stationary and Gaussian random processes can be simulated by employing the technique of Inverse Fast Fourier Transform [38, 39].

For a uniformly distributed band-limited Gaussian white noise, the random pressure, $P^n(t)$ can be simulated as

$$P^n(t_p) = Re[\sum_{n=1}^{M} A_n e^{i\phi_n} e^{i\omega_n t_p}] \tag{C.1}$$

where ϕ_n's are independent random phase angles uniformly distributed between 0 and 2π, ω_n's are the frequencies at which the value of spectral density, S_f are selected,

$M = 2^z$ is the number of simulated points in time, z is a positive integer, $t_p = p\Delta t$ where Δt is the time interval, $p = 1, 2, ..., M$, and

$$A_n = \sqrt{[2S_f(\omega_n)\Delta\omega]} \tag{C.2}$$

The spectral density is defined in equation (4.22) in Section 4.2.3 of Chapter 4.

In order to ensure that the simulated pressure describes its frequency domain counterpart, its mean square value should be close to the integral area under the corresponding frequency spectrum density curve. The root-mean-square value of the simulated pressure should also be the same as the prescribed one calculated from the SPL value, as the process has a mean of zero.

Appendix D

TABLE OF REFERENCES

The table of references shown in this section represents a brief description of the literature cited throughout the thesis. In the table, notations are used and their meaning is explained below:

P: Plate-type structures

S: Shells or curved panels

SP: Stiffened plates

Sine: Excitation varies sinusoidally with time

random: Random Excitation

PT: Point load

DIST: Distributed load

harmonic: Harmonic Excitation

periodic: Periodic Excitation

thermal: effects of elevated temperature

No.	Author	Year	Beams	Plates (stiffened), Shells	Composites	Free Vibrations	Forced Vibrations
1	H.F. WOLFE, C.A. SHROYER, D.L. BROWN and L.W. SIMMONS	1995	X	P	X		Sine, random
2	J MILES	1954		P,S			
3	A POWELL	1958					random
4	B.L. CLARKSON	1968		P,S			random
5	R.D. BLEVINS	1979		P, S			DIST
6	O.C. ZIENKIEWICZ	1977					
7	E.J. RICHARDS and D.J. MEAD	1968					
8	S.H. CRANDALL	1958					
9	S.H. CRANDALL	1963					
10	W.J. TRAPP and D.M. FORNEY, JR	1965					
11	A.H. NAYFEH and D.T. MOOK	1979					
12	M. SATHYAMOORTHY	1987		P			
13	R.A. IBRAHIM	1991					
14	H. CHALLIS and C. STANTON	1979					
15	J.J. STOKER	1950					
16	T.K. CAUGHEY	1963					random white-noise
17	J.M.T. THOMPSON and H.B. STEWART	1986					
18	D.E. NEWLAND	1984					
19	P.D. SPANOS	1981					
20	S.H. CRANDALL	1963					random
21	J. HE	2000				X	
22	T.K. CAUGHEY.	1971					
23	C. MEI and D.B. PAUL.	1986		P			random
24	G. AHMADI, I. TADJBAKHSH and M. FARSHAD	1978		P			random
25	Y.K. LIN	1988					random
26	T.K. CAUGHEY	1963					random
27	N. KRYLOV and N. BOGOLIUBOV	1937					random
28	R. C. BOOTON JR.	1954					random
29	T. SELCUK ATALIK and S. UTKU	1976					
30	F. DINCA and C. TEODOSIU	1973					
31	I. ELISHAKOFF and J. FANG and R. CAIMI.	1995	X				random
32	H.R. BUSBY JR and V.I. WEINGARTEN.	1973	X				random in time
33	R.E. HERBERT.	1964					pure random
34	R.S. LANGLEY	1987	X				
35	I. SIMULESCU, T. MOCHIO and M. SHINOZUKA	1989					
36	I. ELISHAKOFF and P. COLOMBI	1993					
37	R. VAICAITIS	1991		P, SP	X		random
38	M. SHINOZUKA and C.-M. JAN	1972					random
39	M. SHINOZUKA and G. DEODATIS	1996					random
40	A. BLAQUIÈRE	1966					
41	A.W. LEISSA	1969					
42	A.W. LEISSA	1984		P,S		X	
43	J.N. REDDY	1985		P	X	X	
44	S. TIMOSHENKO.	1959					
45	S. WOINOWSKY-KRIEGER	1950	X			X	
46	P.H. McDONALD, JR. and RALEIGH N.C.	1955	X			X	
47	G. SINGH, A.K. SHARMA AND G.V. RAO	1990	X			X	
48	R. BENAMAR, M.M.K. BENNOUNA and R.G. WHITE	1991	X			X	
49	R. BENAMAR, M.M.K. BENNOUNA and R.G. WHITE	1993		P		X	
50	R. BENAMAR, M.M.K. BENNOUNA and R.G. WHITE	1994		P			PT, DIST
51	B. HARRAS, R. BENAMAR, and R. G. WHITE	2002		P		X	
52	R. BENAMAR, M.M.K. BENNOUNA and R.G. WHITE	1990		P	X	X	
53	M.EL KADIRI, R. BENAMAR and R.G. WHITE	1999		P		X	
54	S.R. RAO, A.H. SHEIKH and M. MUKHOPADHYAY.	1993		P / SP		X	
55	R.Y.Y. LEE, Y.SHI and C. MEI	1997		P	X	X	
56	F.MOUSSAOUI, R.BENAMAR and R.G WHITE	2000		S		X	
57	M.M. BENNOUNA and R.G. WHITE	1984	X				PT-sine, random
58	C. HAYASHI.	1964					
59	C.S. HSU	1960					periodic
60	A.V. SRINIVASAN	1966	X	P		X	harmonic
61	J.A. BENNETT and J.F. EISLEY	1970	X			X	harmonic
62	L. AZRAR, R. BENAMAR and R.G. WHITE	1999	X			X	harmonic
63	M.EL KADIRI, R. BENAMAR and R.G. WHITE	2002	X				harmonic
64	A.Y.T. LEUNG and S.K. CHUI	1997		P			Sine
65	H.A. SHERIF	1995		P	X		harmonic
66	N. YAMAKI, K. OTOMO and M. CHIBA.	1981		P			harmonic DIST
67	H.R. BUSBY JR and V.I. WEINGARTEN.	1972	X				harmonic
68	R.Y.Y. LEE, Y.SHI and C. MEI	1997		P	X	X	uniform harmonic DIST
69	C.K. CHIANG, C. MEI AND C.E. GRAY, JR.	1991		P	X	X	harmonic
70	P.RIBEIRO and M. PETYT.	1999	X			X	PT harmonic
71	P.RIBEIRO and M. PETYT	1999		P			harmonic
72	P.RIBEIRO and M. PETYT	1999		P			harmonic
73	R.E. HERBERT	1965	X	P,S			random white-noise
74	R.E. HERBERT	1965	X				Random
75	P. SEIDE	1975					random in time
76	C.B. PRASAD and C. MEI	1987	X				random
77	J.A. SCHUDT	1991					
78	C. MEI and C.K. CHIANG.	1987	X	P			Random
79	C. HWANG and W.S. PI	1972		P			random
80	R.S. SRINIVASAN and P.A. KRISHNAN	1990		P			Random
81	C. MEI and K.R. WENTZ.	1982		P	X		random
82	C.E. GRAY JR. and K. DECHA-UMPHAI and C. MEI	1985		P	X	X	harmonic
83	R. VAICAITIS and P.A. KAVALLERATOS, AIAA-93-1426-CP	1993		P,S			random
84	R. VAICAITIS and R.R. ARNOLD	1990		P	X		random
85	J. DHAINAUT, B. DUAN, C. MEI, S. SPOTTSWOOD and H. WOLFE	2000	X	P,S			random + thermal
86	V. DOGAN and R. VAICAITIS	1999		S			random Pt, Dist, thermal
87	P.D. GREEN and A. KILLEY.	1997					random
88	M.I. McEWAN, J.R. WRIGHT, J.E. COOPER and A.Y.T. LEUNG	2001					harmonic
89	S.C. GALEA and R.G. WHITE	1988		P	X	X	random
90	R.R. CHEN, C. MEI and H.F. WOLFE	1996	X				random thermal
91	A. STEINWOLF, N.S. FERGUSON and R.G. WHITE	2000	X				random
92	Y.K. LIN	1967					
93	M. GHANBARI and J.F. DUNNE	1998	X				random
94	S. TIMOSHENKO, D.H. YOUNG and W. WEAVER, JR.	1974					
95	J. PRESCOTT	1961					
96	R.S. LANGLEY	1987	X				harmonic
97	GB. WARBURTON	1976	X	P,S			
98	C. MEI and K. DECHA-UMPHAI	1985	X				harmonic
99	A.K. CHOPRA	2001					
100	K-J. BATHE	1996					
101	ESDU	1996					
102	V.V. BOLOTIN	1984					
103	A.B. ALPOUR and A.J. McTERNAN	1967					